High Resolution Seismic Reflection Survey to Map Bedrock and Glacial/Fluvial Layers at the U.S. Navy Northern Ordnance Plant (NIROP) in Fridley, Minnesota

Richard D. Miller
Jianghai Xia

Final Report to

U.S. Geological Survey – WRD
Mound View, Minnesota

February 6, 1997

Open-file Report No. 97-12

Kansas Geological Survey
University of Kansas
Lawrence, Kansas

High Resolution Seismic Reflection Survey to Map Bedrock and Glacial/Fluvial Layers at the U.S. Navy Northern Ordnance Plant (NIROP) in Fridley, Minnesota

by
Richdard D. Miller
Jianghai Xia

technical assistance by
David R. Laflen
Joe M. Anderson
Mark T. Roberts
Ken Ross

report preparation by
P. Acker
Mary Brohammer
Ana Villella

**High Resolution Seismic Reflection Survey to Map Bedrock
and Glacial/Fluvial Layers at the
U.S. Navy Northern Ordnance Plant (NIROP) in Fridley, Minnesota**

Shallow seismic reflection in conjunction with downhole velocity profiles and local borehole data allowed delineation of discrete layering within the approximately 120 ft thick glacial drift that overlays the St. Peters Sandstone and/or the Prairie du Chien dolomites beneath the Northern Ordnance Plant, currently the Naval Industrial Reserve Ordnance Plant (NIROP) in Fridley, Minnesota. The primary goals of this study were to determine the feasibility and limitations of the technique and to develop a continuous subsurface image of major acoustic impedance contrasts related to geologic/hydrologic features. Establishing feasibility includes determining the horizontal and vertical resolution potential, optimum acquisition geometries and parameters, best suited equipment for surface and subsurface conditions, level of effort necessary to delineate the geologic/hydrologic features of interest, and to establish a reasonable set of expectations for the technique across the entire facility. Shallow seismic reflection profiles allowed delineation of discontinuous confining units within the glacial drift at this site. A high confidence reflection profile should greatly improve the accuracy of hydrologic flow models in areas with significant lateral variability. The glacial drift that covers the entire site consists of till, outwash, valley train, and lake deposits.

The goals of this survey necessitated the acquisition, processing, and interpretation of a walkaway VSP, three walkaway noise tests, and 1,441 shotpoints of 24-fold CDP data on three different lines. The uphole survey provided excellent ground truth as well as improved event identification and verification through curve modeling. The three walkaway noise tests permitted selection of optimum acquisition geometry and equipment for the CDP profiles and provided a measure of the strengths and limitations of shallow reflection in the various near-surface settings around the site. The CDP profiles collected along the western boundary fence of NIROP, southern extreme of the North 40, and southwest corner of the enclosed facility all possess sufficient resolution potential to image layers as shallow as 20 ft, discontinuities in the upper-drift confining unit, the bedrock (sandstone), and dolomite/sandstone contact. The dramatic change in interval velocities at the water table provided unique challenges to the generation of an accurate time section. The data were collected during two field outings: one between the 19th and 22nd of April and the other on September 28th and 29th.

The walkaway noise testing and check shot surveys were designed and executed to allow evaluation of acoustic signature, optimum acquisition equipment and parameters, near-surface velocity structure, horizontal consistency in reflection character, general resolution potential, signal-to-noise ratio, and impact of cultural noise (i.e., jet aircraft, industrial facility, vehicle traffic, etc.). The walkaway noise test guided the definitive selection of equipment and parameters as well as optimum station spacing and recording geometries. The check shot survey (downhole velocity/one-way travel time) established an approximate velocity structure for the upper 100 ft of sediments in well 13-D. The check shot surveys were necessary to correlate drill/log defined geology with reflections interpreted on CDP stacked sections and allow reflection verification on shot gathers. Several of the shot gathers from site #1 suggest practical vertical bed resolution on the order of 5 ft. It is also clear from the walkaway noise tests that the confining layer(s) and bedrock vary several feet vertically across the length of a spread (192 ft). This evaluation/feasibility study was designed to allow analysis of acoustic characteristics, and more generally, the reflection method, which in turn permitted accurate estimations of resolution and optimization of acquisition equipment and parameters.

With the primary focus of the CDP production survey being delineation of the upper-drift confining unit and bedrock surface, resolution potential is a critical characteristic. Most shallow reflection wavelets recorded during this study possess dominant frequencies in excess of 200 Hz with some upwards of 240 Hz. Based on the downhole survey in well D-13, the top and bottom of the borehole encountered confining units can be separated by as little as 1 msec (4 ft). Theoretically, resolving top and bottom of a bed this thin requires dominant frequencies in excess of 250 Hz, however in practice the reflection frequency band would need an upper corner of around 400 Hz to permit a confident interpretation. Simply identifying a particular layer as present, however, is easily possible with frequencies as low as 100 Hz. Delineating the top and bottom of a bed separated by at least 10 ft is well within the resolution potential of this data set. Using existing drill data around the NIROP site and the walkaway and downhole data as guides, detection of the confining layer and bedrock, when present, is possible across the entire site with the exception of areas contaminated by facility noise and/or less than 50 ft from surface structures. The 24-fold CDP profiles contained in this report possess a horizontal resolution on the order of 15 ft at 50 ft and a practical vertical resolution potential of around 5 ft.

Introduction

Understanding the various factors that control transport and fate of contaminants is critical to current groundwater management and future remediation efforts at the Naval Industrial Reserve Ordnance Plant (NIROP) in Fridley, Minnesota (Figure 1). NIROP has been an active design, fabrication, and testing facility for the Navy for several decades. Currently the facility is cooperatively operated by the Naval Sea Systems Command and FMC. Various by-products have been generated over the last several decades as a result of the industrial activities associated with the fabrication and testing of large ordnance systems. The close proximity of the plant to the Mississippi River and the Minneapolis Water Works river intake encourages an active program to locate source, migration path, and eventual fate of any water transportable product present at NIROP. Current active pump and treat operations could be enhanced and/or modified if an accurate and definitive subsurface profile could be generated with sufficient resolution to map discontinuities and topographic variations on the order of several feet in the upper-drift confining unit.

Localized absence of the upper-drift confining unit (Lindgren, 1990) prevents the horizontal extension of borehole information to the degree necessary for the generation of accurate groundwater flow models. Contaminants introduced at the ground surface during storage, disposal, and use have migrated toward the Mississippi River. Since precipitation recharge and seasonal changes in river levels are the primary hydrologic forces within the unconfined aquifer, the velocity and direction of contaminant transport is strongly influenced by the geologic features within the unconsolidated sediments.

Shallow high resolution seismic techniques possess the necessary resolution potential to delineate changes in the confining unit as inferred from drill data. Seismic reflection is a surface geophysical technique that relies on the reflection of sound waves from abrupt subsurface changes in material velocity and/or density (Appendix B). Shallow land surveys have been successful imaging a shallow bedrock surface (< 100 m) as well as overlying unconsolidated sequences (Miller et al., 1989; Miller et al., 1986; Birkelo et al., 1987; Jongerius and Helbig, 1988; Goforth and Hayward, 1992). The effectiveness and importance of VSPs to accurately correlate two-way travel time reflections on a CDP stacked section with borehole encountered geologic contacts for shallow surveys (i.e., < 100 m) has only recently begun to become apparent (Schieck and Pullan, 1995; Miller and Xia, 1996). Incorporation of VSPs, borehole geophysical logs, and lithologic logs with seismic data

3

MN

line 1

#1

VSP well

NIROP
property line

line 2

#2

#3

main
entrance

East River Road

Mississippi River

line 3

FMC
entrance

approx. trace
of
buildings
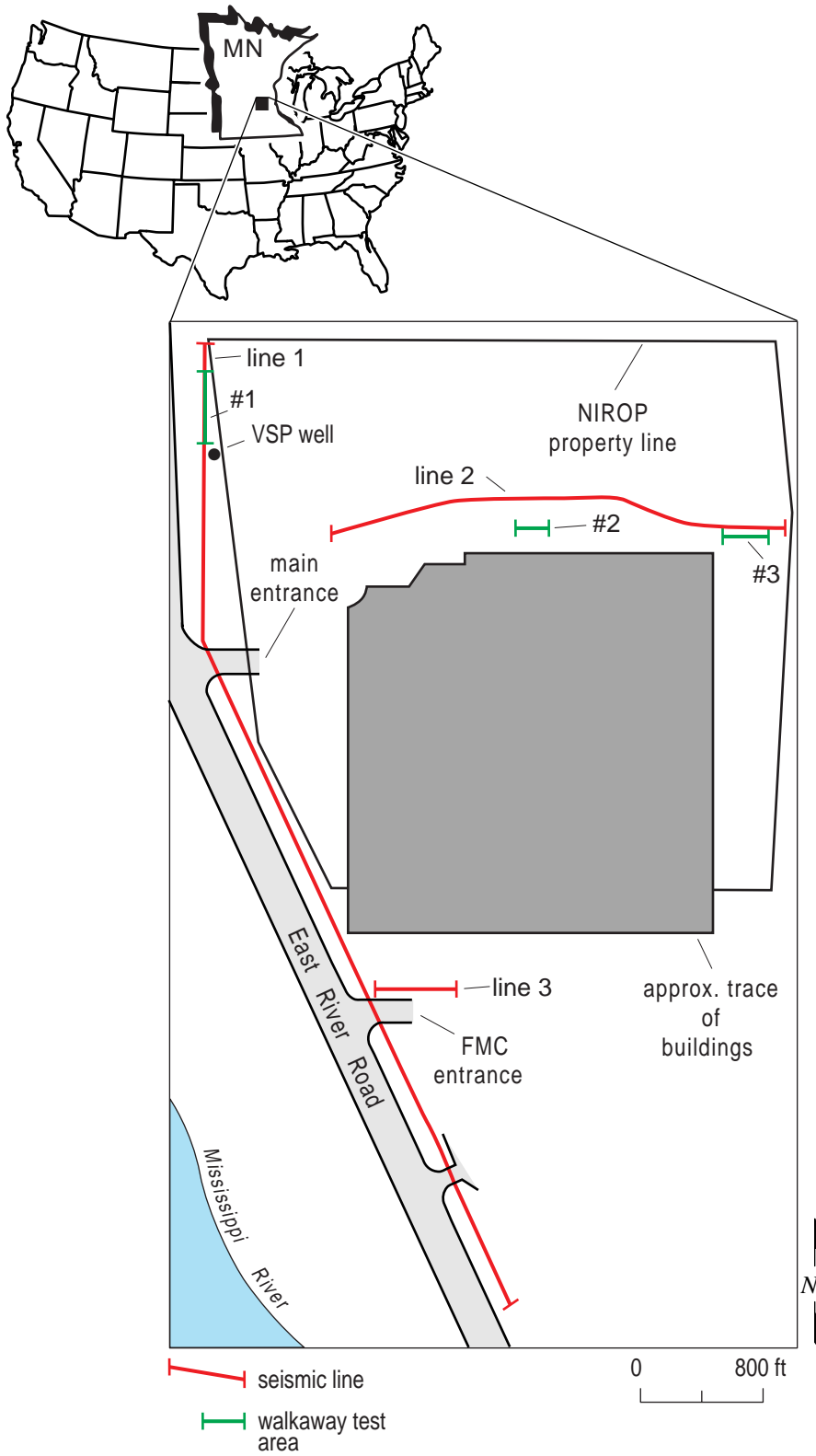
N

0   800 ft

seismic line

walkaway test
area

Figure 1. Generalized site map of U.S. Navy Northern Ordnance Plant, Fridley, Minnesota,
showing seismic lines 1, 2, and 3, walkaway test lines, and VSP well.

should provide the most accurate and horizontally continuous representation of the unconsolidated lithology at this site.

Geology/Hydrology

NIROP is located on an approximately 100 to 150 ft thick sequence of unconsolidated glacial and fluvial sediments overlying a bedrock of either St. Peters Sandstone or Prairie du Chien dolomites (Lindgren, 1990). The focus of this study is the 50 to 100 ft of material between the bedrock surface and the top of the upper-drift confining unit. The unconsolidated sediments that overlays bedrock consist of till, outwash, valley train, and lake and alluvial deposits which are characterized by alternating sands, gravels, silts, and clays. The condition of the upper-drift confining unit as it relates to the hydrologic characterization and therefore the development of transport and fate scenarios for surface introduced contaminant is an extremely important component of the geophysical study at this site. The piezometric surface or water table ranges from 15 to 25 ft below ground surface along the survey lines and is influenced by the Mississippi River, annual precipitation, and the pumping of extraction wells. Hole to hole correlation is not only difficult but very speculative due to the dramatically different appearance and thickness of the clay/silt units observed in boreholes along the lines (Figure 2).

Managing groundwater resources and in certain situations formulating accurate contaminant isolation and extraction programs improves dramatically with the accuracy of the groundwater flow model. Inadequate determination of the spatial variability and hydraulic characteristics of aquifers and confining units in this area would limit the usefulness of numerical groundwater flow models. The importance of compensating for localized discontinuities in the confining unit at this site is evident when considering the hydraulic conductivity (a principal input parameter for hydrologic modeling) of the confining units range from .2 to .00004 ft/d (feet/day) while the hydraulic conductivity of the drift aquifers ranges from 50 to 200 ft/d (Lindgren, 1990).

Data Acquisition

The 24-fold CDP production profile along the western boundary fence, walkaway noise tests, and the VSP/downhole surveys were acquired during April of 1996. A second trip during late September produced 24-fold reflection data along lines 2 and 3. The seismograph used to record data on both trips was a 96-channel Geometrics StrataView. The StrataView amplifies, digitizes the analog signal into a
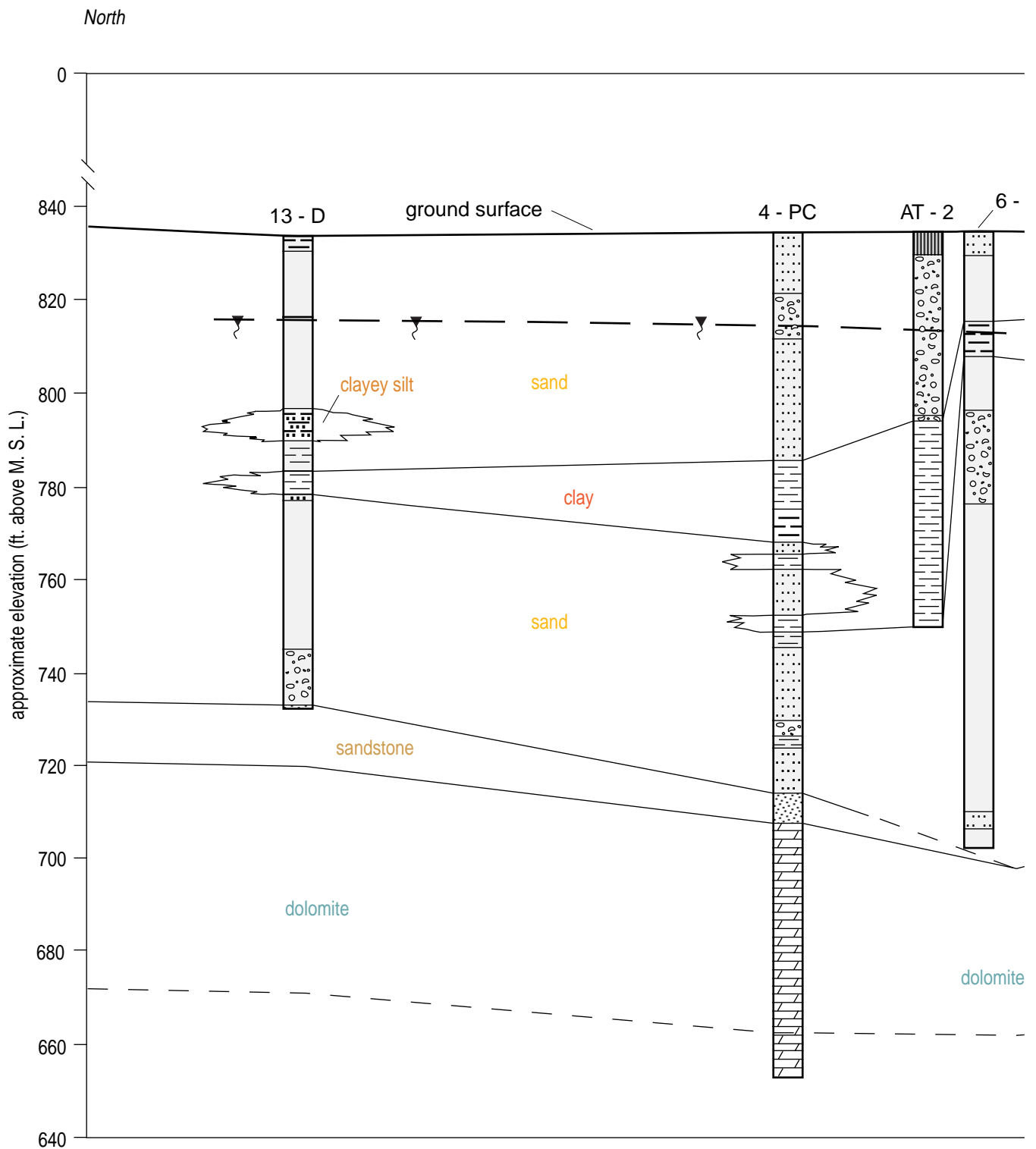
Figure 2a. Geologic cross-section derived from drill data near the East River Road and approximately parallel to seismic line 1 (modified from cross-section generated by RMI Inc., 1995).
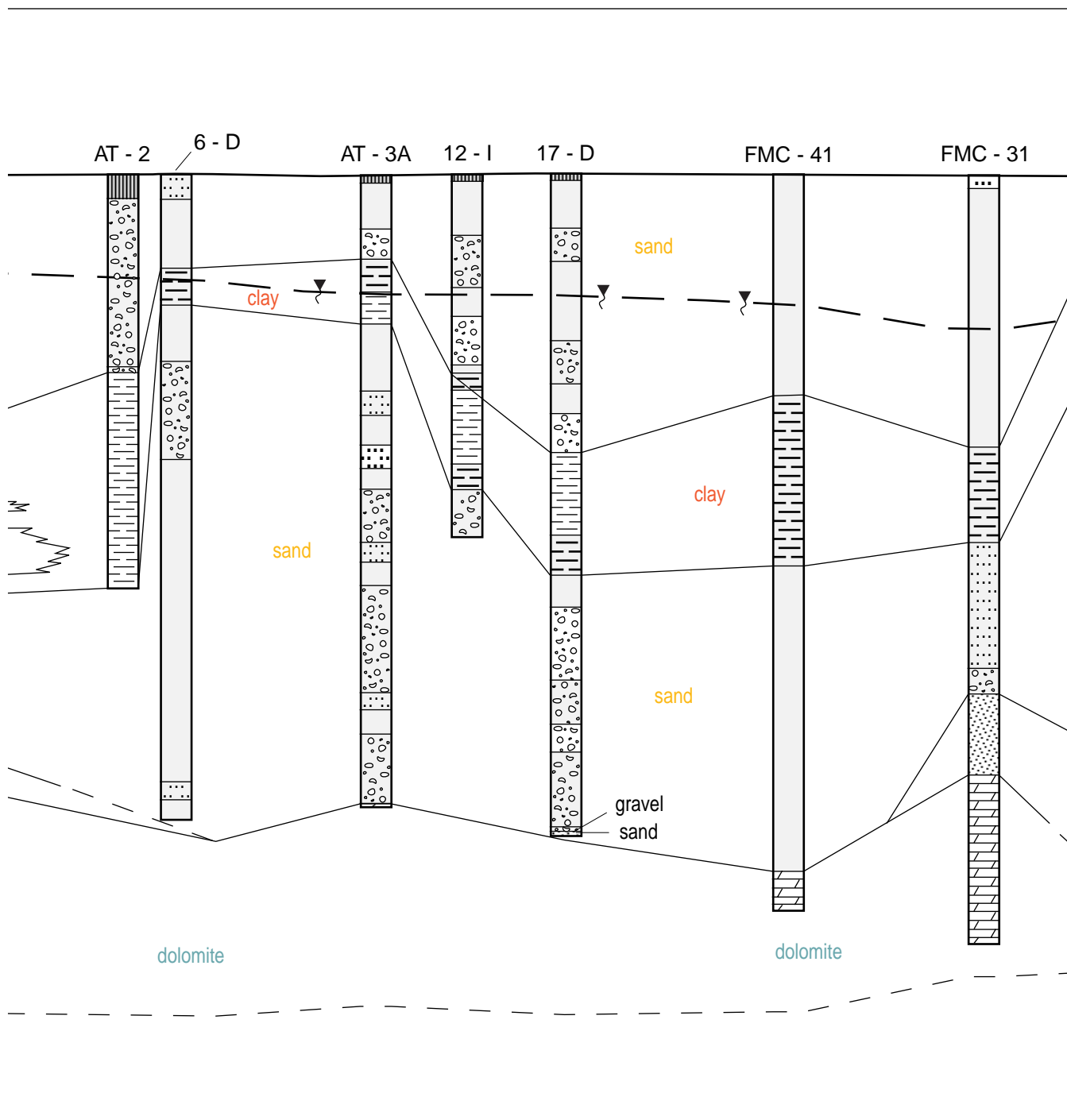
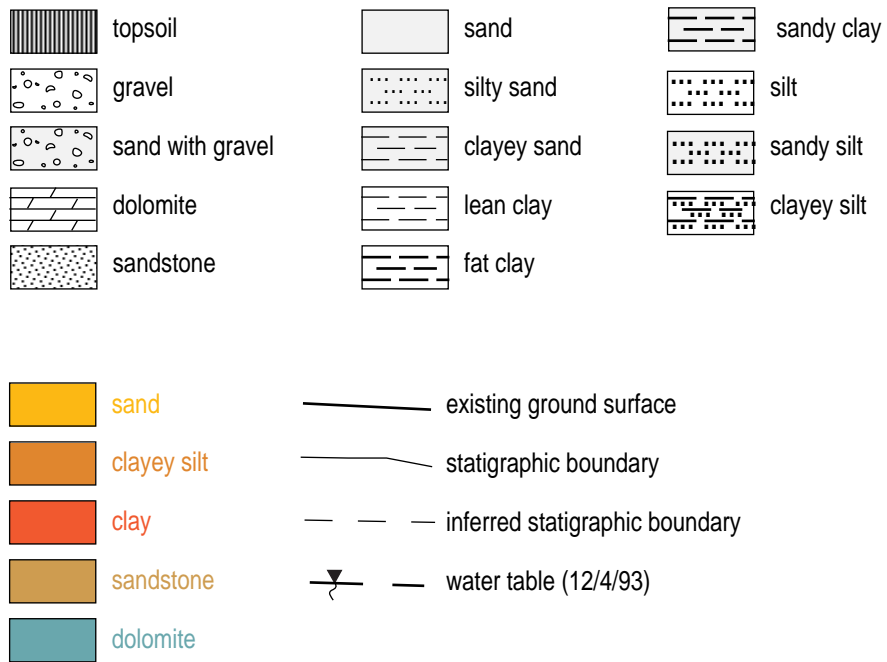AT - 2   6 - D   AT - 3A   12 - I   17 - D   FMC - 41   FMC - 31

sand

clay

sand

clay

sand

sand

gravel

sand

dolomite   dolomite

Figure 2b.

	topsoil		sand		sandy clay
	gravel		silty sand		silt
	sand with gravel		clayey sand		sandy silt
	dolomite		lean clay		clayey silt
	sandstone		fat clay		

	sand		existing ground surface
	clayey silt		statigraphic boundary
	clay		inferred statigraphic boundary
	sandstone		water table (12/4/93)
	dolomite		

Figure 2c.

24-bit word, and stores the digital information on computer hard drives in a demultiplexed format. The dynamic range of the StrataView mitigates the need for analog low-cut filters. CDP data were recorded with a sampling interval of 1/4 msec and a 250 msec record length. Field geometries were designed to maximize productivity without adversely affecting the resolution potential or velocity control of the CDP stacked data. The 30.06 downhole source and 100 Hz geophones were deployed in an asymmetric split-spread configuration with a nominal source-to-nearest receiver offset of 4 ft and farthest receiver offset of about 100 ft.

Downhole velocity check shots were recorded to determine vertical incident travel time from the surface to reflectors. The downhole survey consisted of a series of shots recorded with 10 ft and 50 ft source-to-well offsets and 10 ft downhole receiver intervals between 100 and 220 ft below the ground surface. A single down-hole hydrophone was used to record the downward traveling acoustic wave generated by a 7.3 kg sledge hammer striking a steel plate. Two 100 Hz geophones planted at the ground surface near the well pad provided the quality control (QC) necessary to insure precise time zero and consistency in source waveform. The downhole data were used to calculate average velocities from the surface to sub-surface features and provided ground truth for time-to-depth conversions on CDP stacked sections.

The walkaway noise tests were conducted in areas near proposed seismic lines and as near control wells as possible (Figure 1). The walkaways consisted of source-to-receiver offsets ranging from 4 ft to approximately 388 ft with 2 ft receiver intervals. The 12-gauge auger gun (Healey et al., 1991) (requiring only class C explosives), 12 lb sledge hammer, and 30.06 downhole gun were selected for testing after considering near-surface conditions, target depth, resolution requirements, and environmental constraints. Each source environment was optimized during testing to maximize the performance of each source.

The receivers available for testing included both single 100 Hz Mark Products L-40A geophones and triple 40 Hz Mark Product L-28E geophones wired in series. Survey requirements and site conditions necessitated high quality (spectrally clean throughout bandpass, minimum spurious noise, flat response throughout spectral range) and high output receivers. The need for high frequency signal response from the geophones is based on minimum resolution requirements and the excessive levels of cultural noise that plagued this area. The 100 Hz geophones produced the best response within the frequency band of interest.

All walkaway noise tests are sorted according to source configuration and displayed according to source-to-receiver offset with unique displays for each source. Most of the walkaway sections are trace balanced, bandpass filtered, and plotted in a variable area wiggle trace format. The downhole velocity files are normalized and grouped according to source offset from the well with traces ordered according to increasing hydrophone depth. The source configuration and field parameters for the proposed CDP production lines were based on the analysis of all walkaway tests and the downhole survey.

QC was critical and continuous throughout acquisition and processing. Near-surface inconsistencies, traffic noise, jet aircraft noise, the extremely narrow and changing optimum recording window, and high moisture conditions made strict compliance with QC guidelines and meticulous monitoring of data an absolutely essential aspect of the data acquisition. Based on subtle changes in the near-surface, minor adjustments to some parameters (e.g., source-to-near offset) were necessary to maintain the optimum recording window (Hunter et al., 1984). The seismograph CRT display, nearly real-time digital filtering, and real-time graphical display of noise levels permitted instantaneous monitoring of cultural, air traffic, vehicle traffic noise, cable-to-ground leakage, and geophone plant quality. After each geophone was planted it was tested to insure a cable-to-ground resistance greater than 1000K ohms and an individual geophone continuity of 500 ohms ($\pm$20 ohms). As well, each geophone underwent a modified tap and twist test. No shot was recorded if background noise voltage levels on active geophones was greater than 0.05 mV. The ability of the seismograph to real-time monitor noise levels, signal quality (through digital filtering), and unacceptable geophone plants and the roll-switch's built-in earth leakage and continuity meters minimized the chances a recorded shot would not be maximized for the site and equipment.

Data Processing

Data from this study were processed on an Intel Pentium-based micro-computer using $WinSeis$, a set of commercially available algorithms. Display parameters were determined based on scale of existing data sets, optimum exaggerations, and workable formats. During this study, the only operations or processes used were those that enhanced the signal-to-noise ratio and/or resolution potential as determined through evaluation of high confidence reflections identified directly on field files.

The primary intent of a walkaway noise test is to allow the comparison of various source, receiver, and instrument settings and configurations as they relate to overall improvements in the signal-to-noise ratio and frequency content. Walkaway tests are ideally suited to the identification of individual events within the full wave field. Phase velocity and wave types are a couple of the most important pieces of information extractable from walkaways. The relationship of velocity and wave type to spread geometries and offsets needs to be completely analyzed and understood for acquisition parameters and equipment to be optimized (Pullan and Hunter, 1985). Assumptions or partial analysis of these key properties could result in artifacts or improperly recorded data. Processing of walkaway data for this study was limited to trace organizing, gain balancing, and digital filtering. Walkaway data from each source configuration or comparison parameter are displayed in a source-to-receiver offset order (Appendix A).

For most basic shallow high-resolution seismic reflection data, CDP processing steps are a simple scaled-down version of established petroleum-based processing techniques and methods (Yilmaz, 1987; Steeples and Miller, 1990). CDP data presented in this report followed a processing flow similar to those used for routine petroleum exploration (Table 1). The main distinctions relate to the conservative use and application of correlation statics, precision required during velocity and spectral analysis, two-stage NMO correction, f-k filter to remove wide angle reflections, and the accuracy of the muting operations. A very low (by conventional standards) allowable NMO stretch (< 20%) was extremely critical in minimizing contributions from the very shallow reflected energy at offsets significantly beyond the critical angle. Limiting wavelet stretch through muting maximizes resolution potential and minimizes distortion in the stacked wavelets (Miller, 1992). Processing/processes used on this data have been carefully executed with no *a priori* assumptions. Extreme care was taken to enhance through processing only what can be identified on shot gathers and not to create coherency on stacked sections.

Some basic petroleum processing techniques make assumptions that are violated by most shallow reflection data sets. Applying these processes could dramatically reduce data quality or worse, generate artifacts. Particular processes, such as deconvolution and some forms of trim statics, assume large numbers of reflections with a random reflectivity sequence and a broad range of reflection frequencies (Yilmaz, 1987). Migration is another process that, due to non-conventional scaling, many times appears to be necessary when in actuality geometric distortion may be a simple scale exaggeration (Black et al., 1994). The low-pass nature and

Table 1
Processing flow

Primary Processing
format from SEG2 to KGSEGY
preliminary editing (automatic bad trace edit with 10 msec noise window)
trace balancing (150 msec window)
digital filtering (bandpass 25-50 250-375)
spectral balance
first arrival muting (direct wave and refraction)
surgical muting (removal of ground roll based on trace-by-trace arrival)
assign geometries (input source and receiver locations)
elevation correction to multiple, floating datums
sort into CDPs (re-order traces in common midpoints)
velocity analysis (whole data set analysis on 100 ft/sec increments)
spectral analysis (frequency vs amplitude plots)
NMO correction (station dependent ranging from 1350 to 3,500 ft/sec)
correlation statics (2 msec max shift, 7 pilot traces, 100 msec window)
digital filtering (bandpass 25-50 250-375)
secondary editing (manual review and removal of bad or noisy traces)
CDP stack
amplitude normalization (whole trace with 40 msec delay)
correct to flat datum (48 ft above sea level)
display

Secondary Processing
f-k filtering
f-k migration

deconvolution (spiking and second zero crossing)

coherency enhancing tendency of f-k migration improved the geometric accuracy and confidence in interpreted CDP stacked sections displayed in this report. Consistency in arrival and apparent orientation of individual reflections after each process was critical to ensuring the authenticity of final interpretations.

Results — Walkaways and Downhole Analysis

Unequivocal identification and verification of reflections on shot gathers is not only necessary, it is mandatory for meaningful interpretations of shallow seismic data. Matching modeled NMO curves based on borehole velocity information with reflection hyperbola interpreted on shot gathers is the most conclusive means to both verify and analyze reflections. This combination incorporates ground truth (borehole velocity), geometric curve fitting (forward and inverse modeling), and event identification directly from single-fold shot gather data. Too many times the power of seismic processing software and lack of careful attention to

detail results in stacked seismic reflection data that inaccurately represents the sub-surface and are justified based on consistency with existing drill data and geologists' models.

As spelled out in the proposal for this work, the testing and verification of interpretations will be a top priority. Data from this project goes through rigorous verification techniques that include modeling (both forward and reverse), step-by-step event verification, cross comparisons of borehole and surface seismic, and interpretations on CDP stacks that incorporate shot gather interpretations.

Downhole velocity data acquired by lowering a single hydrophone to specific depths and then measuring the time it takes an acoustic wave to travel from the ground surface to that point in the subsurface provided valuable ground truth, comparison of true average velocity against curve matched moveout velocities, and assistance interpreting reflections easily identifiable on shot gathers. The downhole survey was acquired in observation well D-13. The piezometric surface at the time of the survey was about 17 ft from ground surface. Due to the characteristics of this particular hydrophone, about 8 ft of head was necessary for the hydrophone to respond according to specifications. Data were acquired at both 10 ft and 50 ft offsets from the well head (Figure 3). Closer offset data is generally preferred, but in the event the casing/grout provides a seismic response, tube wave energy overpowers the reflected or direct arrivals, or the near surface around the well has been altered and corrupts the data, the longer offset data allows verification or cross-checking.

Based on the downhole survey (Figure 3) and the interpretation of borehole (D-13) geology, the following is the most likely reflection (time) to reflector (depth) correlation (Figure 4):

time	depth	geologic contact
30 msec	= 15 to 20 ft	Top of water table (piezometric surface)
41 msec	= 38 ft	Top of clayey silt
43 msec	= 46 ft	Top of clay
60 msec	= 100 ft	Bedrock surface (St. Petersburg Sandstone)

The average velocity as determined from the borehole acoustic survey increased rapidly with depth. The average velocity from ground surface to 25 ft was around 1400 ft/sec, 65 ft to the ground surface 2,500 ft/sec, and the average from ground surface to 100 ft was measured to be about 3,300 ft/sec. An average interval velocity of 5,100 ft/sec was measured between 25 and 65 ft and is consistent with saturated unconsolidated sands/gravels. Between 65 ft and 100 ft, however, the average

uphole survey

source offset = 10 ft source offset = 50 ft
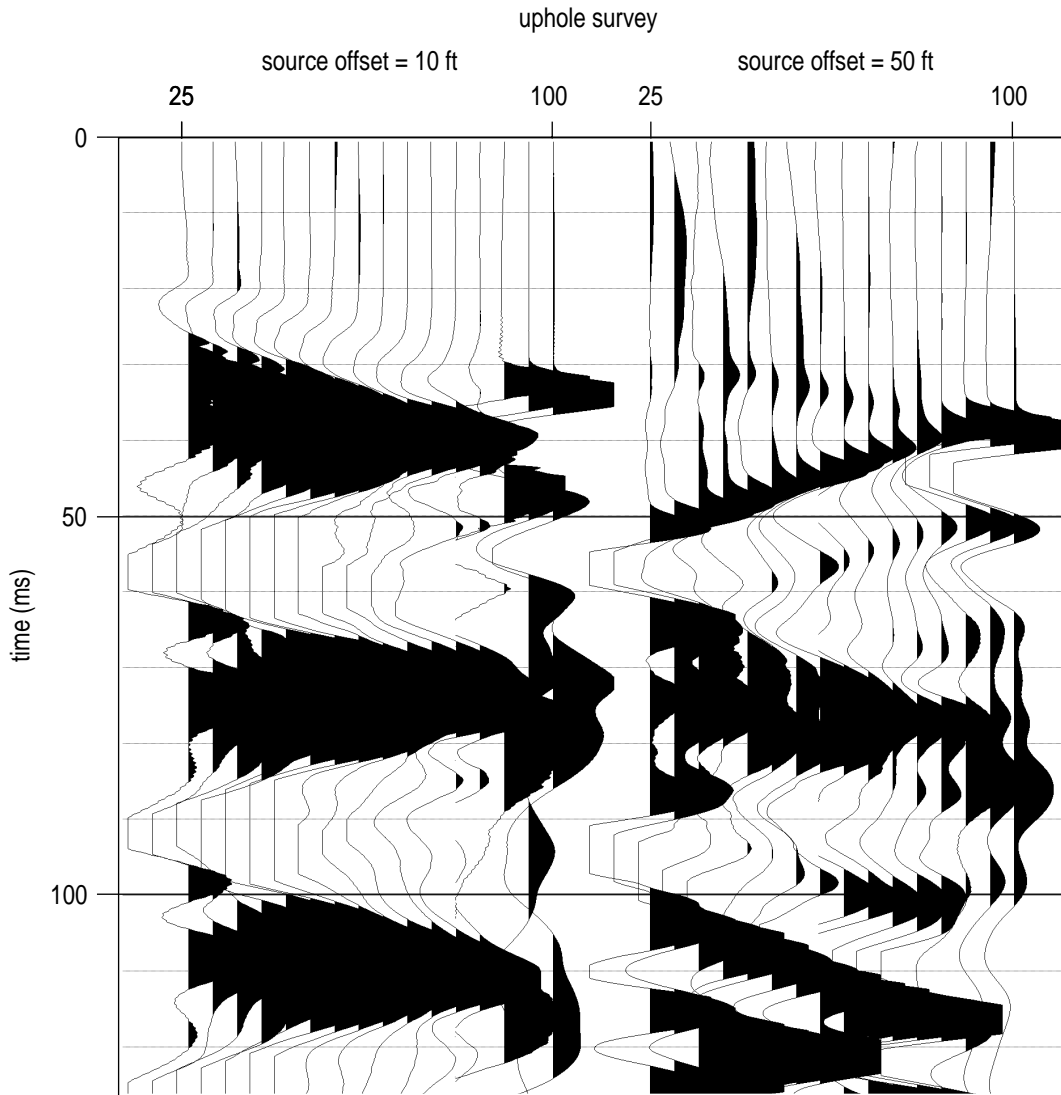
average velocity from surface to 25 ft $\dfrac{25}{0.018}$ $\dfrac{ft}{sec}$ ≅ 1,400 ft/sec

average velocity from surface to 65 ft $\dfrac{65}{0.0258}$ $\dfrac{ft}{sec}$ ≅ 2,500 ft/sec

average velocity from surface to 100 ft $\dfrac{100}{0.03}$ $\dfrac{ft}{sec}$ ≅ 3,300 ft/sec

average interval velocity from 25 to 65 ft $\dfrac{40}{0.078}$ $\dfrac{ft}{sec}$ ≅ 5,100 ft/sec

average interval velocity from 65 to 100 ft $\dfrac{35}{0.0042}$ $\dfrac{ft}{sec}$ ≅ 8,300 ft/sec

Figure 3. Uphole velocity survey using a sledge hammer and hydrophone. Two source offsets were used to insure tube wave arrivals could be distinguished. Interval and average velocities are calculated.
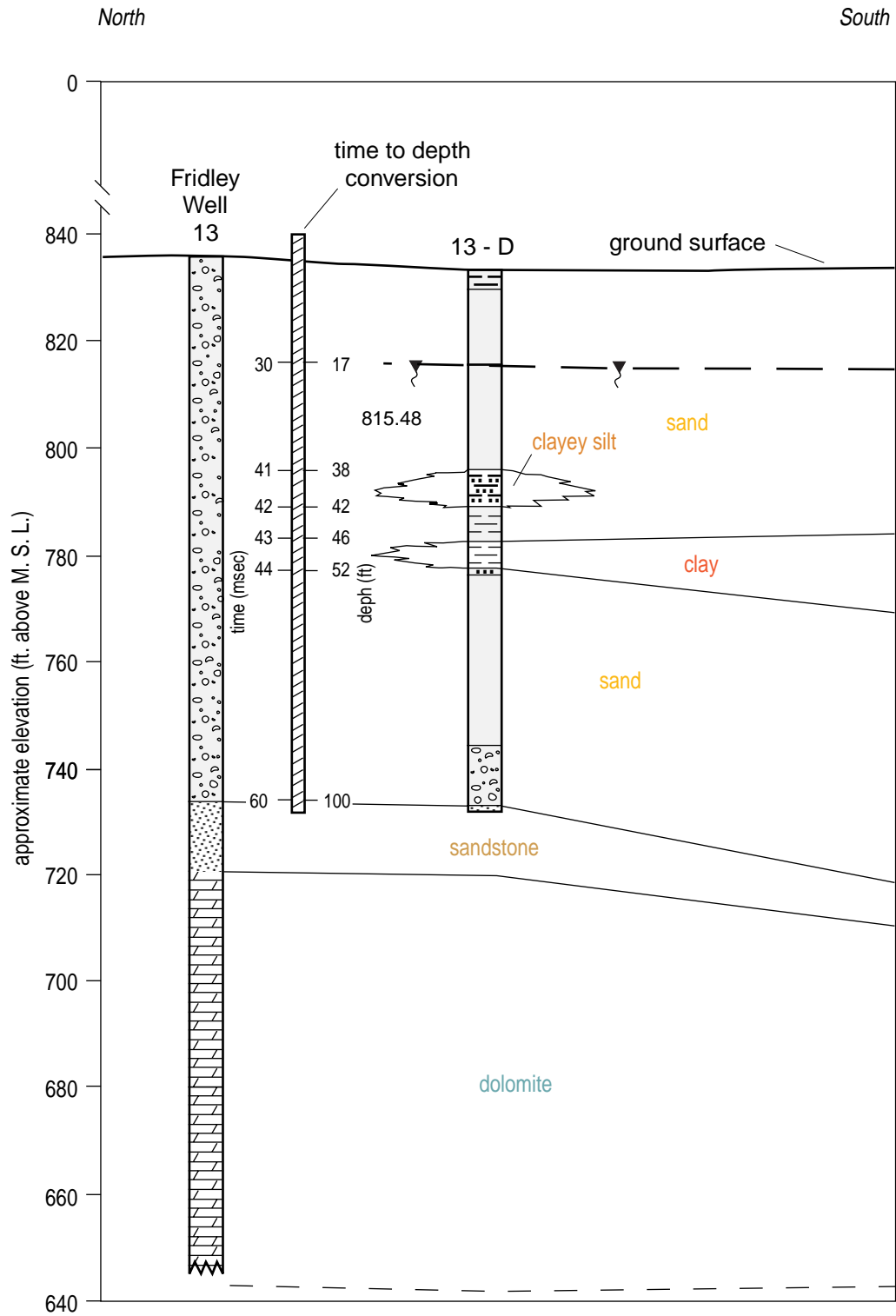
Figure 4a. Two-way time-to-depth correlations from uphole survey and borehole-interpreted geology.

sand with gravel		lean clay
dolomite		sandy clay
sandstone		sandy silt
sand		clayey silt

sand

clayey silt

clay

sandstone

dolomite

existing ground surface

statigraphic boundary

inferred statigraphic boundary

water table (12/4/93)
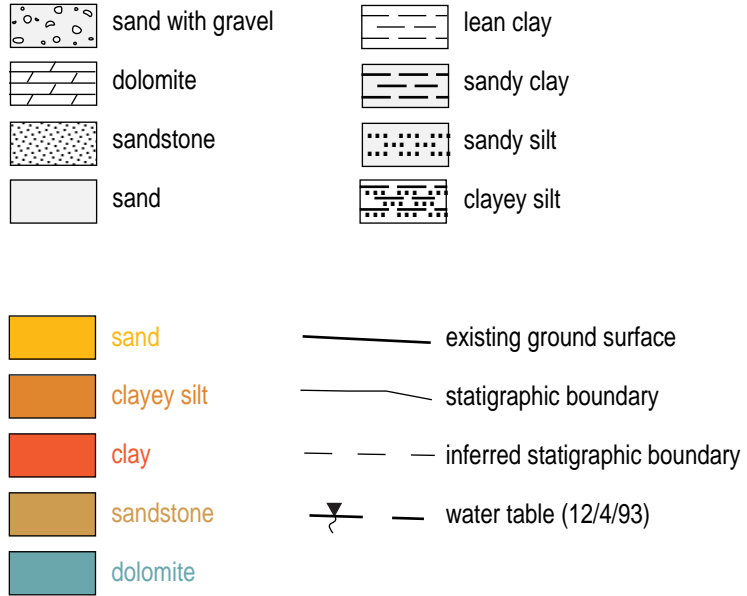
Figure 4b.

velocity increases dramatically to around 8,300 ft/sec and is likely the result of increased clay/silt or till concentrations. Time-to-depth conversions were based on average velocity values determined using first arrival interpretations made on downhole data (Figure 3).

The walkaway shot gathers possess high signal-to-noise ratio reflection data and demonstrate the obvious variability in data characteristics with changes in acquisition equipment and site conditions (Appendix A). Changes in the data characteristics exemplify the need for a good testing program prior to execution of a survey such as the one planned here and also demonstrates the need to have a sizable repertoire of acquisition equipment available for testing. Any reflection program needs to be tuned for the acoustic and logistical conditions at a particular site.

Comparing the three sources tested at walkaway site #1, the downhole 30.06 possesses the highest signal-to-noise and resolution potential. The predominant negative characteristics of the sledge hammer was the ratio of air coupled wave to reflection energy, the potential for inconsistent source energy, variable surface coupling, and the slight degradation of resolution potential due to vertical stacking. The auger gun was more energetic but possessed a lower reflection frequency band-width. The decrease in reflection frequencies is likely a result of the higher level of energy released (Knapp and Steeples, 1986). When comparing the 30.06 data to either sledge hammer or auger gun data, it is evident the digitally filtered downhole 30.06 data possess a higher upper corner frequency in the reflection bandwidth, higher dominant frequency, and more minimum phase wavelet characteristics.

Results — CDP Stacked Sections

Shallow seismic reflection is a method that lends itself to over-processing, inappropriate processing, and minimal involvement processing. Interpretations must take into consideration not only the geologic information available but also each step of the processing flow and the presence of reflection events on raw unprocessed data. Identification and confirmation of reflection hyperbola on walkaway noise tests is essential and best accomplished through mathematical curve fitting, match to borehole-derived velocity structure, and observation of file-to-file consistency. Walkaway noise tests are designed so the subsurface is over-sampled horizontally and the source-to-farthest-offset is about twice the depth of interest. This allows all aspects of the complete wave field (especially the reflections) to be thoroughly appraised.

Modeling reflection arrivals as interpreted on shot gathers is not only critical, it should be required by law. Too many times seismic data will magically go from QC plots quickly provided for viewing in the field with hand waving interpretations to CDP stacked section with lots of color. Even more amazing, the seismically interpreted geologic section matches perfectly the conceptual picture provided prior to commencing the seismic survey. The only way to have confidence in a processed and interpreted CDP stacked section is to follow reflections from shot gathers to stacked section along each step of the processing flow.

Shot gathers recorded during the acquisition of the CDP profile along the western perimeter fence clearly possess several interpretable reflection arrivals (Figure 5). The data were recorded end-on, symmetric split spread, and asymmetric split-spread. Arrival time and optimum source-to-receiver offset of reflection events interpreted during acquisition dictated which field geometry was selected. The proof of authenticity of coherent events interpreted as reflections on CDP stacked sections is directly related to how well they correlate to reflections observed on shot gathers and model-verified from downhole velocity data. Reflections on field files from this site possess dominant frequencies ranging from about 180 Hz for the shallowest coherent reflection to over 300 Hz for the reflection at about 70 msec on shot gather (B) (Figure 5). With dominant reflection frequencies ranging from 180 to 250 Hz depending on reflector depth, the vertical resolution potential is about 4 to 5 ft and the horizontal is around 15 ft at 50 ft of depth. The resolution potential of this survey and any seismic survey should be and generally is used as a guide for evaluating whether the technique has the potential to effectively image the target(s) of interest.

For this data set, downhole velocity data were used to produce synthetic reflection curves and arrival times for each significant interface (Figure 6). After studying these curves it becomes painfully obvious that this data set cannot be processed using standard processing flows designed to flatten reflection curves and mute overstretched wavelets in a single pass. If the 1150 ft/sec reflection at about 35 msec is moved out as part of an accurate time varying velocity function which included the 3400 ft/sec bedrock reflection, everything arriving before the direct wave would be muted. This would include all reflections within the optimum window for depths from about 70 to 150 ft.

Specialty processing flows were developed to insure the stacked data was truly representative of reflections observed on field files (Figure 5). The extreme range of velocities over this very small depth interval required near traces to be corrected for

source-to-receiver offset (ft)
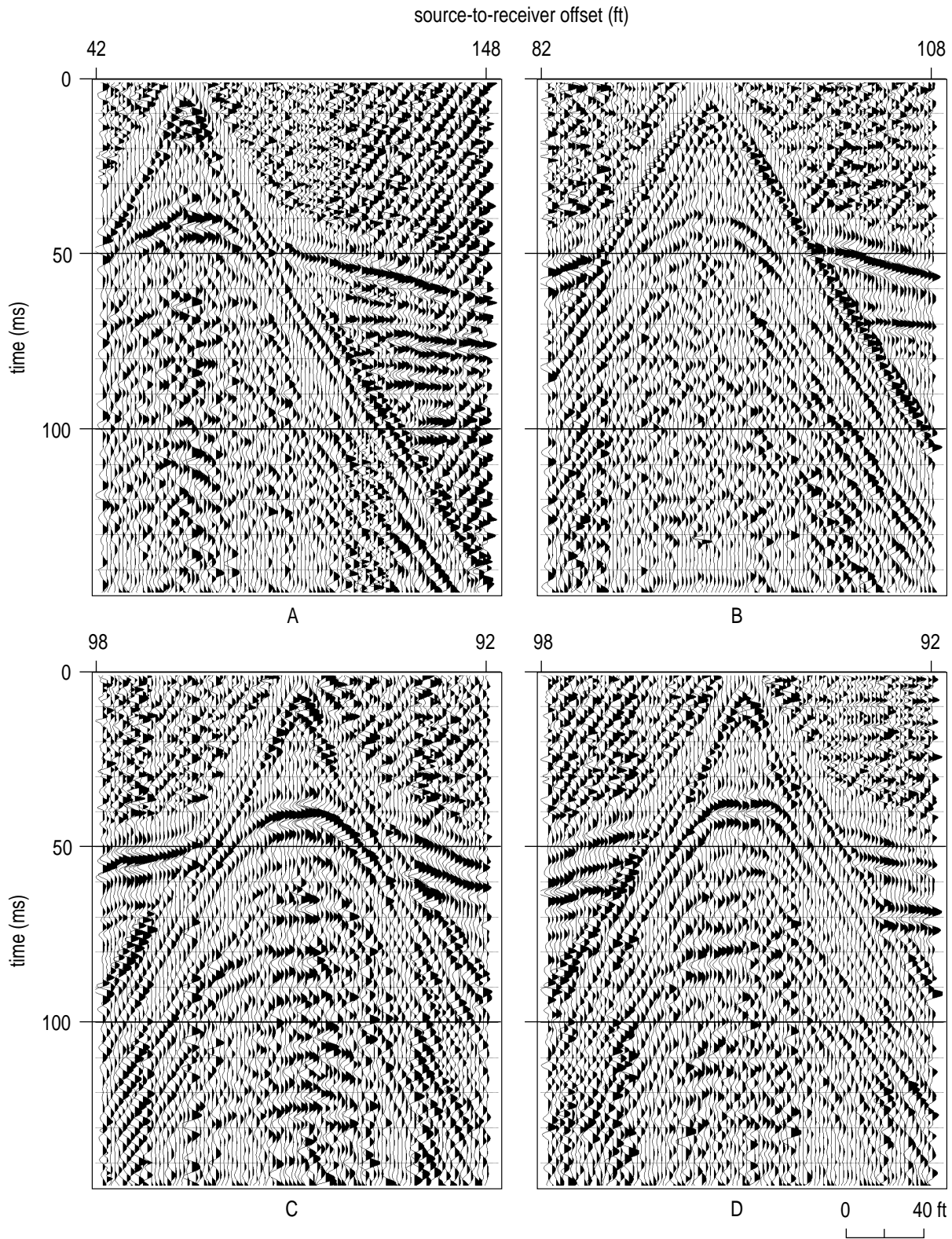
Figure 5. Digitally filtered (spectral balanced) shot gathers from along line 1. Source/receiver geometries included symmetric and asymmetric split spreads. Reflection arrivals are easily interpretable on all four shot gathers.

source-to-receiver offset (m)

A
Vnmo = 1250 ft/sec   To = 33 msec

B
Vnmo = 1850 ft/sec   To = 41 msec

C
Vnmo = 2360 ft/sec   To = 44 msec

D
Vnmo = 7000 ft/sec   To = 85 msec

E
Vnmo = 6000 ft/sec   To = 66 msec

F
Vnmo = 3400 ft/sec   To = 57 msec

0   40 ft
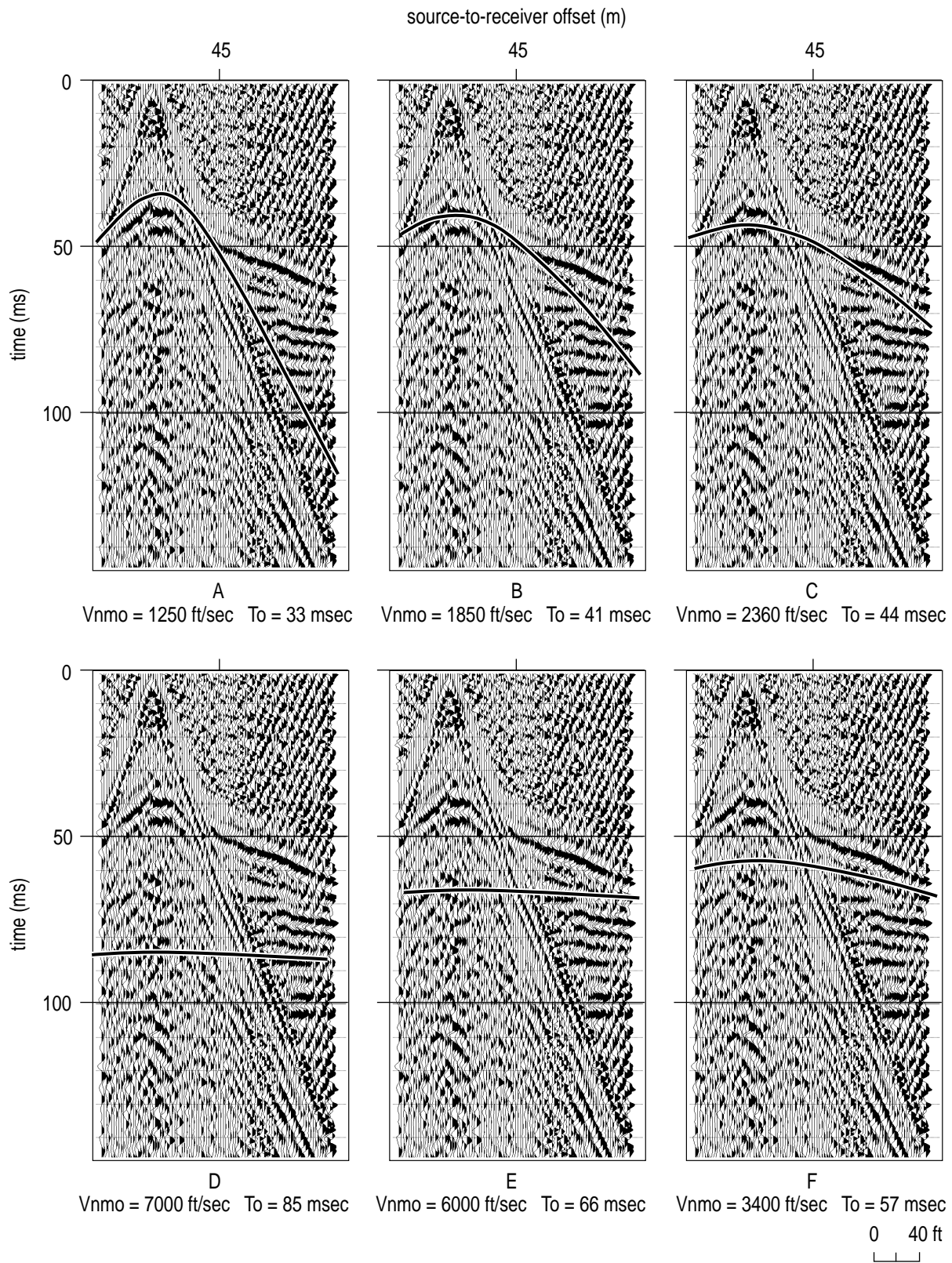
Figure 6. Selected shot gathers with six different normal moveout velocity curves overlaying the
filtered data. Indicated velocities and curves selected based on uphole velocity survey.

non-vertical incidence separately from the far traces and then rejoined as a single data set. To effectively stack the shallowest reflection, the direct wave and wide angle reflections from that shallow layer were removed with a very narrow slice f-k filter (Figure 7). Without this extra step, or not recognizing the necessity of this extra step, a bogus interpretation would have resulted. This data area is unusual with respect to the velocity gradient between about 10 ft (just above the water table) and just below the bedrock surface. If a "standard" or even a "shallow reflection modified" processing flow were used on this data, interpretations on a stacked section would be incorrect and consist of stacked coherent artifacts or ground roll.

The water table is commonly used as a guide for making near-surface static corrections (Hunter et al., 1984) since it can generally be assumed the piezometric surface is flat. In this data the shallowest reflection which is from a depth reasonably close to the water table fluctuates relatively severely, with no apparent mirrored movements in deeper events. This implies the undulations are not related to near-surface static and therefore the reflector must have true structure represented by these undulations. The characteristics of this shallow event have lead to the conclusion that it is not a direct reflection from the piezometric surface but likely a reflection from a saturated clay at or near the piezometric surface.

Two criteria are used to classify this reflection as from a saturated clay and not water table: 1) arrival time and velocity does not have a real good correlation to the borehole velocity, and 2) observed variability in reflection depth with little or no change in stacking velocity would require an excessive amount of variability in the piezometric surface. Interpreting this event as the clay requires file-by-file analysis of the unstacked data. There are places across line 1 where these the wavelet (doublet) diverges (CDPs 340, 770, and 1390, to name a few), which is a characteristic of variable degrees of bed tuning (Miller et al., 1995). This diverging implies that this wavelet likely contains information from more than one reflecting interface. These places are likely candidates for bed thickening and don't necessarily indicate truncation or erosional channels.

The three CDP profiles were collected in areas with the highest concentration of monitor wells and borings, the least amount of cultural noise, and the greatest potential to enhance characterization of the near-surface at this site (Figure 8). The near-surface provided good source and receiver coupling along the west perimeter fence. The primary obstacles and noise sources along line 1 included traffic on East River road, three vehicle access roads, noise from activities within the facility, power lines, a gopher colony, and intermittent rain. The moisture conditions in the

source-to-receiver offset (ft)
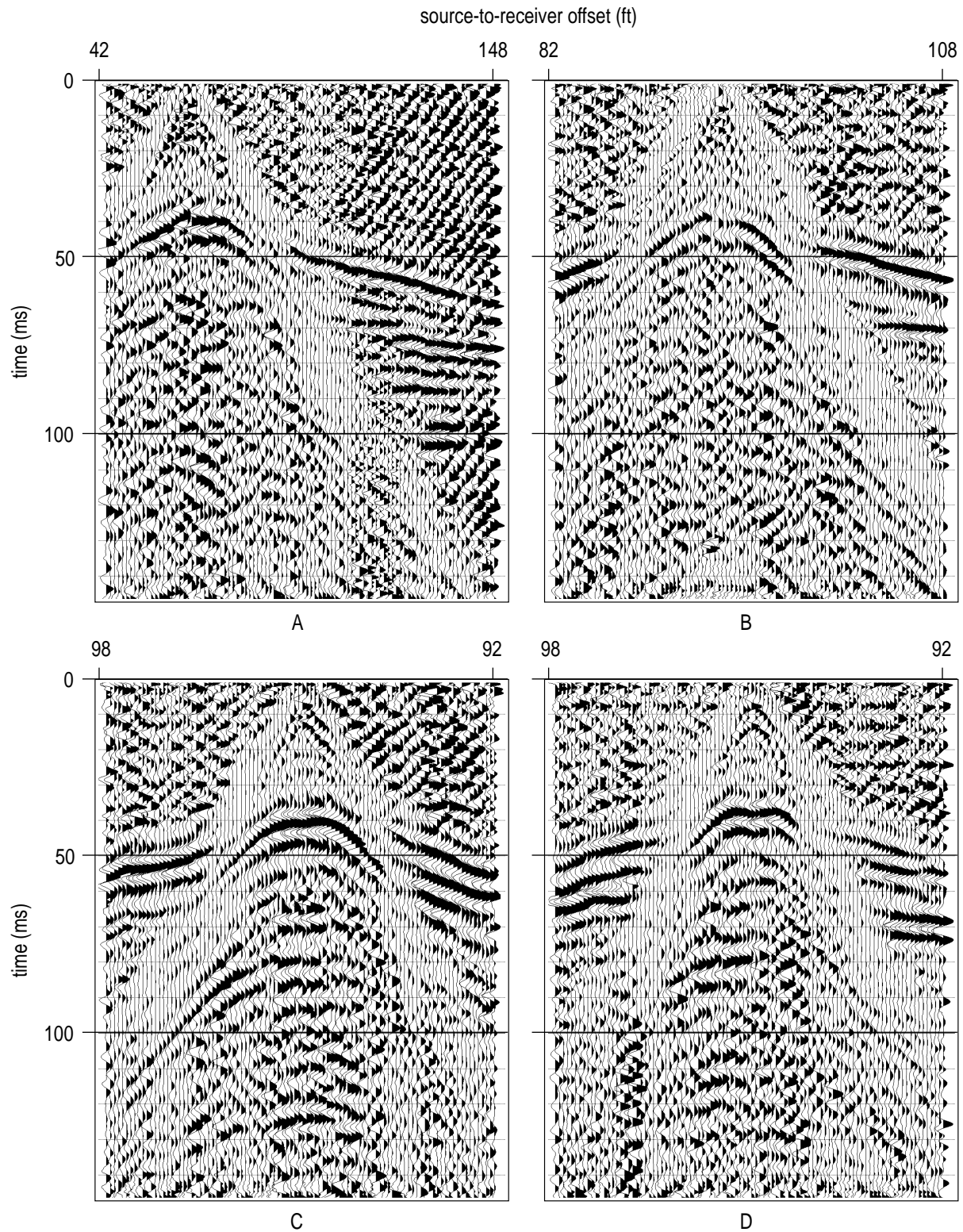
Figure 7. Results of the application of an f-k filter to digitally filtered data. The f-k filter was designed to remove the long offset portion of the shallowest reflection curve and the air-coupled wave.

line 1

12-D

13-D

180

line 2

1575 1553

1660

1740

2-PC

1838

AT-4

NIROI

4-PC

700

1120
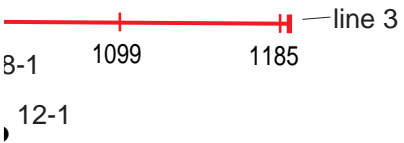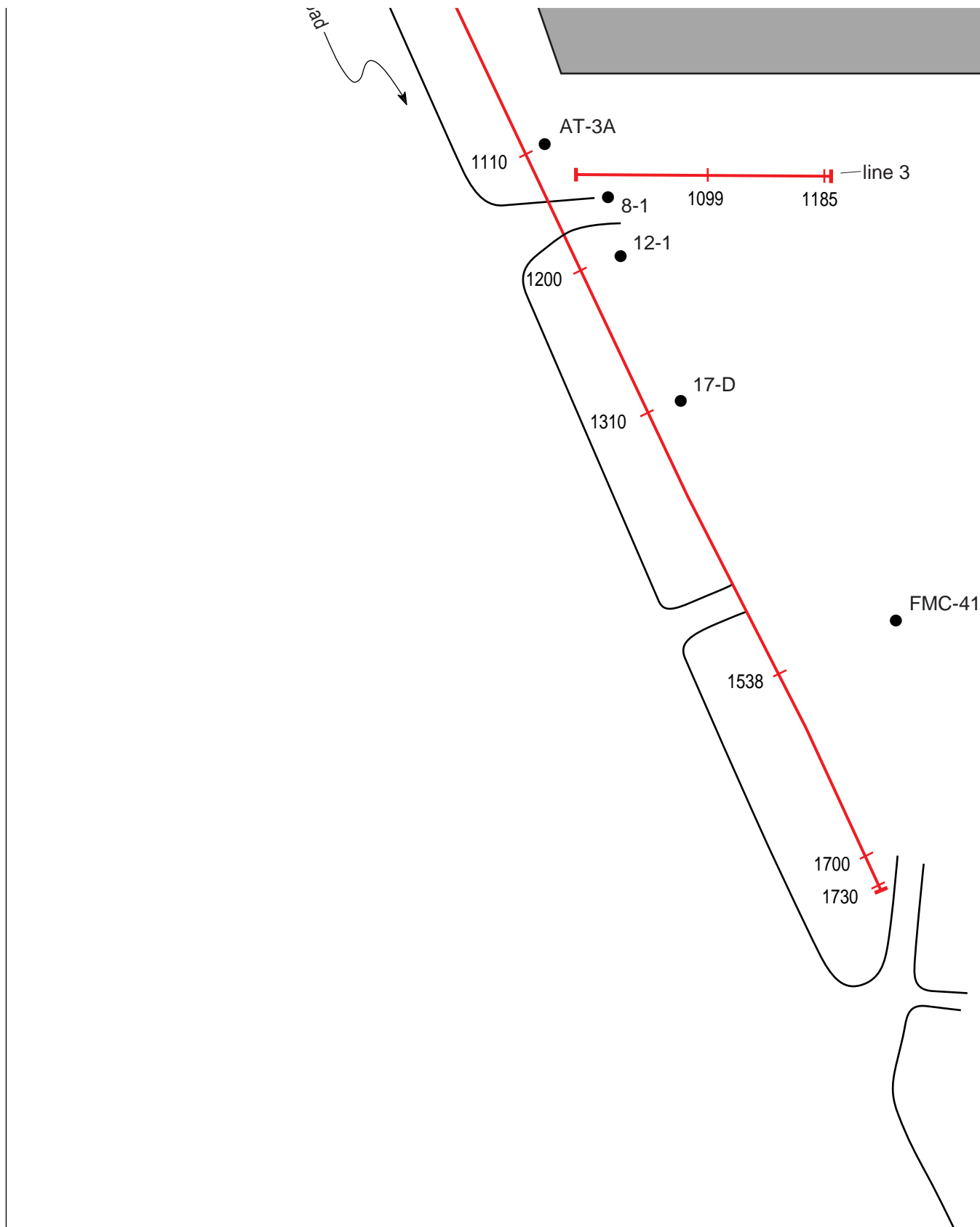seismic line and station number

FMC-31   well number and location
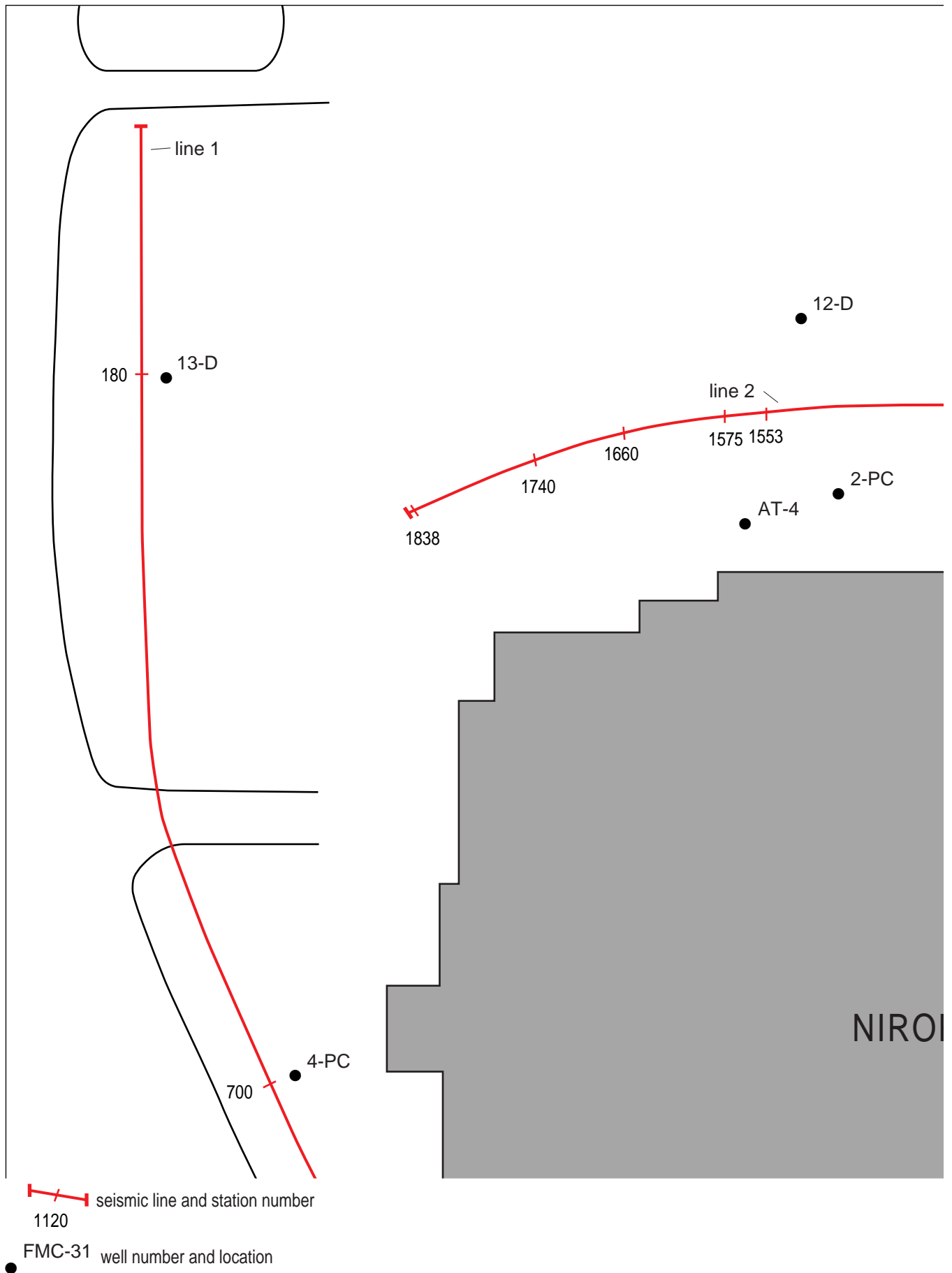
Figure 8a. Detailed site map of U.S. Navy Northern Ordnance Plant, Fridley, Minnesota, showing approximate station numbers of CDP profiles relative to the facility and nearby wells.
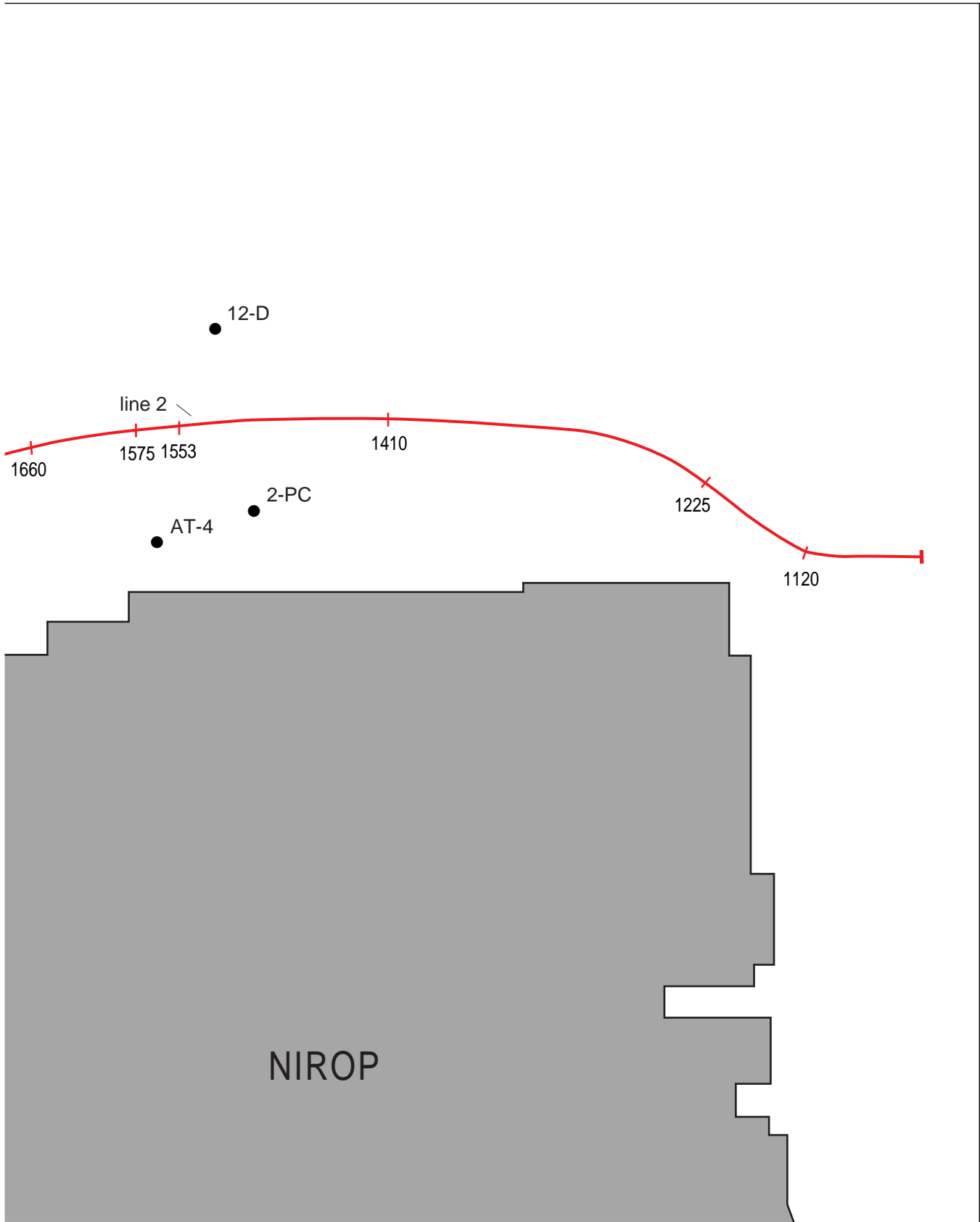
12-D

line 2

1575 1553

1660

1410

2-PC

AT-4

1225

1120

NIROP

1120 seismic line and station number

FMC-31 well number and location

Figure 8b.

NIROI

4-PC

700

East River Road

AT-2
6-D

930
940

AT-3A

1110

line 3

1099   1185

8-1

12-1

1200

17-D

1310

FMC-41

1538

seismic line and station number

1120

FMC-31   well number and location

Figure 8c.

NIROP

line 3

3-1   1099   1185

12-1

17-D

FMC-41

1538

seismic line and station number
1120

FMC-31 well number and location

Figure 8d.

AT-3A

1110

road

line 3

1099   1185

8-1

12-1

1200

17-D

1310

FMC-41

1538

1700

1730
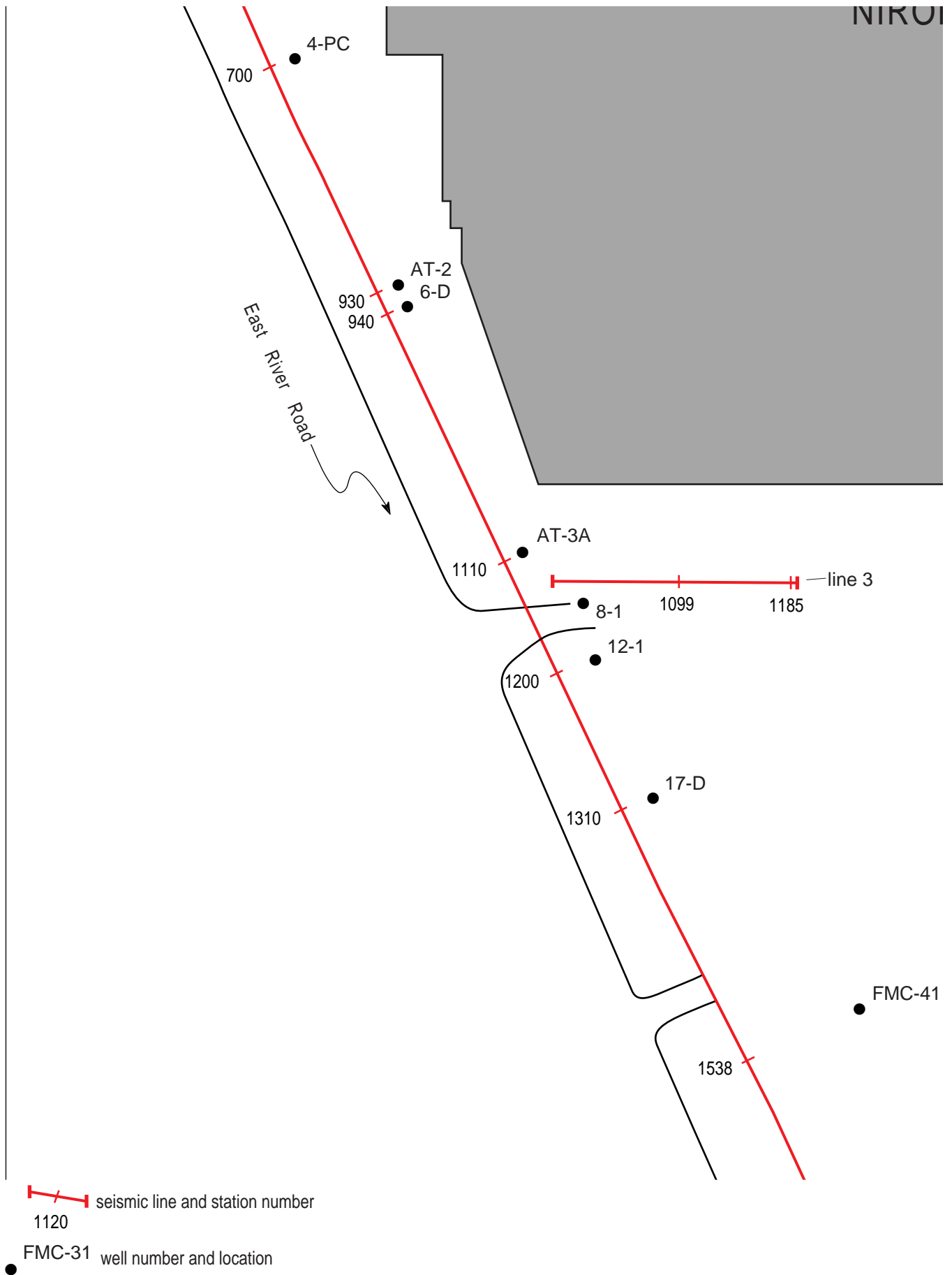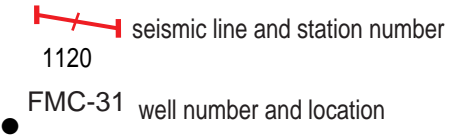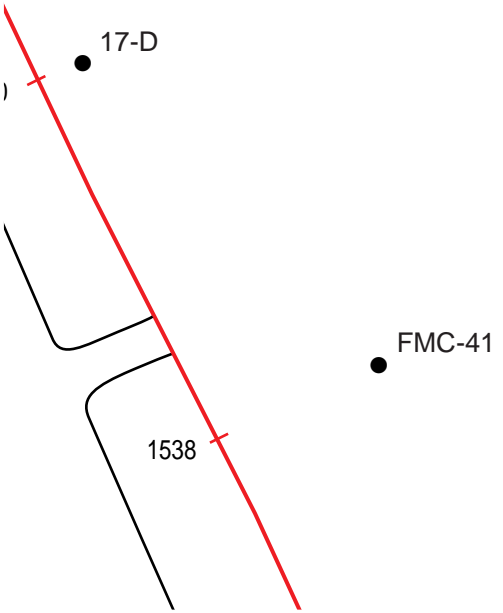
seismic line and station number

1120

FMC-31   well number and location

Figure 8e.

line 3

3-1   1099   1185

12-1

17-D

FMC-41

1538

1700   FMC-31

1730

N
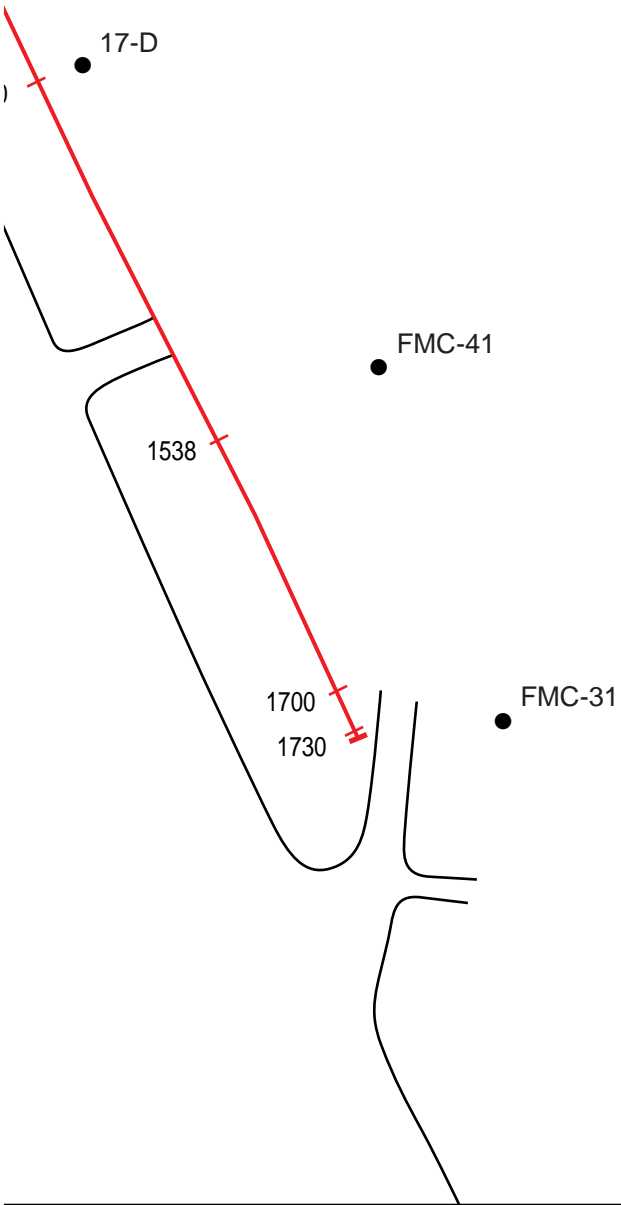
seismic line and station number

1120

FMC-31   well number and location

0   200 ft

Figure 8f.

near-surface were outstanding for seismic data acquisition. Data quality along line 1 varied from fair to excellent with no area sufficiently undersampled or poorly sampled to adversely effect the interpretation of the data. Lines 2 and 3 were collected during a second trip to the site when the near-surface conditions and weather were not as favorable. Line 2 is an east/west line collected along the southern extreme of the North 40. The line crossed areas with near-surface materials recently altered as part of environmental restoration activities. Even with these unfavorable near-surface conditions the data quality was better than expected. Line 3 is a west/east line that was acquired to explore the three-dimensional nature of the reflection events identified on the CDP stack of line 1 near the north parking lot entrance to the FMC portion of the facility. The data were collected in a grass strip between asphalt drives. Data quality was quite good on the west end of the line but diminished to the east as changes in the source-receiver geometry occurred to avoid the asphalt drives.

The number and diversity of the reflections evident on the CDP stacked section of line 1 is suggestive of several different episodes of material deposition (Figure 9). Many of the wells used to help interpret this seismic section are slightly off-line, but are close enough to assist with correlation of reflections to reflectors. The bedrock reflection is interpreted with a high degree of confidence. The correlation to borings is excellent with sub-bedrock reflectors interpretable in several places along the line. The focus of the acquisition geometry was to image reflectors between water table and bedrock. Therefore, in some places reflections from interfaces deeper than the bedrock surface are evident but delineating them across the section or to depths greater than a couple hundred feet is not possible with this data set. The potential quality of a stacked section focusing on sub-bedrock layers is best demonstrated through observations of field files at the beginning of the line where the longest source to receiver offsets were recorded.

The bedrock reflection clearly changes characteristics across line 1. This change in wavelet character seems to be fairly consistent with changes in the bedrock surface from sandstone to dolomite as indicated on drill data. The downhole survey collected in well 13-D and the stacking velocity determined from analysis of the seismic data places the bedrock reflection at a two-way travel time of 60 msec around station 185. The bedrock is interpreted in yellow across the entire section regardless of suggested changes in lithology of the bedrock surface (Figure 10). The bedrock reflection is interpreted with some degree of confidence across the entire stacked section.
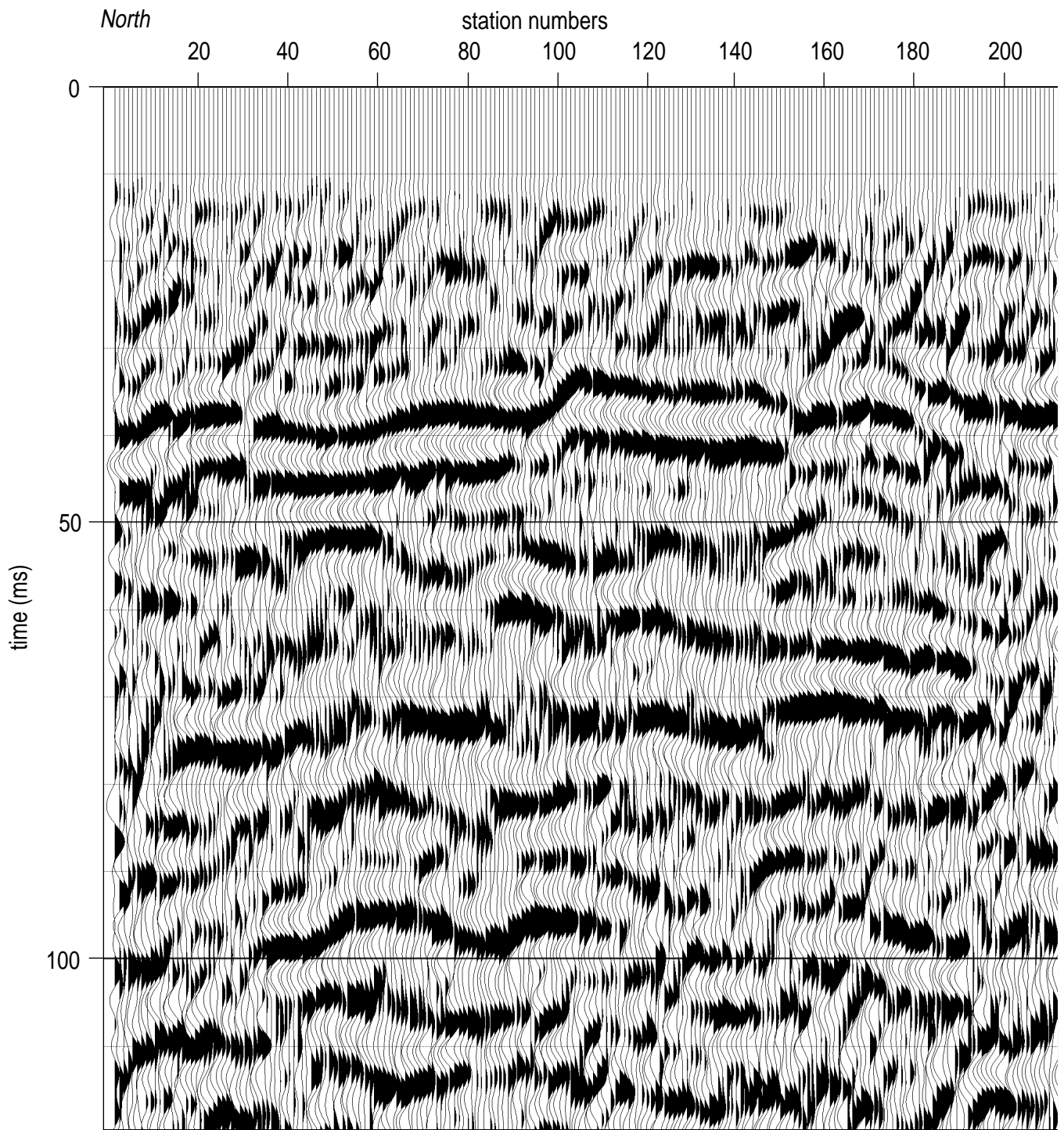
Figure 9a. CDP stacked section of line 1 along East River Road. Display scale designed to be consistent with display parameters of other engineering reports from this site.
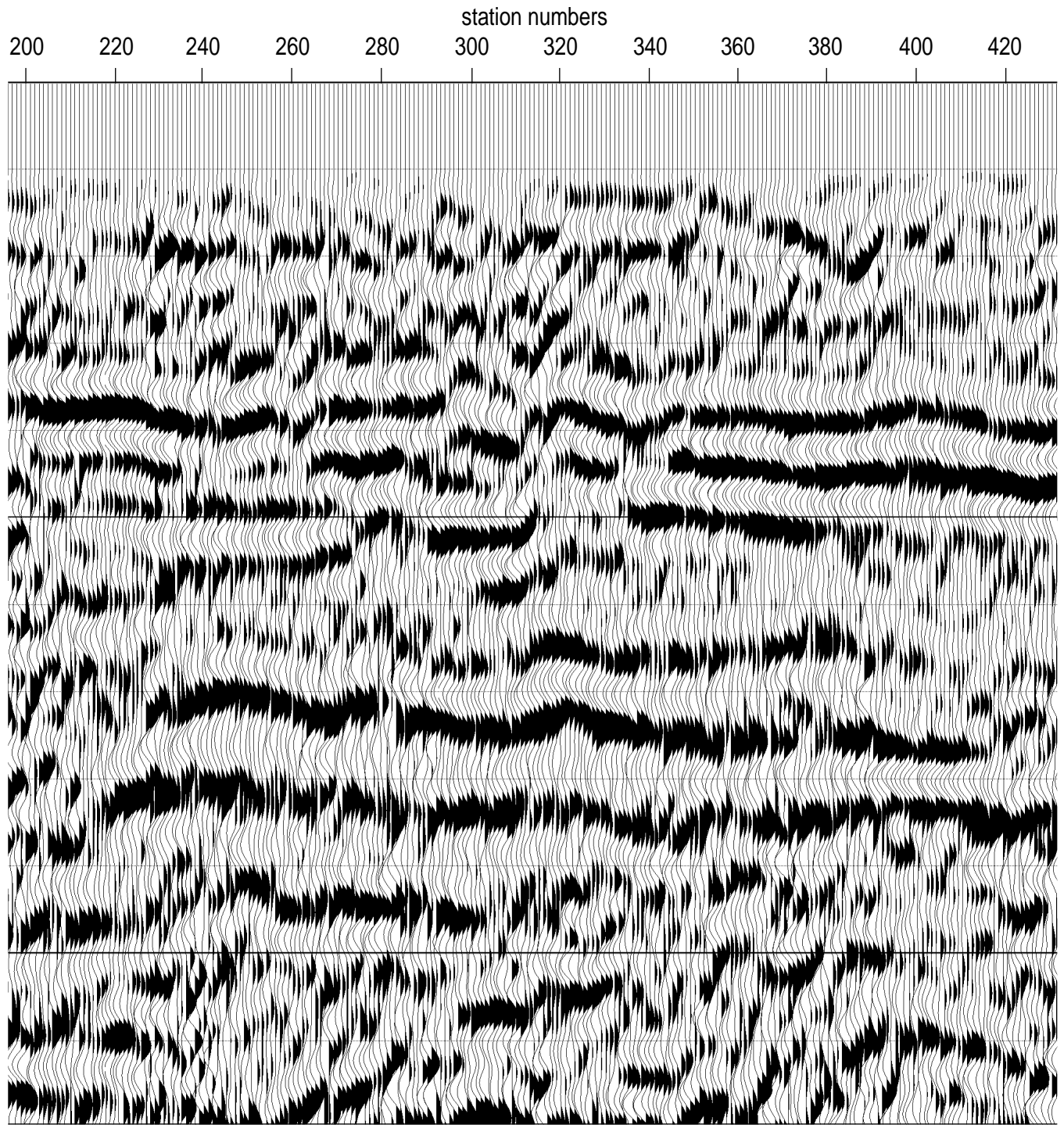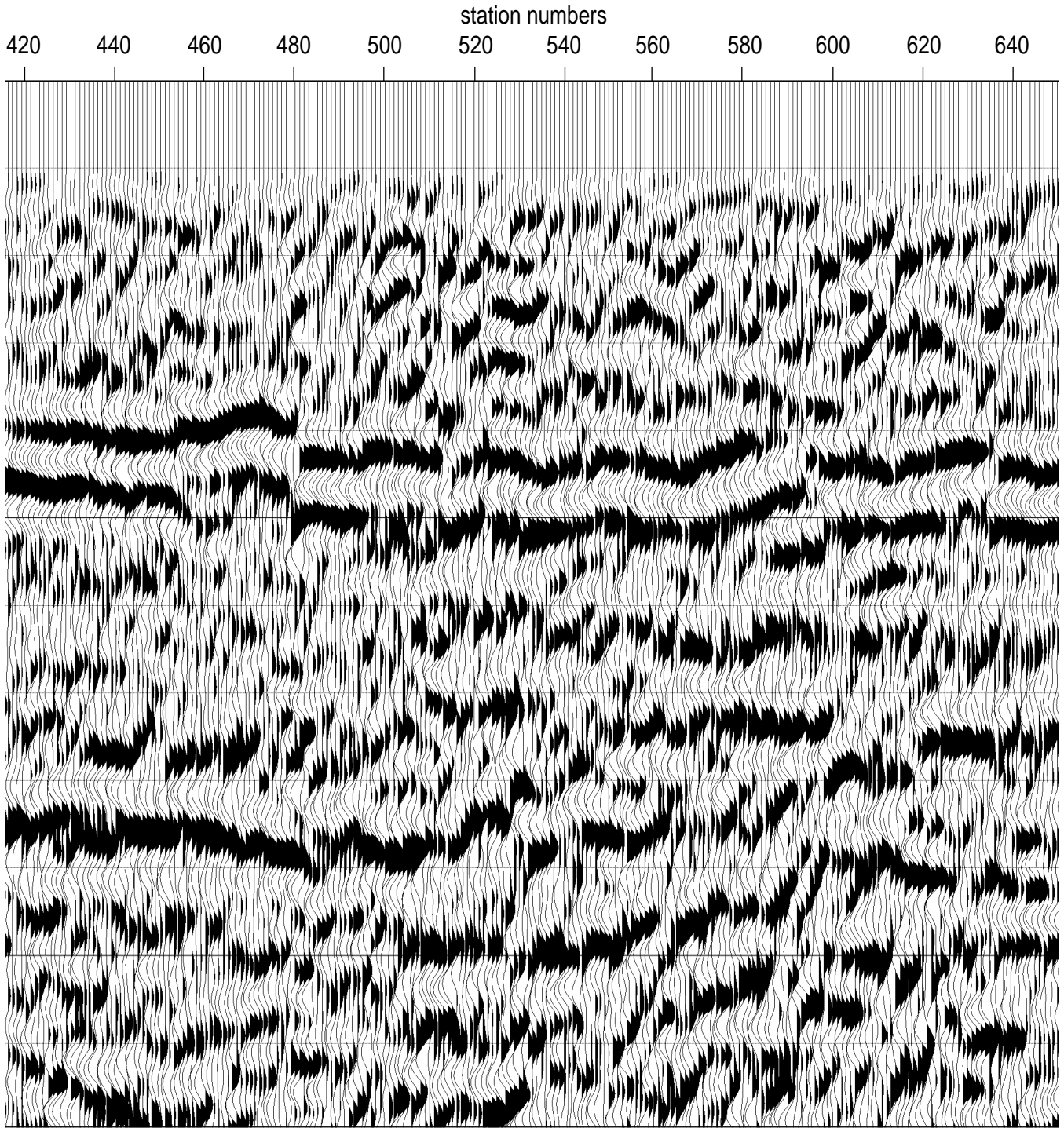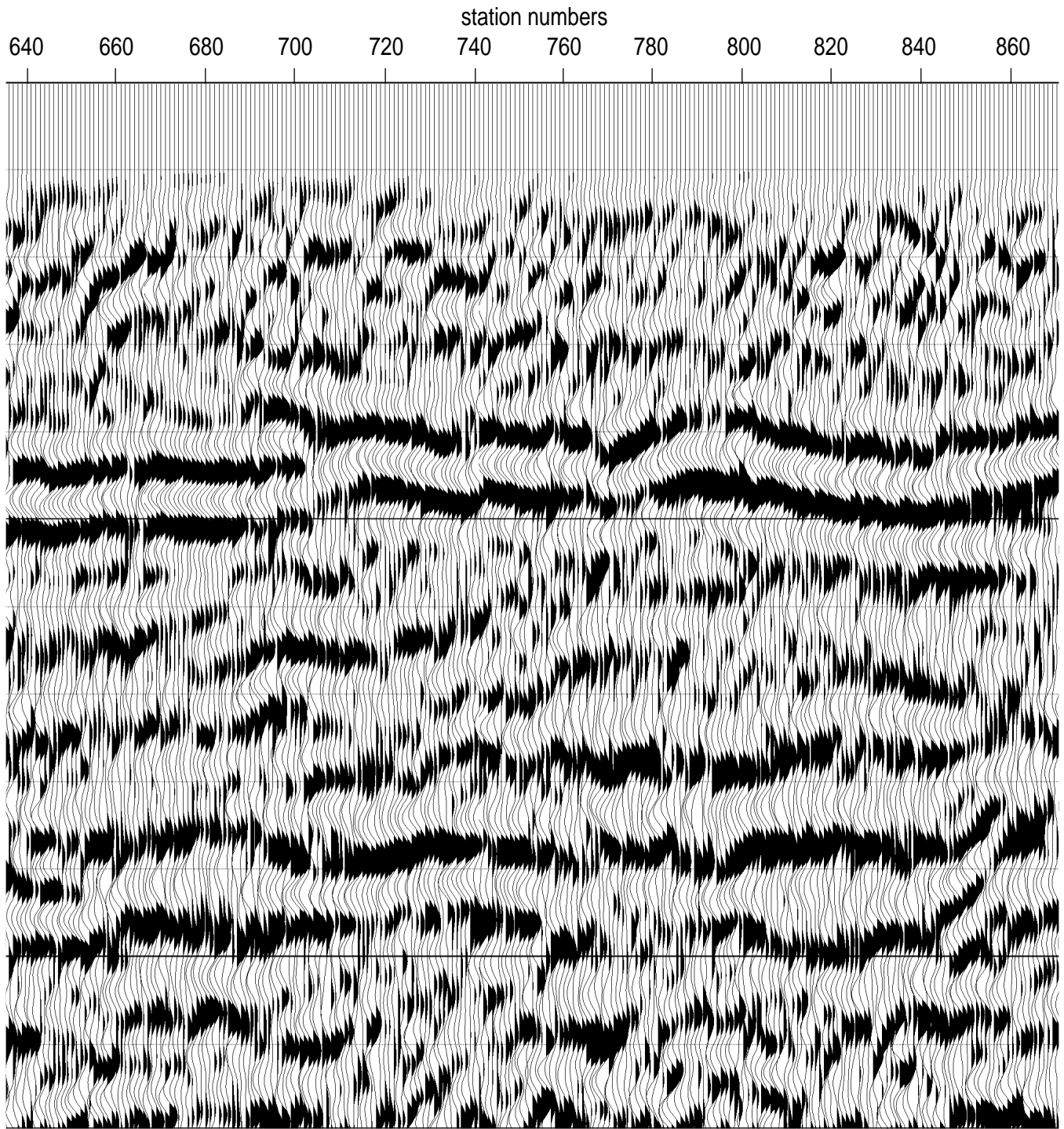
station numbers

Figure 9b.

station numbers

Figure 9c.

station numbers

Figure 9d.

station numbers

Figure 9e.

station numbers

1080 1100 1120 1140 1160 1180 1200 1220 1240 1260 1280 1300

Figure 9f.

station numbers

Figure 9g.

station numbers   *South*

1520   1540   1560   1580   1600   1620   1640   1660   1680   1700   1720

0   80 ft
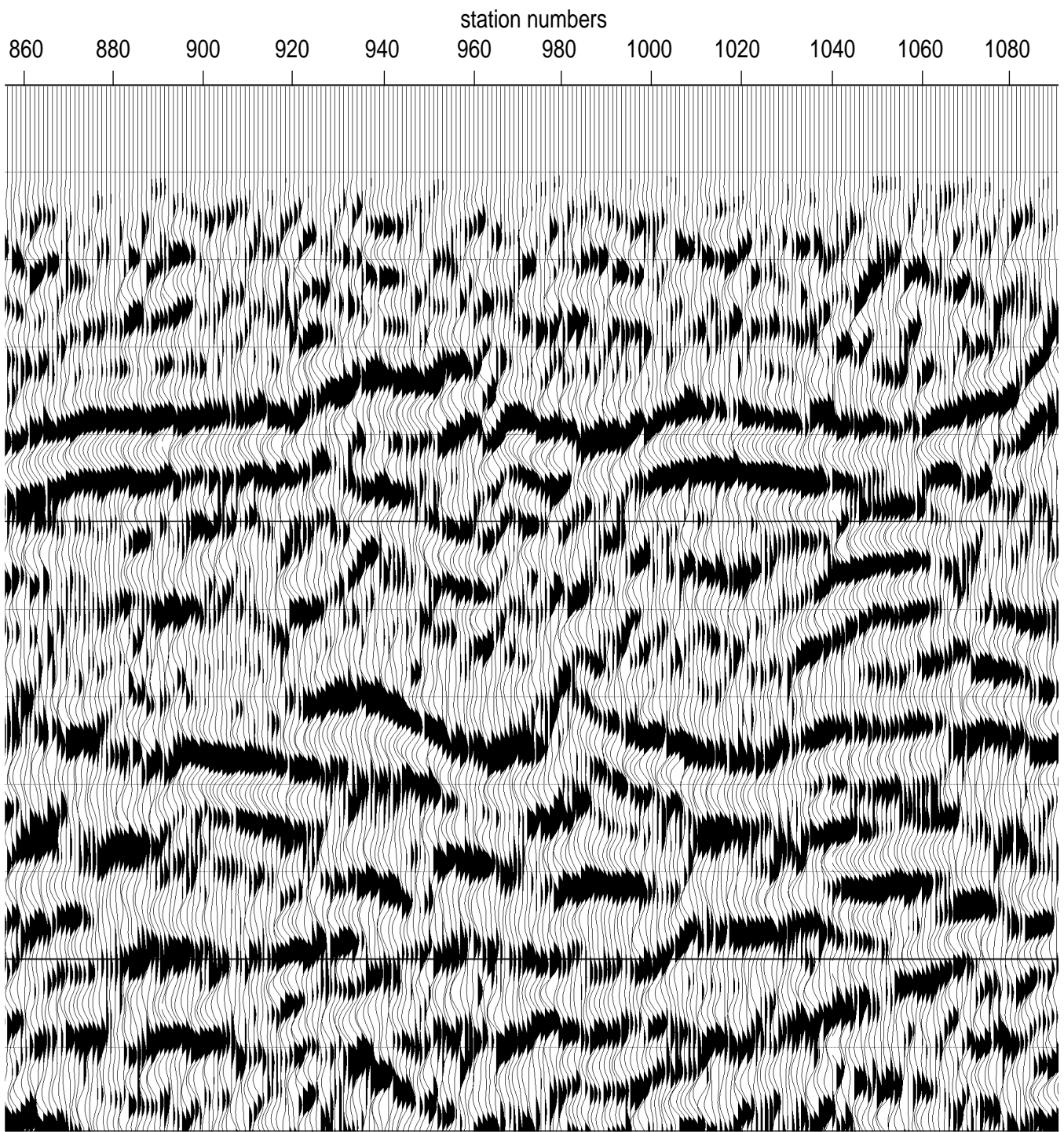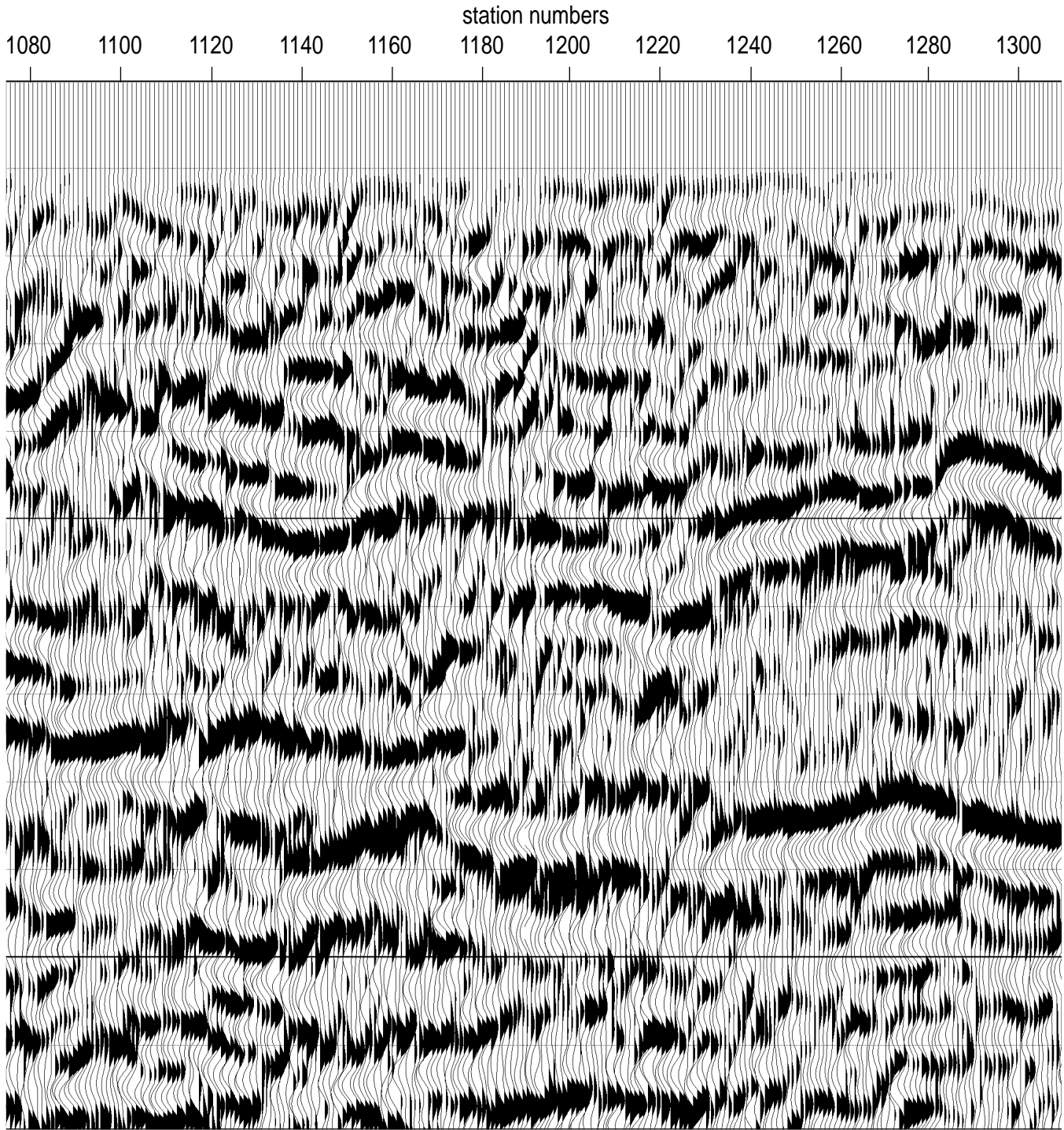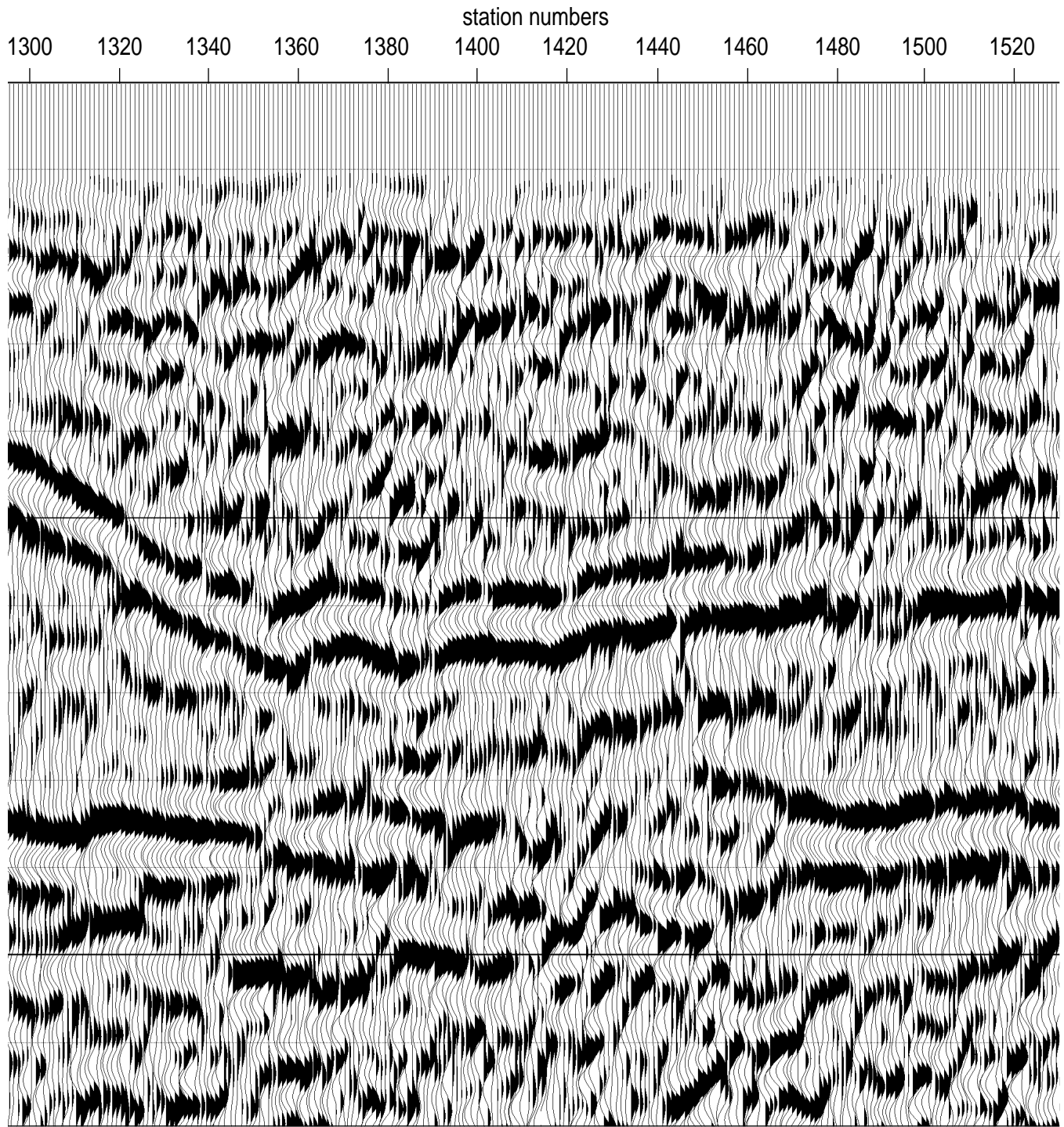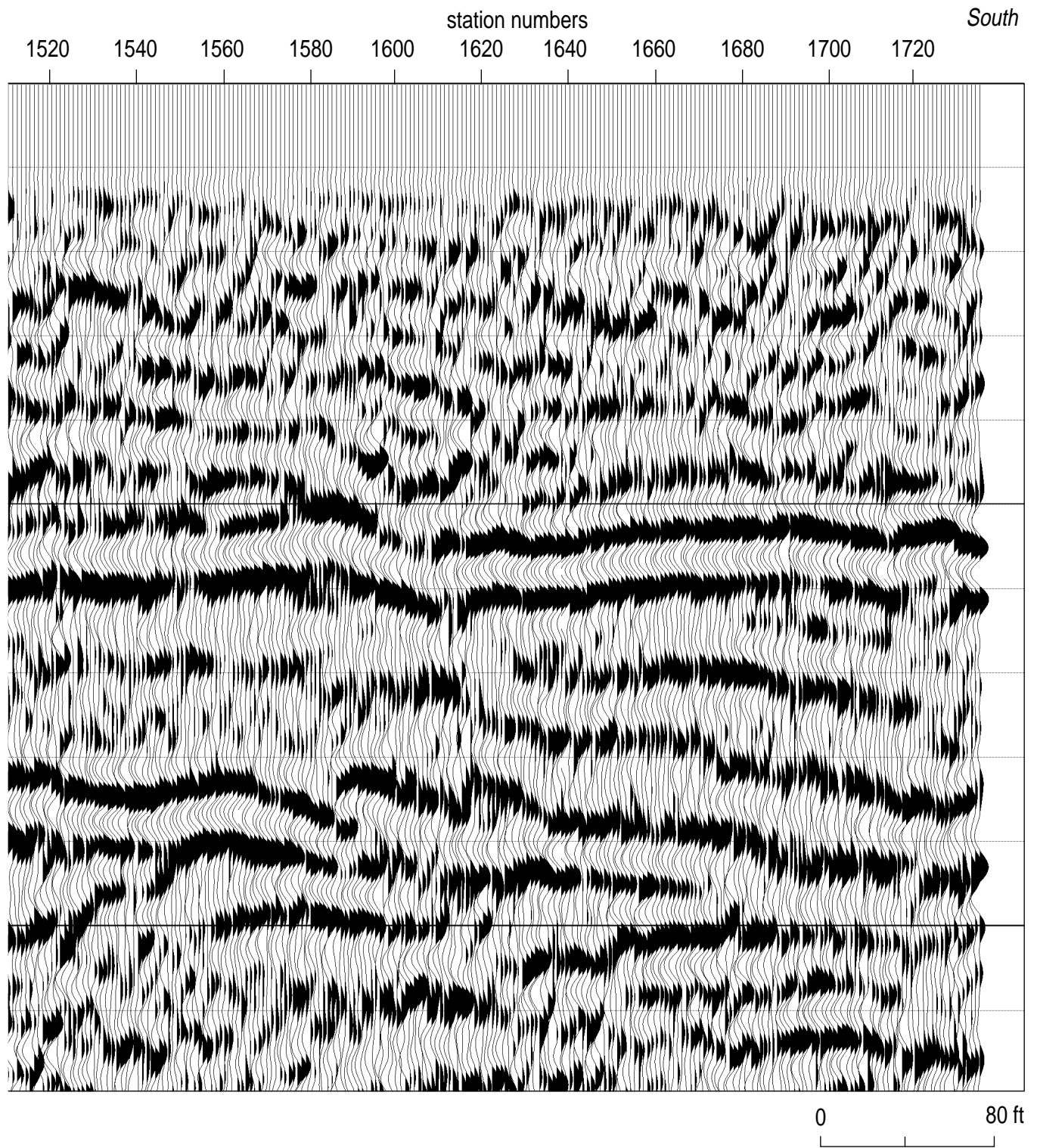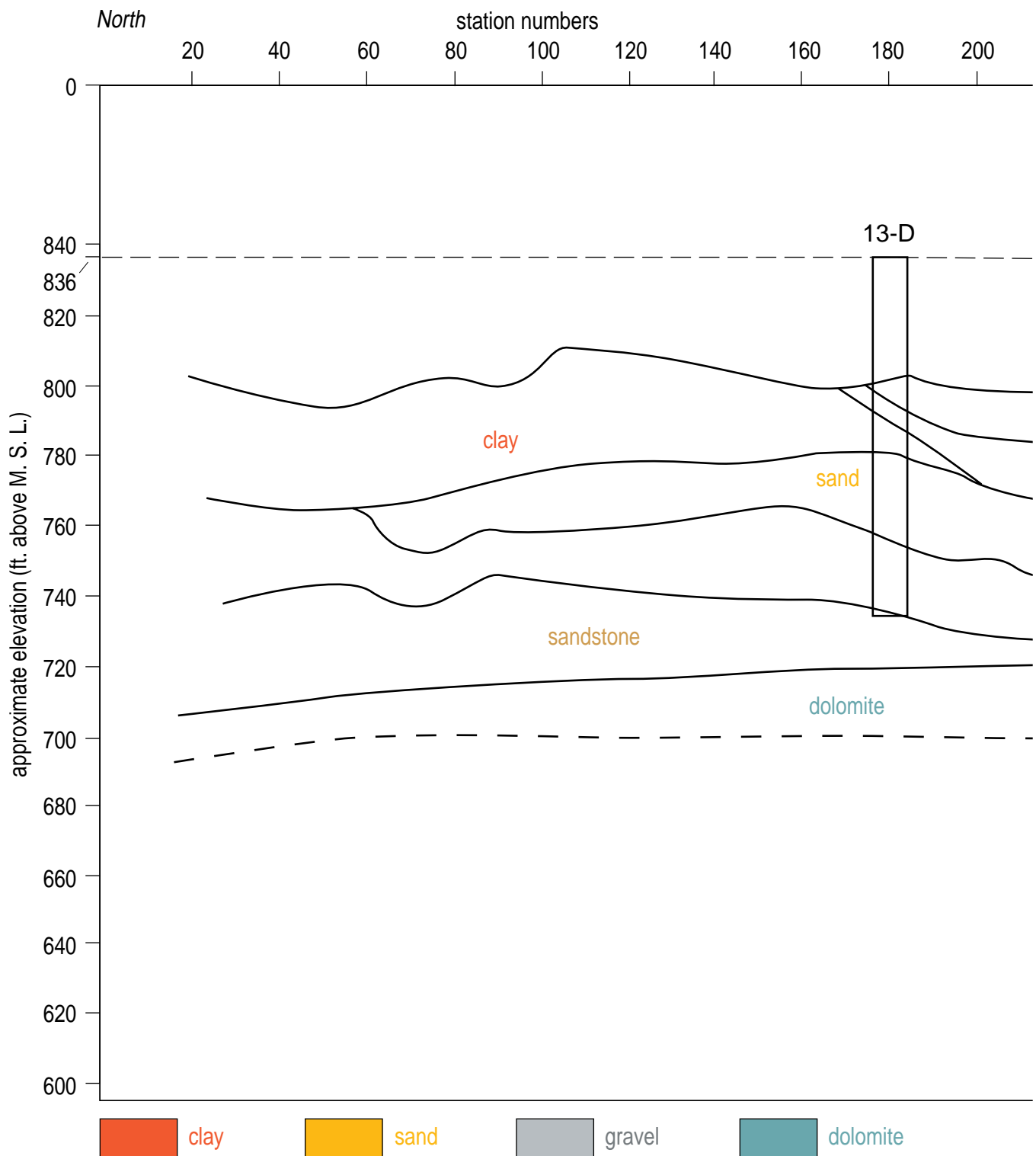
Figure 9h.

Figure 10a. Interpreted CDP stacked section of line 1 along East River Road incorporating borehole information as interpreted by RMI Inc. (1995). Geologic interpretations were made only if extrapolation from well identifications was possible.

station numbers

200 220 240 260 280 300 320 340 360 380 400 420

clay

silty sand

gravel

clay
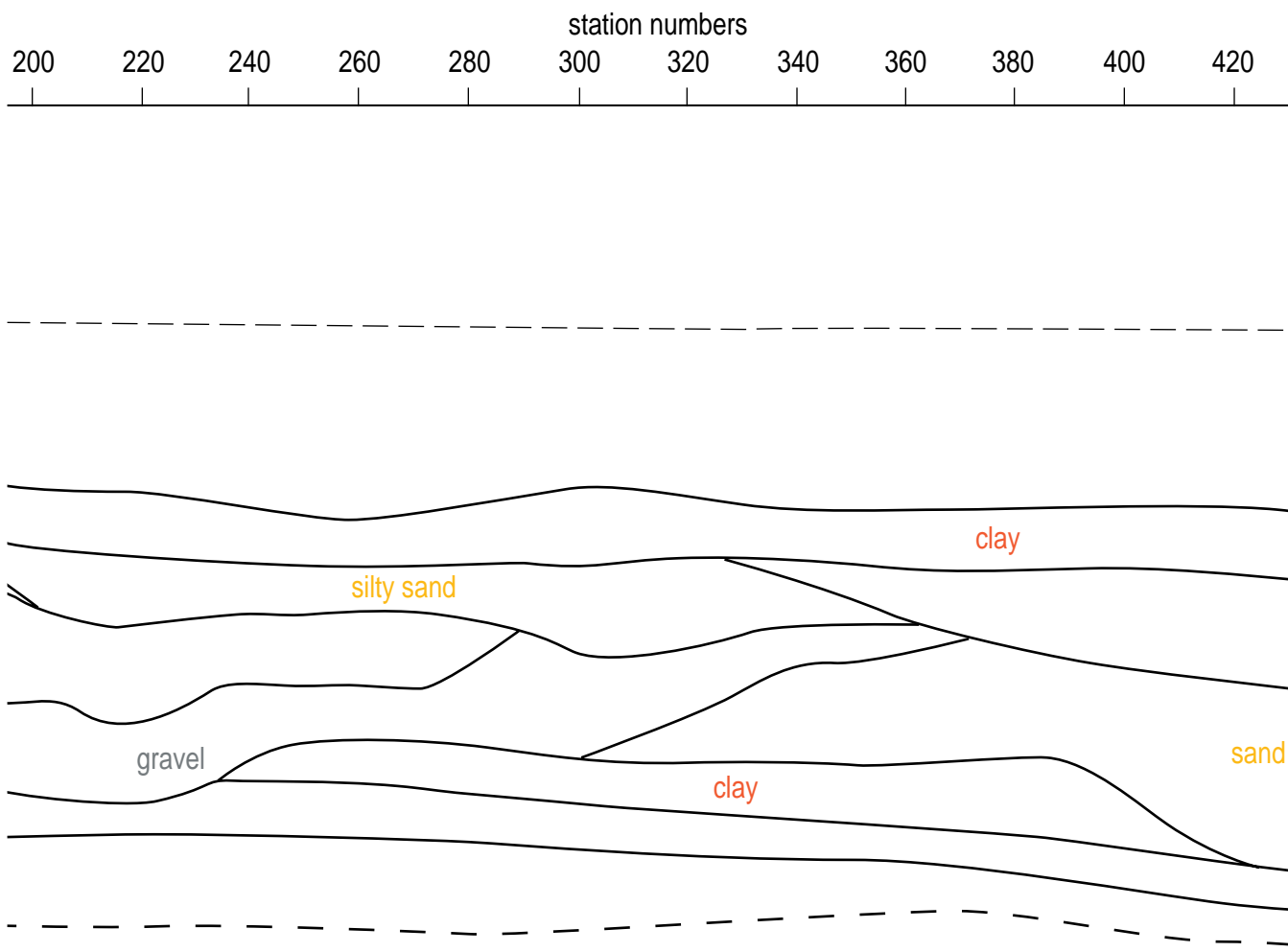
sand

sandstone   undefined reflections

Figure 10b.

station numbers

420 440 460 480 500 520 540 560 580 600 620 640

unknown

silty sand

sand

clay

sandstone

dolomite
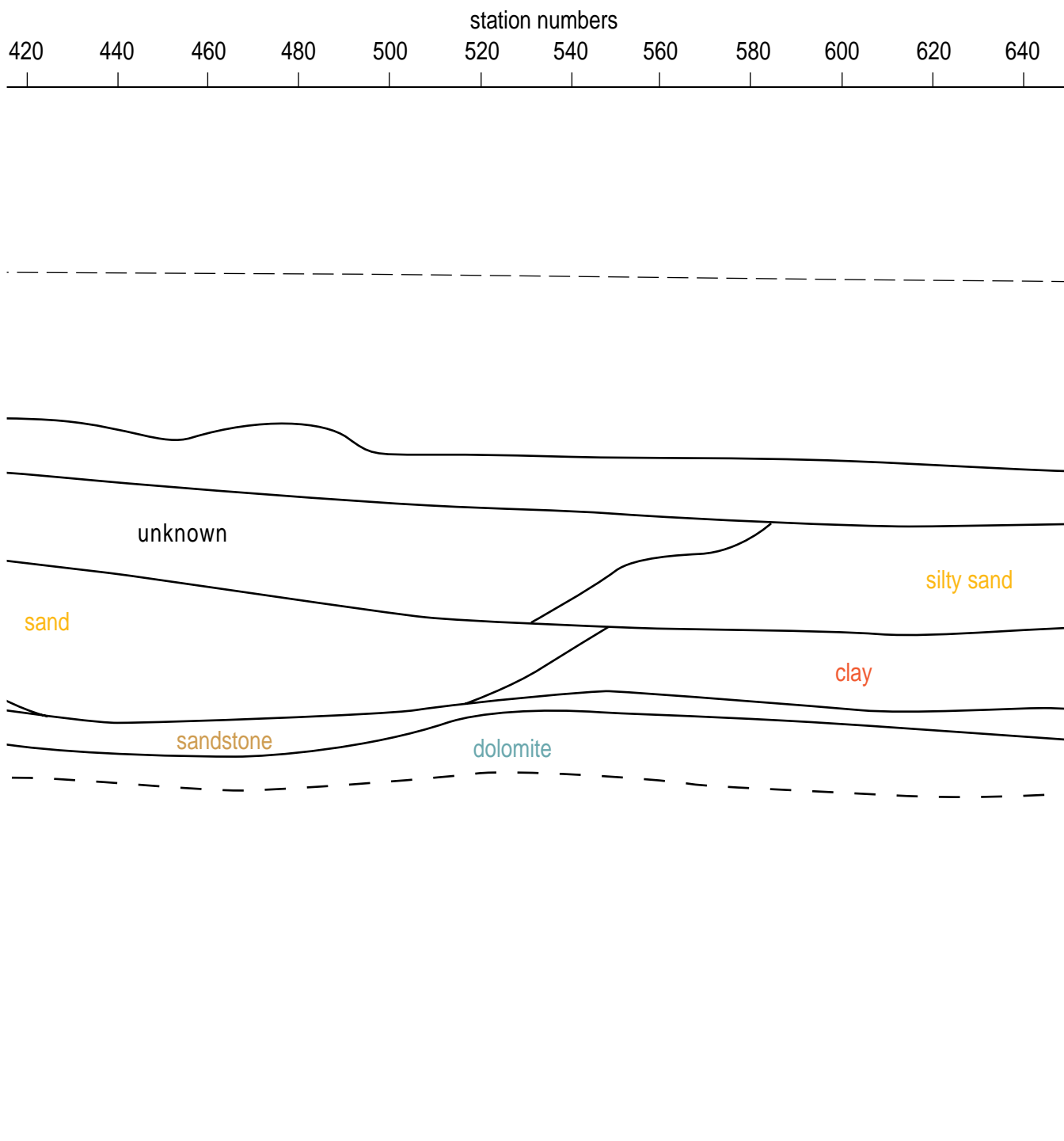
Figure 10c.

station numbers

640 660 680 700 720 740 760 780 800 820 840 860

4-PC

clay

silty-clay

gravel

silty sand

sandstone

dolomite

Figure 10d.

station numbers

860　880　900　920　940　960　980　1000　1020　1040　1060　1080

AT-2　6-D

? clay ?

? clay ?

?

? clay ?

sand

sand

silty sand

?　?

?

nite

Figure 10e.

station numbers

1080   1100   1120   1140   1160   1180   1200   1220   1240   1260   1280   1300

AT-3A   12-I   17

?

clay

gravel

nd   sand

gravel   sand

sand   gravel

gravel sand

dolomite

Figure 10f.

station numbers

1300   1320   1340   1360   1380   1400   1420   1440   1460   1480   1500   1520

17-D   F

nd

sandy gravel   sand

Figure 10g.

station numbers

| 1520 | 1540 | 1560 | 1580 | 1600 | 1620 | 1640 | 1660 | 1680 | 1700 | 1720 |

South

FMC-41

FMC-31

clay

sand

dolomite

0   80 ft

Figure 10h.

The comparatively unique geometries observed in the bedrock reflection at 60 msec and the next deeper reflection at 70 msec suggests two distinct reflections and not a single reflection with doublet style waveform. Between the north end of the line and station 184 the bedrock surface generally dips to the north with subtle undulations in its surface. Around station 210 the bedrock reflection becomes difficult to interpret and a reflection from within the unconsolidated materials seems to form a channel feature directly above the uninterpretable bedrock reflection. It is possible that this missing reflection could be a channel cut with sufficiently severe dip on the flanks to be unimaged with reflection techniques. The bedrock is very coherent and gently dips to the south between about stations 210 and 400. At around station 400 the reflection seems to lose amplitude. This could be due to a more diffuse reflecting surface, a higher degree of reflectance in units above bedrock, or near-surface problems. Based on wavelet consistency it appears the bedrock has a large scour or channel cut into the rock surface between stations 470 and 700. An alternate interpretation would place a rise in the bedrock surface at about station 500, somewhat analogous to a plateau or terrace. The channel cut seems most consistent with the data and is therefore the preferred interpretation.

The bedrock surface possesses a very well defined topographic high beneath stations 750 to 820. Comparing well 4-PC with the seismic data character, this high is likely sandstone with dolomite present as bedrock on both sides of the high in the interpreted channels. From about station 850 south to station 1000 the bedrock surface is represented by a very discontinuous reflection, possibly indicative of undulations or topographic changes too severe to effectively image with this technique. The bedrock low beneath station 890 could be deep enough to have dolomite as the bedrock surface. The sandstone is likely present on the north side beneath stations 840, but dolomite is probably bedrock from 870 south. The suggestion that the bedrock is dolomite from 870 south takes into consideration both the wavelet character and reflection times of the interpreted bedrock as well as the presence of dolomite in well AT-3A. The bedrock surface possesses a very gradual dip to the south from about station 1000. The bedrock surface beyond that point seems much more abrupt with respect to localized variability in the reflection surface. The interpreted bedrock surface is very consistent with both the well data and generally accepted models of the bedrock in this area (Lindgren, 1990).

Reflections within the unconsolidated material between the ground surface and bedrock on line 1 can generally be characterized as laterally variable in both structure and lithology. This suggestion of variability is based on consistency in

individual reflection wavelet characteristics, the large number of changes in reflection geometry, and attempts to correlate borehole data to the seismic reflection data. Time ties between lithologic contrasts and acoustic events on the seismic section are quite good. A very representative and detailed geologic cross-section resulted from this seismic section (Figure 10).

A very strong reflection event at about 35 msec north of the well located near station 150 possesses a very well defined undulation or wave in the reflection surface (Figure 11). Based on the arrival time and wavelet characteristics, this event is interpreted as the top of the non-permeable layer identified as the upper-drift confining unit. The apparent monocline in the shallow high amplitude reflection is likely some kind of terrace associated with a meander of the Mississippi River. The unique topography of this reflection event in comparison to deeper events all but eliminates any possibility this event is the water table with changes in topography of this event the result of near-surface static. Undulations of this kind in the reflector surface could act to pool or guide fluid movement.

Reflection arrivals between the high amplitude event interpreted as the top of the upper-drift confining unit at about 35 msec and the bedrock reflection at about 70 msec possess several very distinctive arrival geometries suggestive of channel cut-and-fill features. The reflection at 50 msec beneath station 40 is altered by interference and tuning effects from convergence with the 35 msec event beneath station 140. The 50 msec reflection is from a depth of around 75 ft. This tuning or interference suggests reflection separation that is less than one wavelength (or about 20 ft). The 50 msec reflection between station 60 and about station 90 is characterized by a shallow channel feature. This channel is about 8 to 10 ft deep and about 60 ft across. Tracing the 50 msec reflection from left to right across the stacked section from about station 90, a very subtle undulation in the surface of the event is evident. The unique wavelet interference pattern could represent the presence of some channel infill between stations 130 and 150. The geology as interpreted in the well located at about station 150 is very consistent with the reflection events as interpreted on this section.

At well 13-D the 50 msec reflection splits or thickens into a lens-looking feature (Figure 9). Between well 13-D and 4-PC a massive reflection event appears to dip to the south and form a syncline, possibly representative of a 200 to 400 ft wide and 45 ft deep channel. This channel ranges in depth from around 50 ft (45 msec) to almost 100 ft (60 msec) between stations 350 and 700. This large channel feature
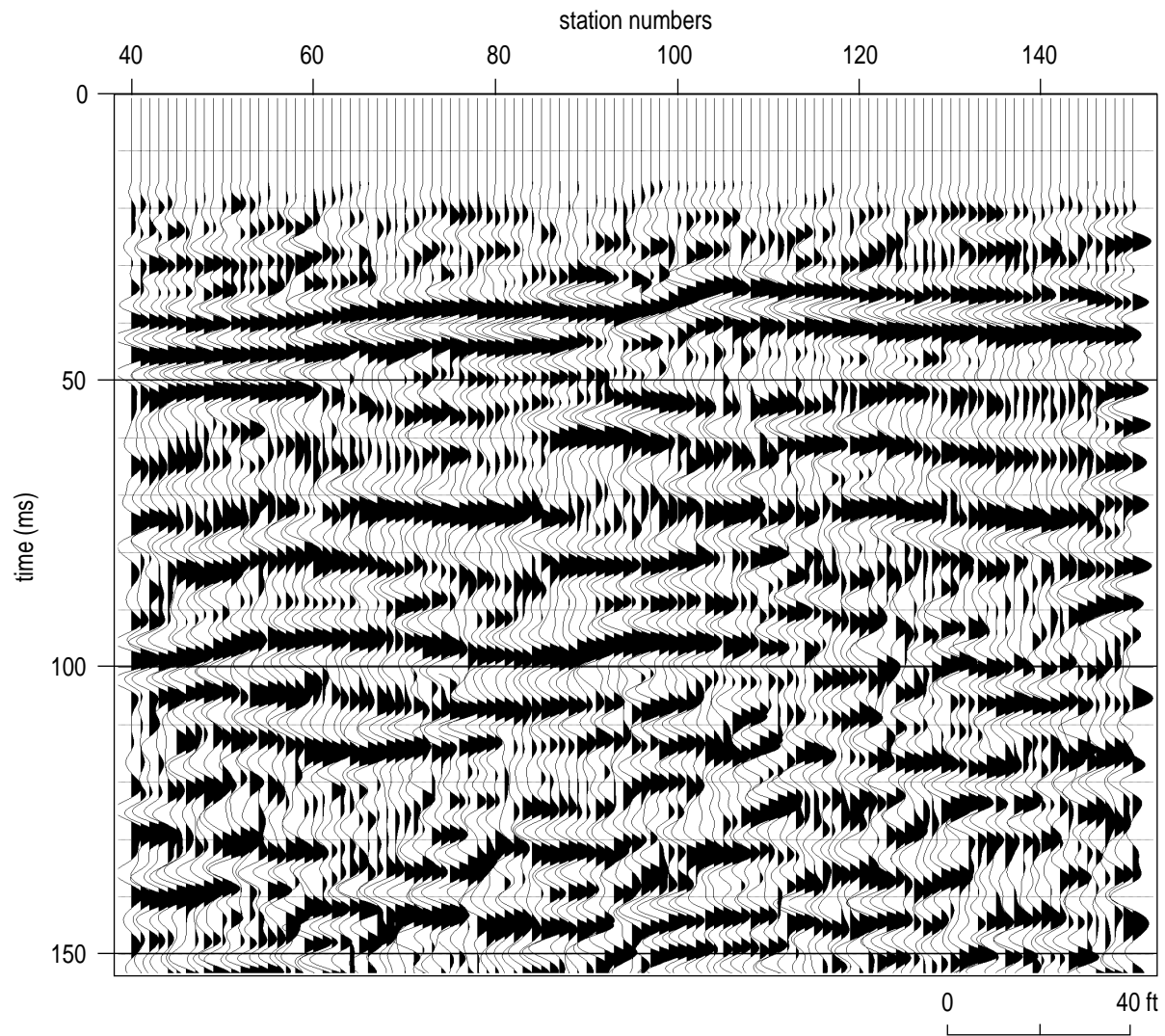
Figure 11. Portion of 24-fold CDP stack of line 1 expanded to provide more horizontal detail. Subtle stratigraphic features are evident in several places.

within the unconsolidated material is much wider but generally centered on the bedrock low previously interpreted to be centered on station 570.

At well 4-PC, several layers are present but only the shallowest reflections (< 50 msec) have a possibility of being continuous (Figure 9). At well 4-PC there appears to be some indication that several layers are either dramatically thinning or possibly becoming discontinuous. It is most likely that much of the variability in the shallow part of the section in this area is due to fairly significant changes in bed thickness and not discontinuous beds. If the beds were discontinuous there should be a much more dramatic change in reflection amplitudes and some edge effects might be present.

Examining the portion of the stacked section between stations 870 and 1200 in greater detail unveils several very interesting features and characteristics of the reflecting units (Figure 12). It is clear that the shallow reflection appears very discontinuous at about station 960 to the point that it is very reasonable to interpret the termination of the 35 msec event as an erosional truncation. The reflections that proceed south from that point at about 40 msec are likely completely different units. As well the bedrock surface beneath station 980 possesses a very unique structure. The apparent high at that location seems to divide two different bedrock channels with relatively unique geometric shapes. The complexity of the bedding between the shallowest interpretable reflection and bedrock is apparent within the zone with a discontinuous upper drift confining unit.

The massive clay unit interpreted in well A-2 is clearly present on the seismic data (Figure 9). If the drill data had not been available, the interpretation of this thick clay reflection would likely have been the same. The thick clay terminates or thins by several orders of magnitude beneath station 860. It is most likely that this thick clay terminates with a shallower northward dipping layer continuing south from well 13-D. In the area between stations 870 and 1150 it is very difficult to say if any reflection besides bedrock is continuous. There are clearly lenses or stringers of clay/sand throughout the area, but it appears that even the shallower events are either not present or very thin. Based on the seismic data alone it would be reasonable to suggest the clay is missing between stations 930 to 980 and again between stations 1060 and 1200. It would not be unreasonable to suggest that, from the termination of the massive clay unit at station 870 to the appearance of another high amplitude reflection at about station 1200 (both around 50 msec), no continuous thick clay units are present.
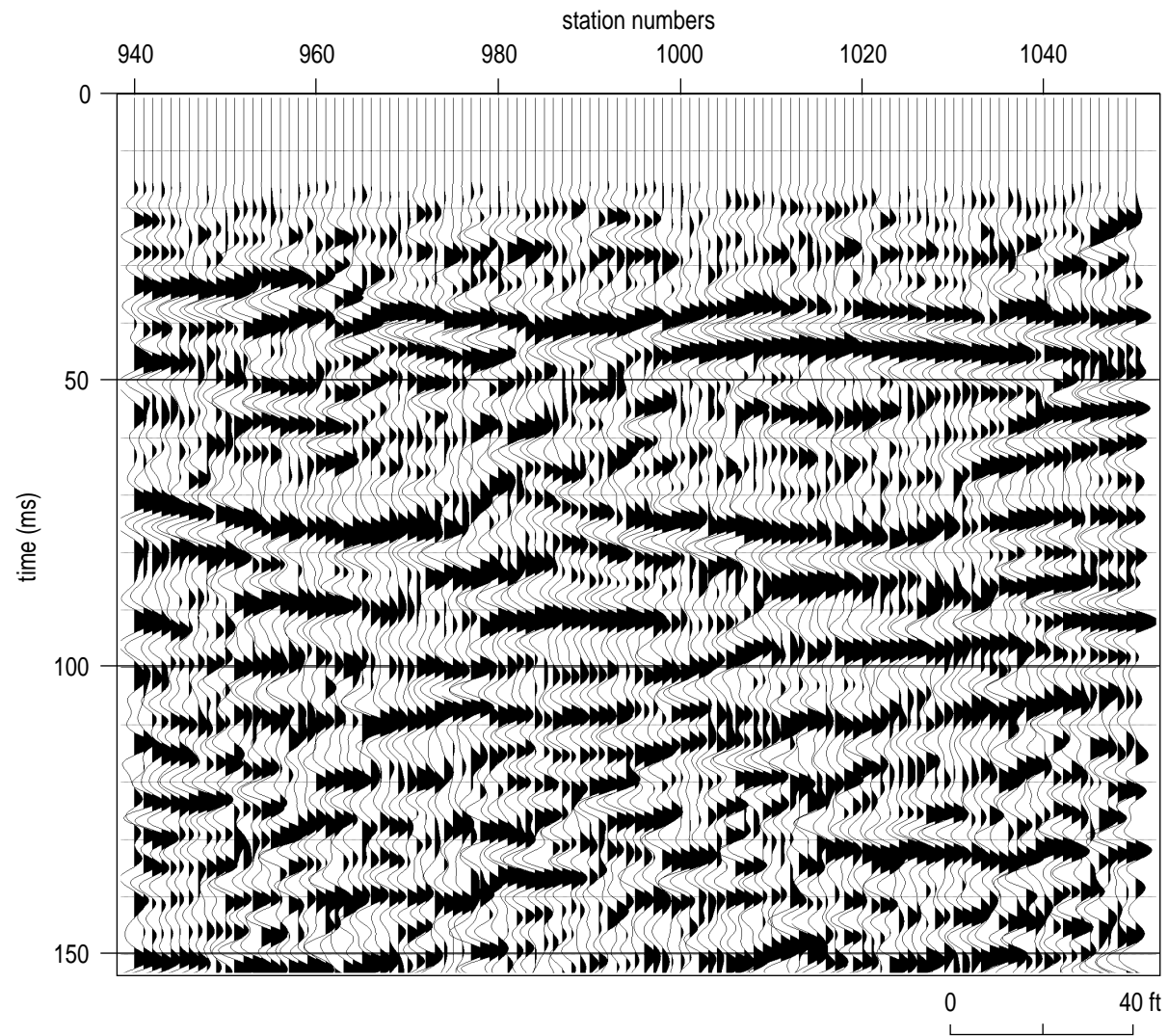
Figure 12. Portion of 24-fold CDP stack of line 1 showing several relatively dramatic geometries associated with both the bedrock surface and the shallowest reflecting layer.

The shallowest reflection that has been correlated to lithology or hydrology becomes significantly deeper north of station 1200 (Figure 13). This drop in reflection depth is not related to changes in near-surface velocity, so it must represent real geology. The reflector drops 50 ft vertically across 120 ft horizontally. A feature with these dimensions could be expected in many modern river systems. From about station 1200 to the north end of the line, with the exception of several shallow reflections cutting and cross cutting above the high amplitude intra fluvial/glacial reflection at about 50 msec, the section is relatively continuous to a point near the extreme south end of the line. At the far south end of the line the bedrock is interpreted to rise by almost 30 ft and then dip to the north. This portion of the interpretation is very speculative and required incorporation of borehole data off-line by a couple hundred feet. Based on the interpretation of line 3, correlation to wells that far from the seismic line might give completely inaccurate guidance. Without the borehole data this feature would have likely been interpreted as a dipping bedrock etched with several channel features within the unconsolidated section.

The shallowest coherent reflection interpretable across most of the CDP profile becomes very erratic around station 1300 (Figure 13) and then flattens, becoming quit well behaved between about station 1600 and the south end of the line (Figure 14). The monocline interpretable between station 1280 and 1360 dramatically affects the hydrologic setting of this site. The steep dip of this confining layer will likely act as a barrier to northward movement of fluids with a specific gravity greater than that of water. The relative flatness of the bedrock surface is conclusive evidence that this feature is real and not the result of uncompensated static. This feature is unique considering the relative uniformity of reflection events south of about station 1500 (Figure 14). The strong bedrock reflection and less distinctive reflections from within the unconsolidated layers are consistent with undisturbed alluvium over bedrock settings previously investigated using shallow seismic reflection techniques.

The CDP stacked section from line 2 is not nearly as high quality as line 1, but it does contain a significant amount of very useful information (Figure 15). Information from the three wells near enough to the line to possibly be useful are extremely difficult to correlate to the seismic data. This is not a complete surprise when considering how fast the layers within the unconsolidated portion of the section change both lithologically and structurally. This can be observed on the CDP stack of line 1 (Figure 9) and the geologic cross-section derived from the borehole information (Figure 2). The most prominent reflection is the slightly lower
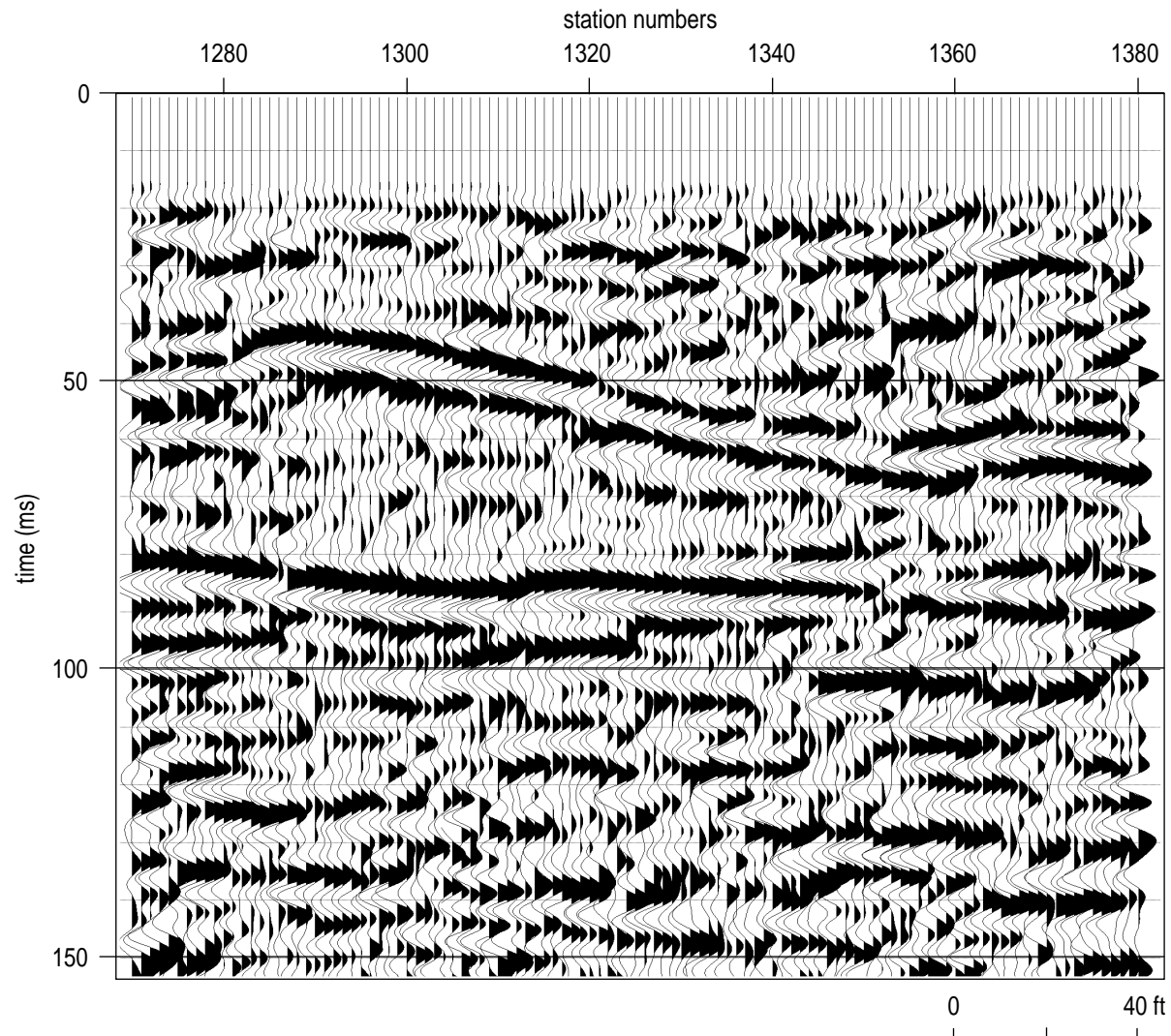
Figure 13. Portion of 24-fold CDP stack of line 1 showing shallowest reflection dipping toward the south, seemingly independent of the apparent dip on the bedrock event.
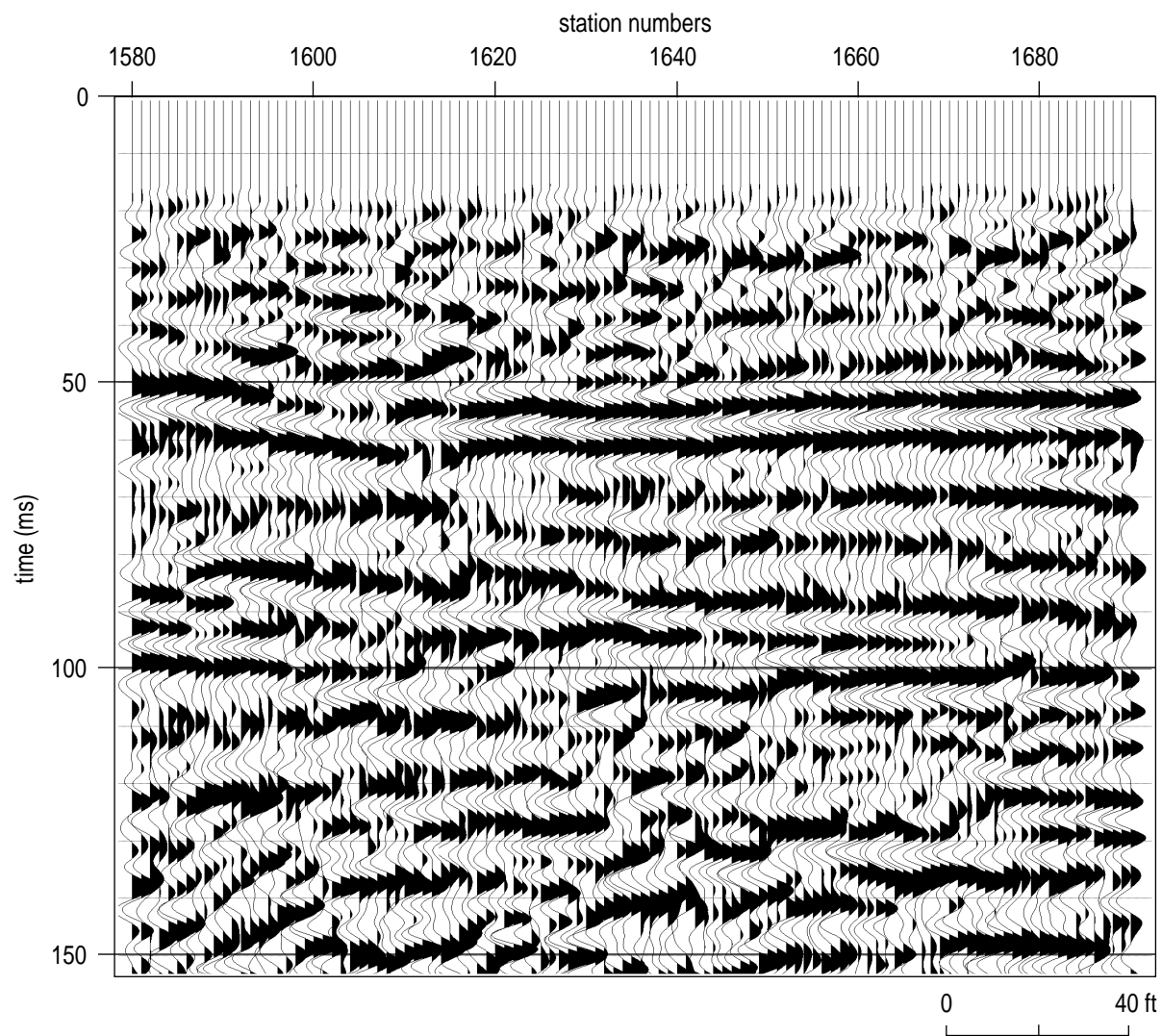
Figure 14. Portion of 24-fold CDP stack of line 1 representing several relatively consistent stacked reflection events.
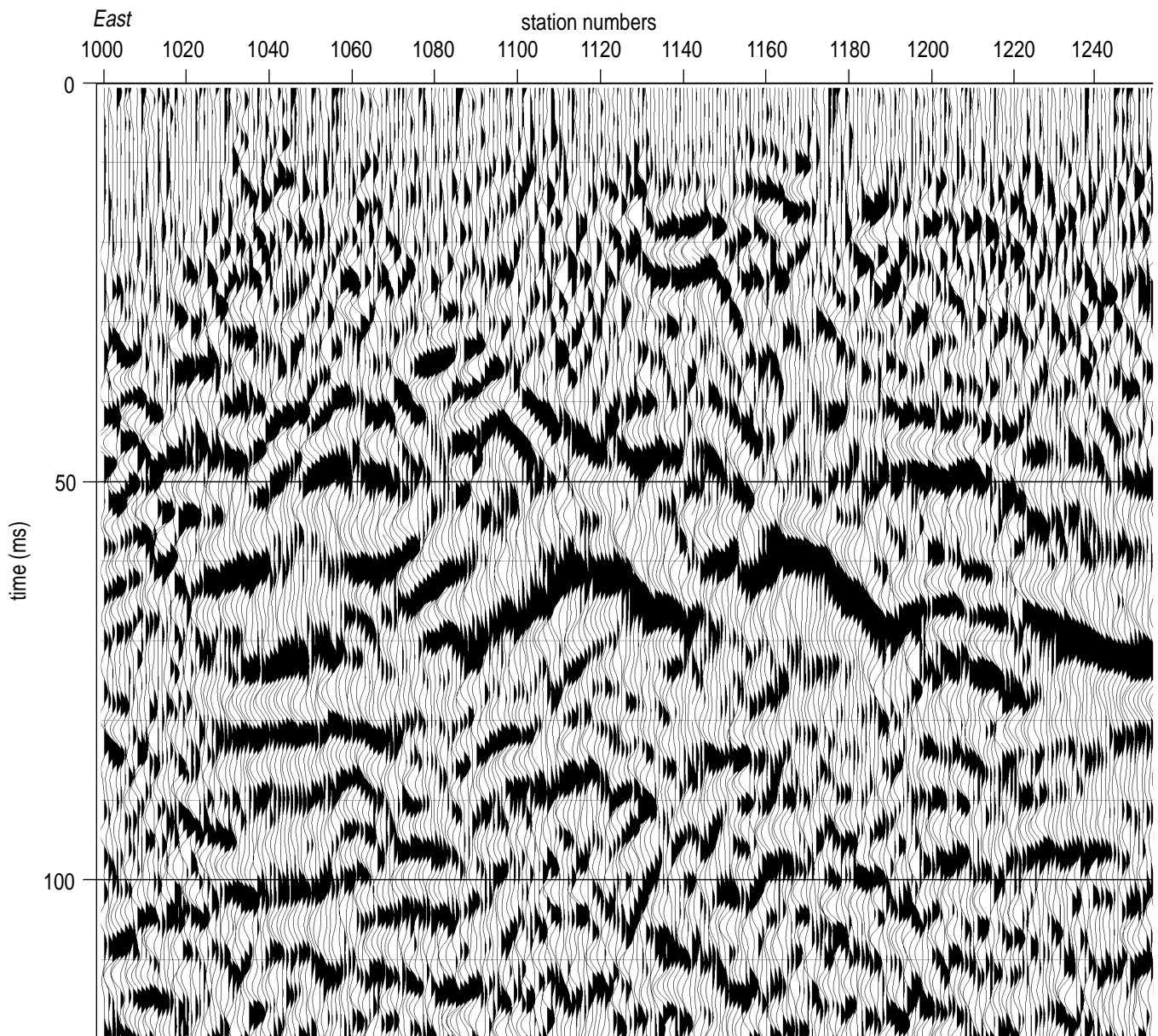
Figure 15a. CDP stacked section of line 2, North 40 area. Stacked data quality is not as high on line 2 as line 1, likely due to the poorer near-surface conditions on line 2 in comparison to line 1.
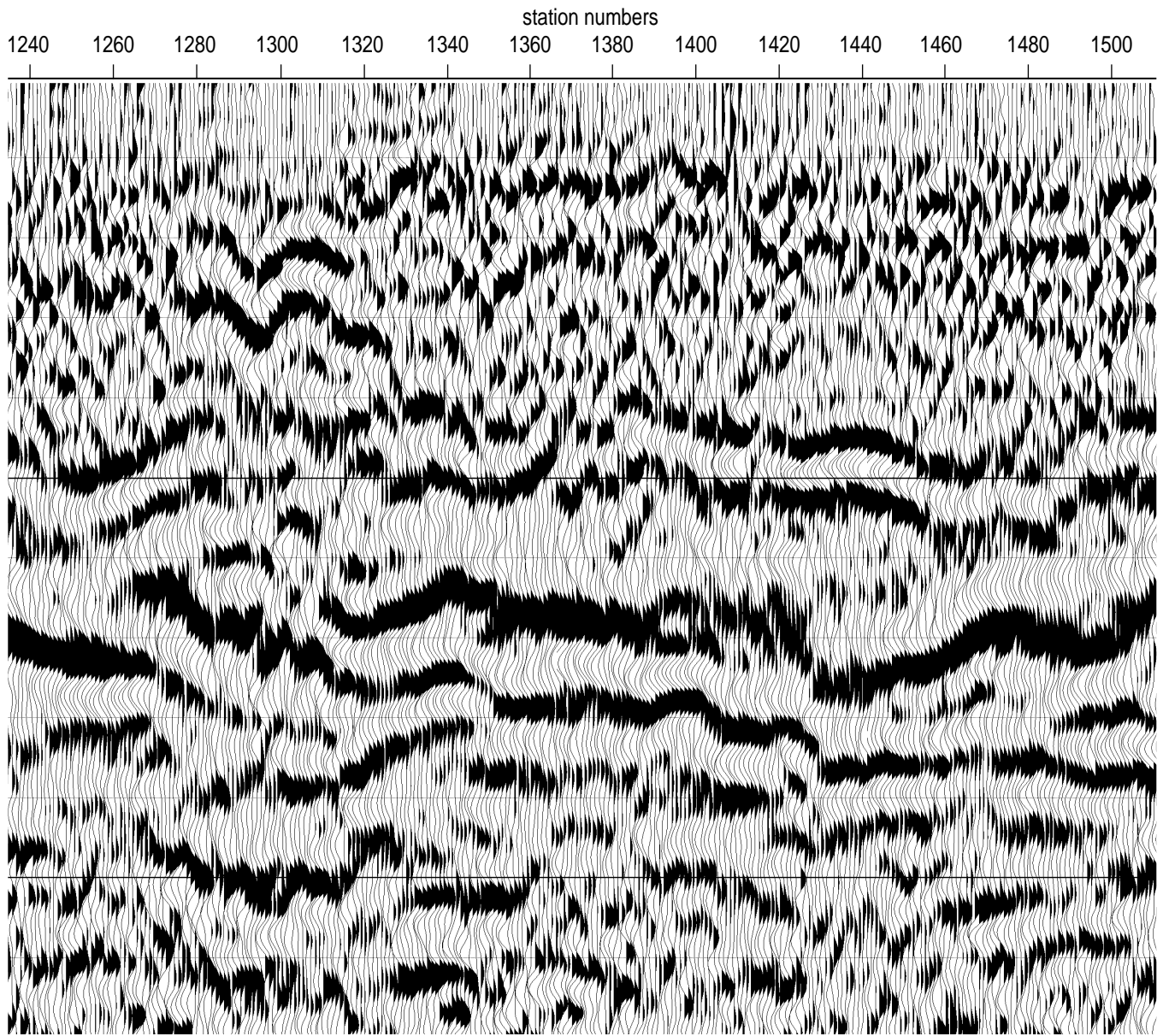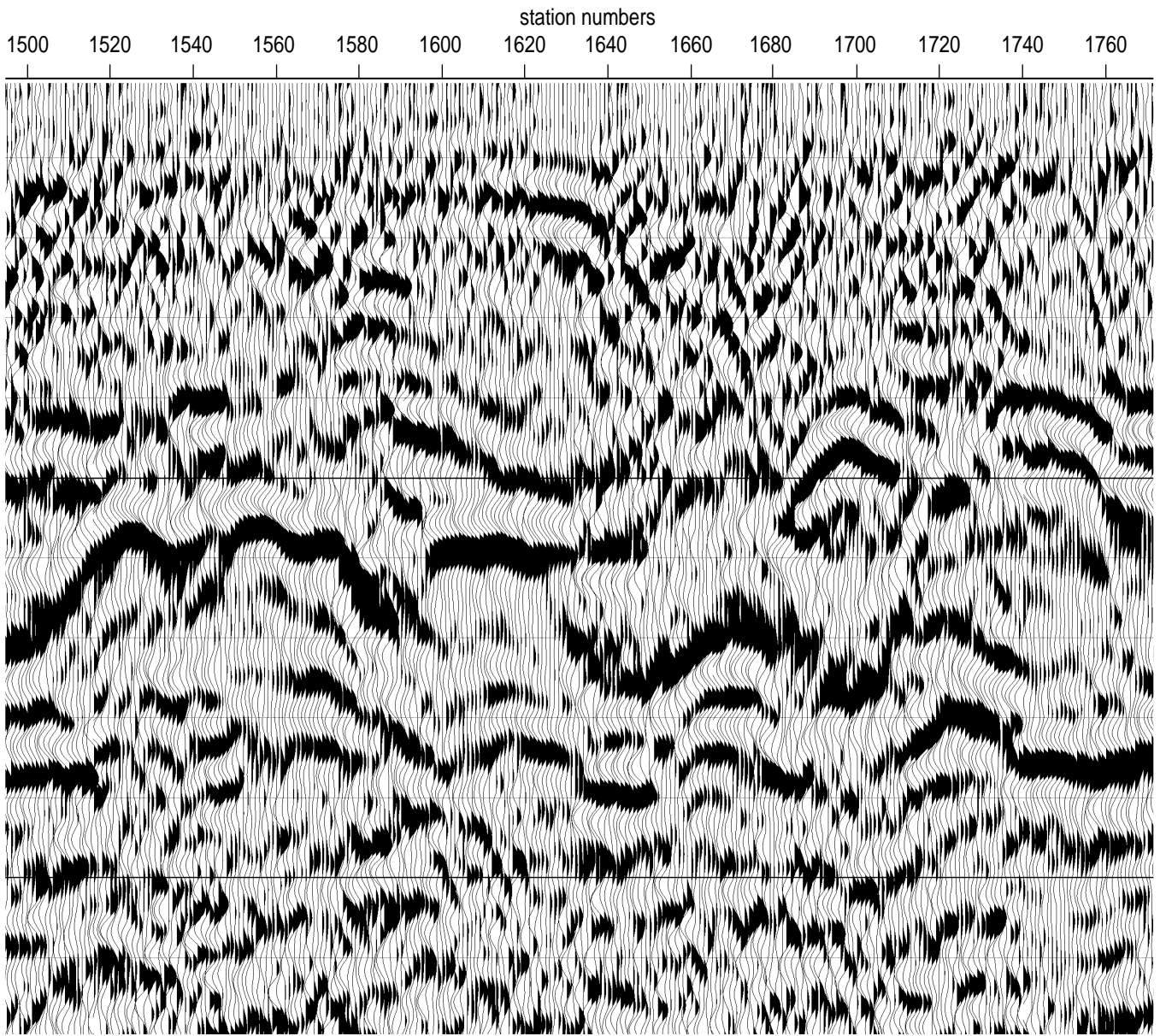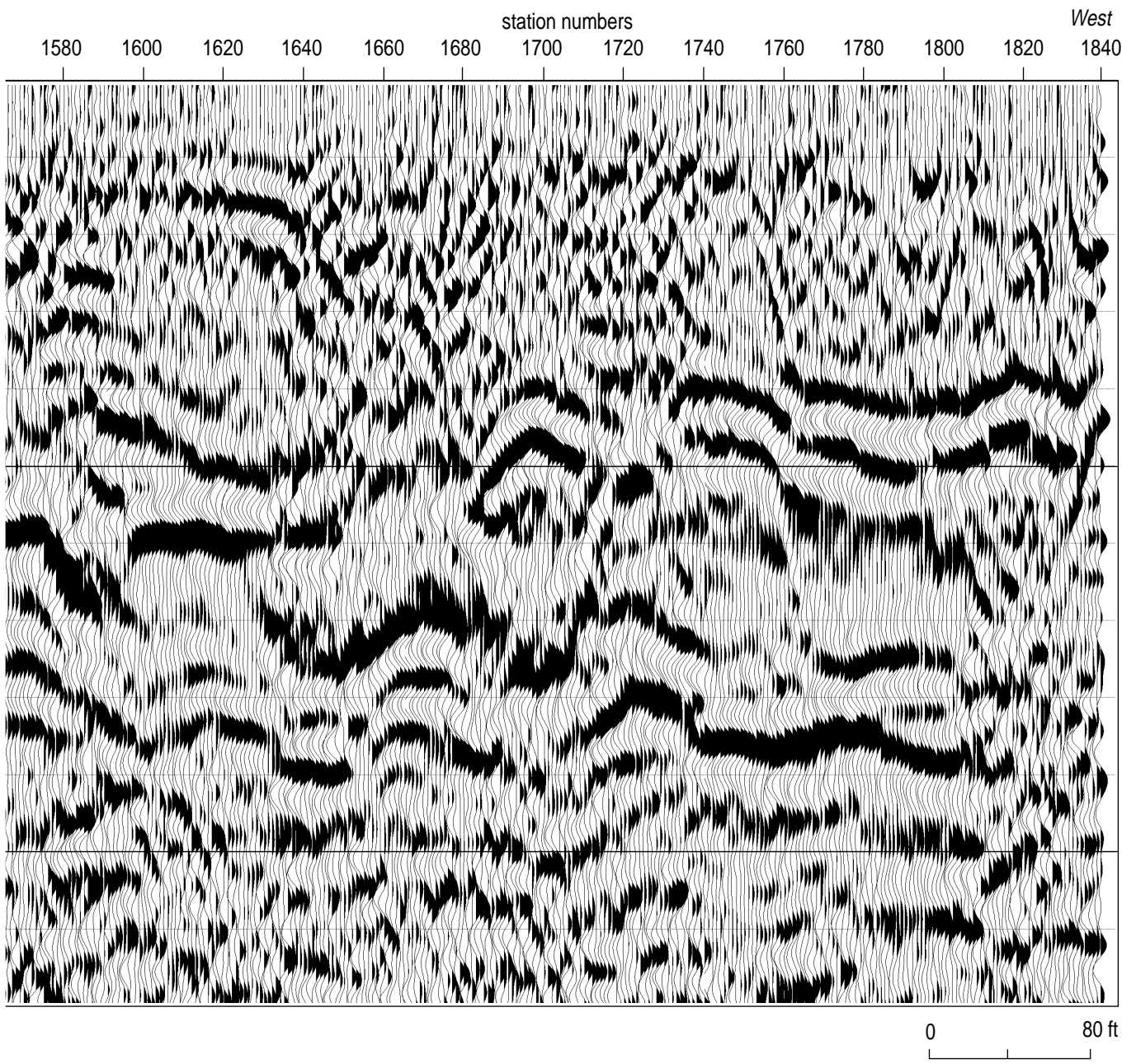
station numbers

1240 1260 1280 1300 1320 1340 1360 1380 1400 1420 1440 1460 1480 1500

Figure 15b.

station numbers

1500 1520 1540 1560 1580 1600 1620 1640 1660 1680 1700 1720 1740 1760

Figure 15c.

station numbers   *West*

1580   1600   1620   1640   1660   1680   1700   1720   1740   1760   1780   1800   1820   1840

0   80 ft

Figure 15d.

frequency event ranging in depth from 50 to 80 msec across most of the section. A shallow reflection event is also interpretable across most of the line nominally above 50 msec.

The bedrock reflection is much more difficult to confidently interpret on this section than on line 1. This lack of a consistently confident bedrock reflection could be due to several factors. The most likely is related to near-surface conditions and the obvious decrease in the depth of penetration of acoustic energy along this line. Also to consider is the unique characteristics of the lower frequency reflection present across most of the line. This event seems very diffuse with a dominant frequency more than 50 percent less than other reflections above bedrock. This dramatic difference in spectral properties could be indicative of material, com-paction, "sharpness" of the layer contacts, etc., with anyone of these completely or partially responsible for the observed decrease in bedrock reflection clarity.

Boreholes with geologic data available along this line are offset from the line and concentrated between stations 1450 and 1700. Correlation of these wells to each other is somewhat speculative and making the jump across to the seismic line is even more difficult to do confidently. The extreme horizontal variability in the unconsolidated sediments, as evident in places along line 1, make confident ties difficult. Interpretations of the seismic reflection data were done using the nearby wells as a guide only, with no direct tie to the profile (Figure 16). Consistent with line 1, the confining layer when present is a high amplitude and high frequency event allowing confident interpretation.

The coherency, geometry, and wavelet characteristics of the reflection at about 50 msec change several times across the expanse of this survey line (Figure 15). The reflection character and arrival time on the far west end of the line is very consistent with data recorded along line 1. This similarity is unique for this line and leads to the suggestion that the confining layer identified from about 1780 to the west end of the line is likely equivalent in terms of geometry and geology to the shallow confining layer interpreted on the north end of line 1. Several very pronounced diffraction-looking arrivals are interpretable beneath stations 1745 and 1705 with appexes at or within the shallow confining unit. These diffraction-looking arrivals are very likely bed terminations and represent breeches in the confining layer. The reflection arrivals within the expanse between stations 1740 and about 1440 is con-sistent with a very discontinuous confining layer. The data in this area are very similar to those observed between stations 870 and 1150 on line 1. From about station 1440 east to around station 1180 the reflection coherency of the confining
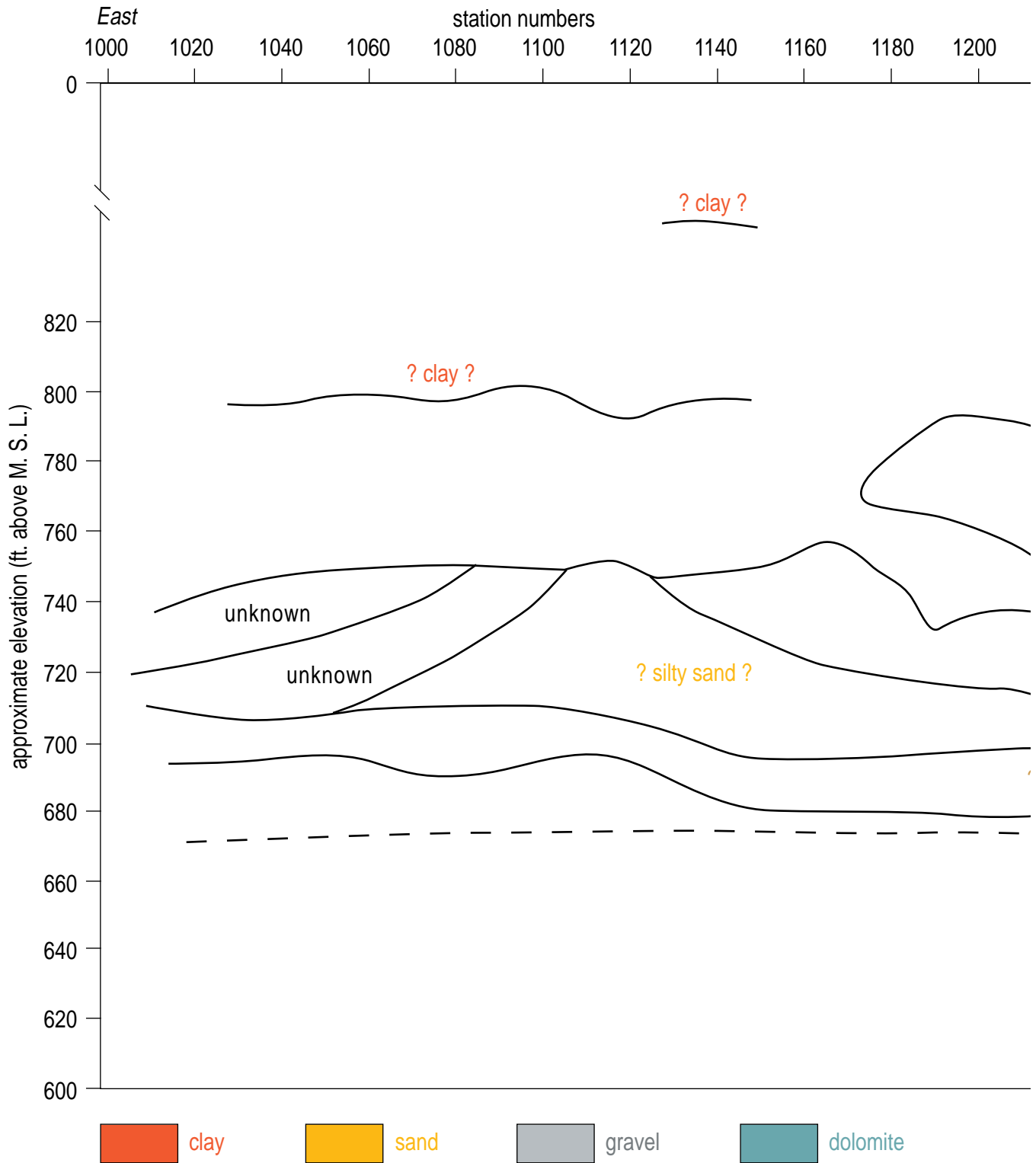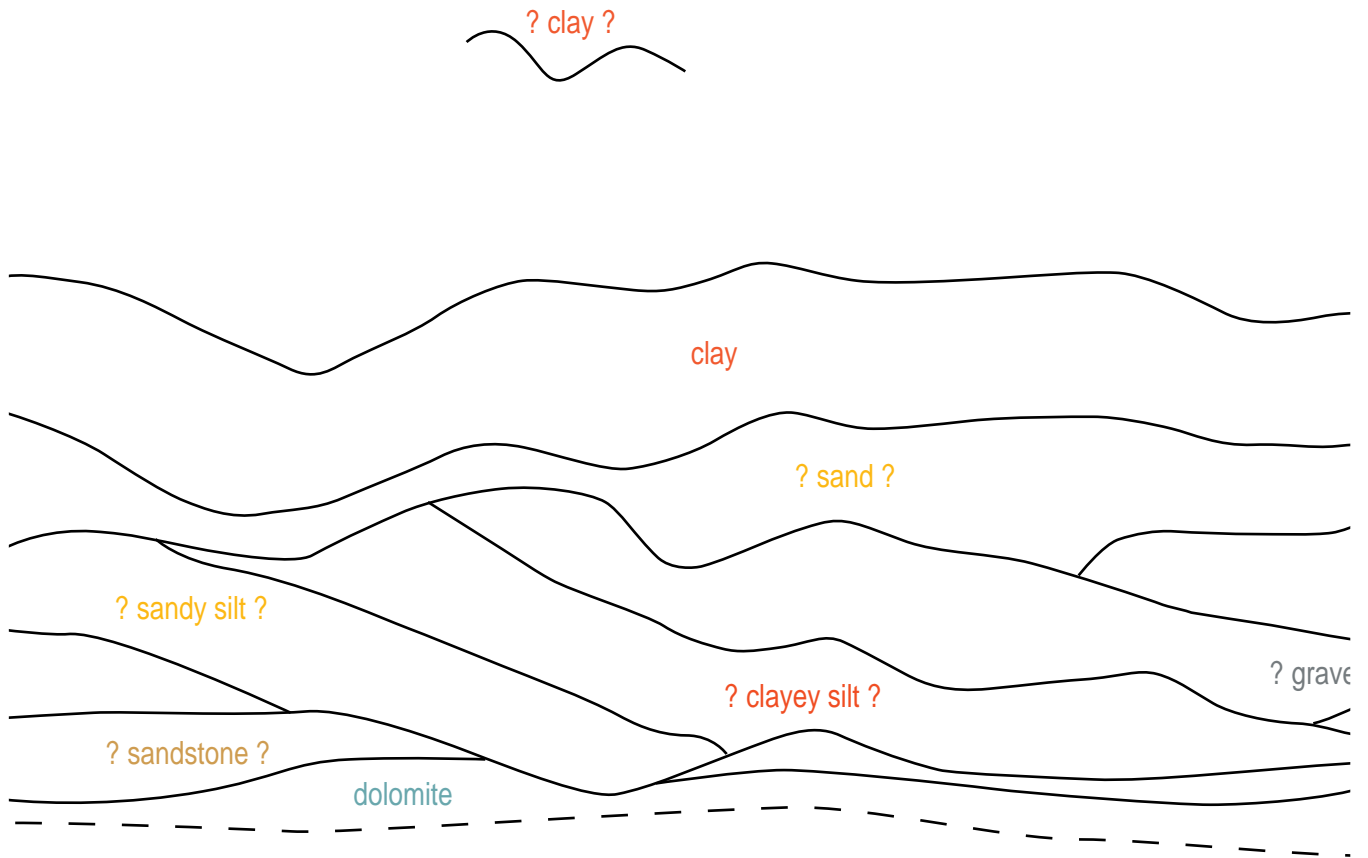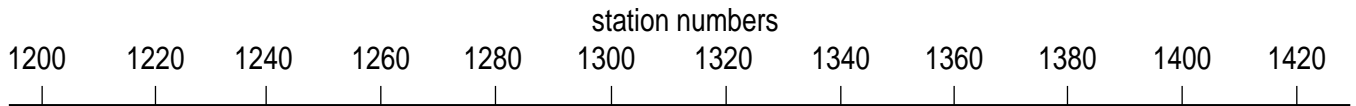
18

Figure 16a. Interpreted CDP stacked section of line 2, North 40 area. Geologic units were assigned by extrapolating well information adjacent to the survey line at offset distances ranging from 100 to 1000 ft.

station numbers

1200   1220   1240   1260   1280   1300   1320   1340   1360   1380   1400   1420

? clay ?

clay

? sand ?

? sandy silt ?

? clayey silt ?

? grave

? sandstone ?

dolomite

sandstone

Figure 16b.

station numbers

| 1420 | 1440 | 1460 | 1480 | 1500 | 1520 | 1540 | 1560 | 1580 | 1600 | 1620 | 1640 |

clay

clay

? silty sand ?

san

? gravel ?

? silty sand ?

dolomite

Figure 16c.

station numbers

West

1620 1640 1660 1680 1700 1720 1740 1760 1780 1800 1820 1840

clay

lay

clay

sand

? silty- and ?

unknown

? sandstone ?

0 80 ft
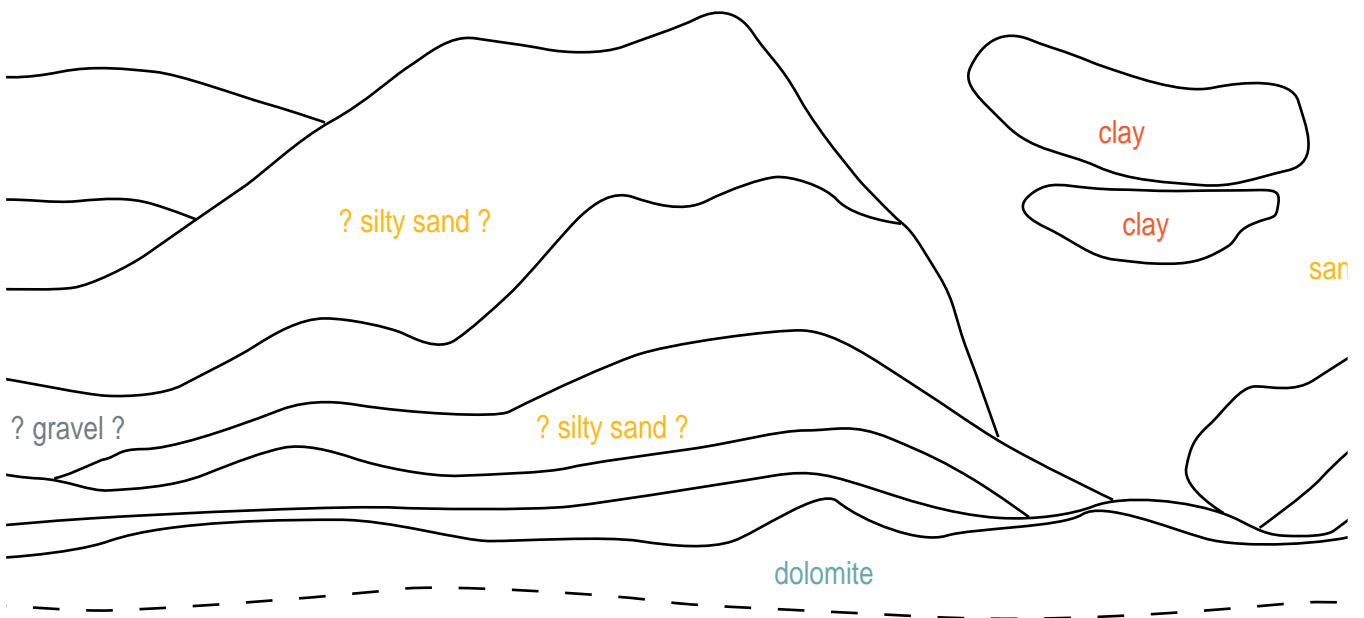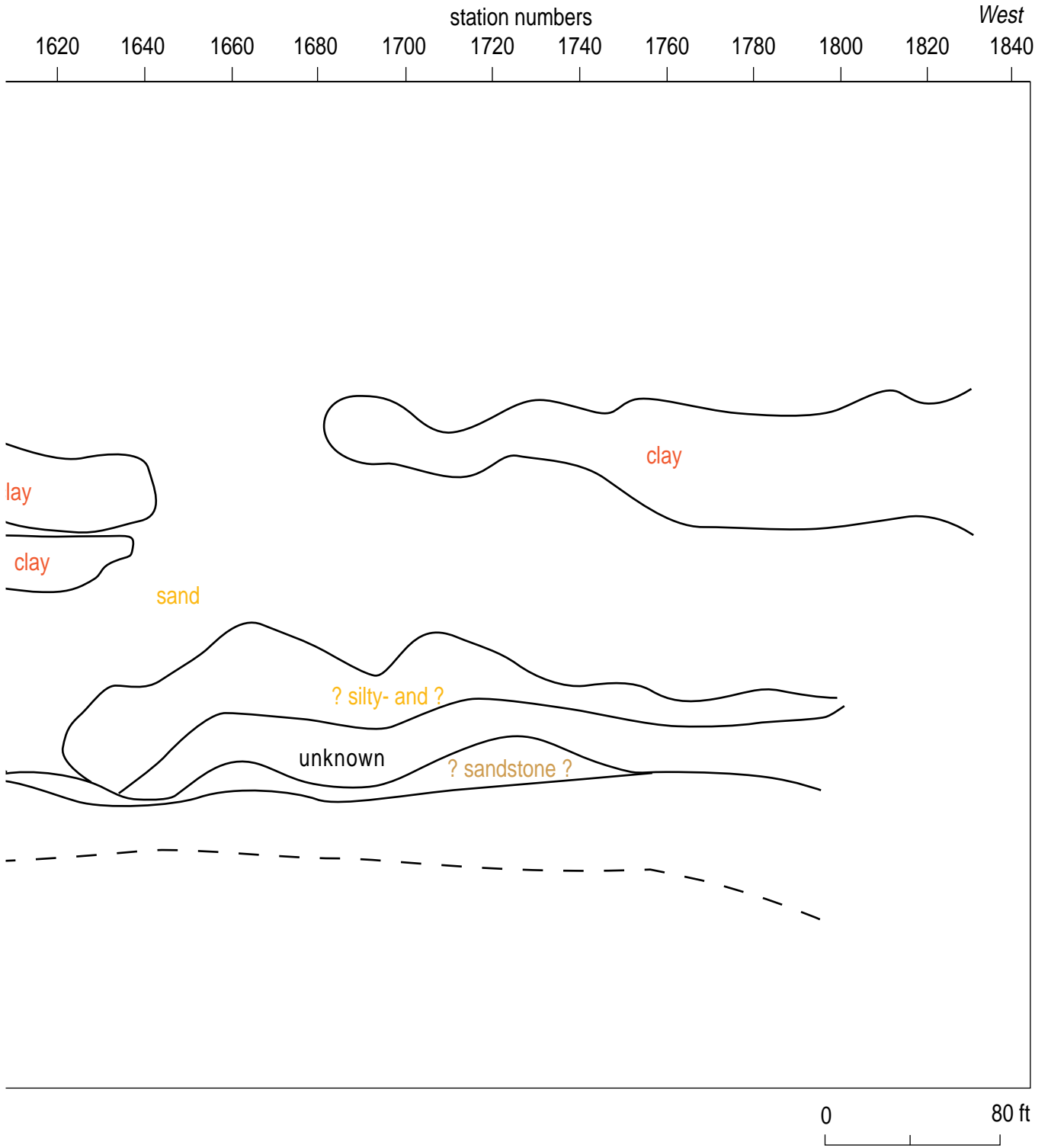
Figure 16d.

layer is relatively good, and it is reasonable to interpret this area as underlain by a continuous confining unit. East of station 1180 the data quality becomes very erratic with several diffraction-looking features. If these are diffractions, which would be suggestive of bed termination or point source features, it is very likely the confining unit is not continuous between stations 1040 and 1180.

The lower resolution of this section in comparison to line 1 is evidenced by the lower frequency, more smeared-out looking prominent reflection between 50 and 80 msec (Figure 15). Interpreting this packet of events as a series of non-uniform layers and lenses with very diffuse boundaries containing varying com-binations of materials such as sand, silt, clay, or gravel is consistent with nearby borehole data and the interpretation of bed tuning. The most dramatic features within this particular packet of reflections is the mound centered on about station 1560. Based on the borehole information, this mound could be an extension of the pile of silty-sand encountered in well PC-2. This mound rapidly diminishes to the west to the point it is likely only a thin layer overlying bedrock. Immediately west of the mound beneath stations 1600 to 1640 a relatively flat layer interpreted as clay beneath a lens also interpreted as clay (Figure 16). It is very possible this could be the clay-silt-clay sequence similar to that interpreted in well AT-4. Extrapolating geology interpreted in boreholes to the seismic line one step further, it is possible if a bore-hole were drilled at station 1590, a thick sand layer similar to that encountered in borehole 12-D might well be present. The break in reflection coherency between stations 1580 and 1600 is very suggestive of this very type of extremely variable subsurface. Interpretations of possible material types at the interfaces imaged by the seismic reflection technique at this site are very speculative as a consequence of the extreme variability in subsurface and the lack of borehole data directly on the line.

The bedrock is interpreted based on reflection characteristics and apparent continuity. The very low signal-to-noise ratio in some places makes confident identification of the bedrock surface very difficult in some areas along the line. It is especially difficult to identify the bedrock surface on the eastern half of the profile.

Line 3 was acquired to determine the three-dimensionality of the confining layer imaged near one of the edges as interpreted on line 1 (Figures 17, 8, and 9). The approximately 20 msec of apparent change in reflection depth between stations 1030 and 1060 is equivalent to about 15 to 20 ft vertical in about 60 ft horizontal. These dimensions are not unrealistic for a major river system like the Mississippi. The apparent change in reflector depth dramatically demonstrates the high degree of variability in the shallow confining layer and is more evidence in support of this
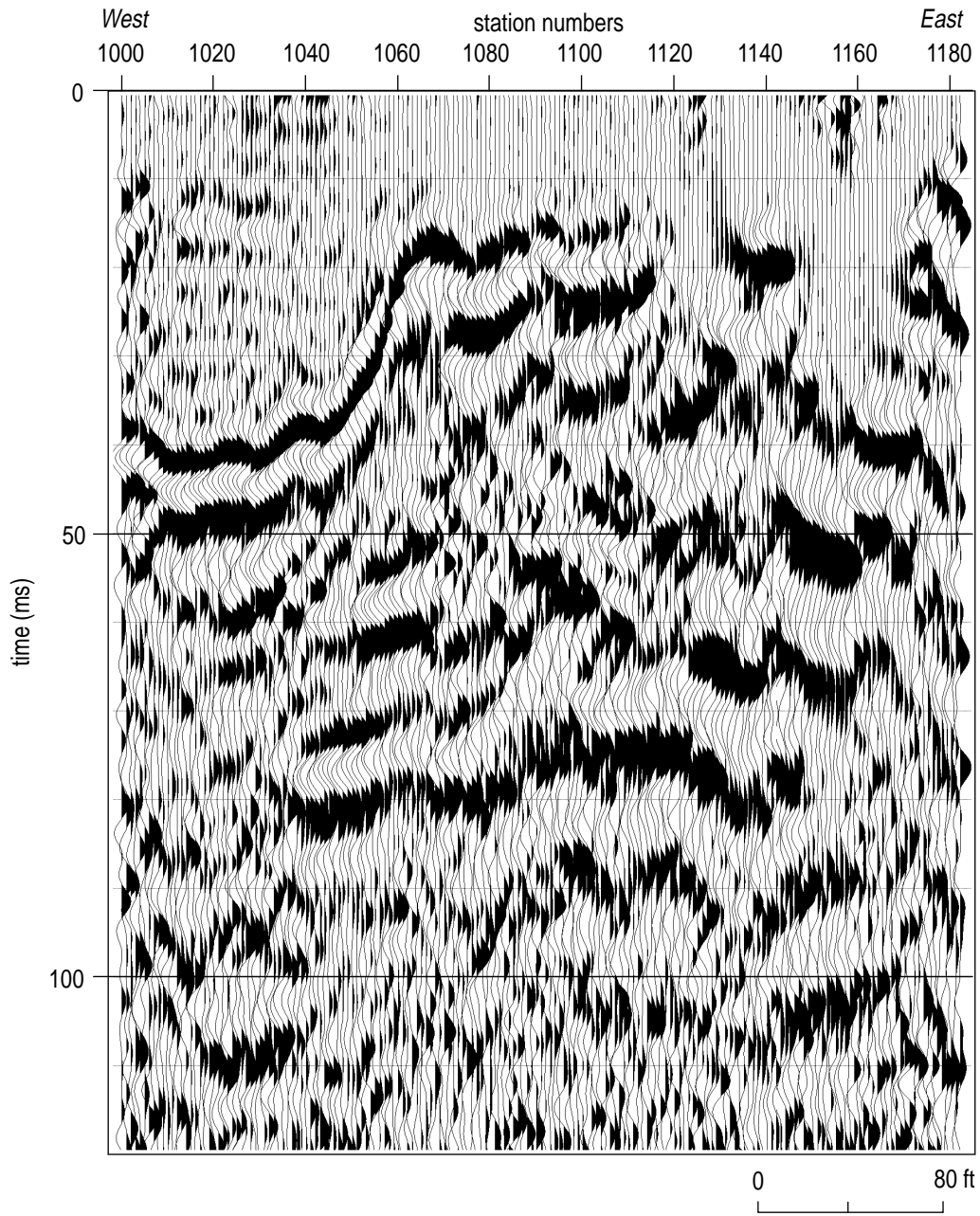
Figure 17. CDP stacked section of line 3 located along the southwest corner of the facility. Reduced fold and non-optimized source-to-receiver offsets result in deterioration of data on the eastern extreme of the line.

shallowest reflection event as being related to geology and not purely hydrology. The bedrock reflection is only interpretable over a very short distance due to the lack of longer offsets recorded on this very short line.

Interpretations of geology on this line were very speculative since well information was only available on the western extreme of the line (Figure 18). Complicating interpretations was the extreme change observed in the confining layer depth. Bedrock is interpretable from stations 1040 to about 1140 at a depth of between 60 and 70 msec. Acoustic returns from layers between the confining unit and the bedrock were very chaotic and extremely difficult to correlate across sufficient horizontal distances for confident interpretations. The terrace interpreted in the confining layer between stations 1060 and 1030 is an example of a subtle feature uninterpretable from drill data alone that could dramatically impact the movement of or act as a barrier to contaminants released at or near the surface.

Conclusions

The seismic data possess the potential to dramatically improve horizontal resolution of the drill data at this site. A geologic cross-section generated from the seismic data shows the very discontinuous nature of layers presently inferred between boreholes to be continuous. Micro-features (channel cuts, bed termina-tions, terraces, etc., less than 100 ft horizontal) can be interpreted on stacked seismic data between wells that significantly enhance the overall accuracy of the geologic cross-section. It is very possible to probable that no layers with the exception, of course, of bedrock are continuous across the length of the profile. The horizontal and vertical resolution potential of the stacked data is very consistent with that observed in raw field data.

Confirmation drilling would greatly enhance the confidence in any inter-pretation. An area between about stations 860 and 1100 on line 1 possess the least continuity and is the most likely candidate for an area without significant reflecting interfaces. Key features to focus a confirmation drilling program on include: the bedrock anomaly around station 560, the absence of reflecting interfaces around station 980, and a significant change in the elevation of the strong 45 to 50 msec reflection between stations 1300 and 1355. Any drill hole located between 870 and 1150 should encounter a section of material distinctly different from outside that zone. Drilling on line 2 should include a borehole that intersects the mound interpreted at station 1560 and the clay layers interpreted at station 1620.
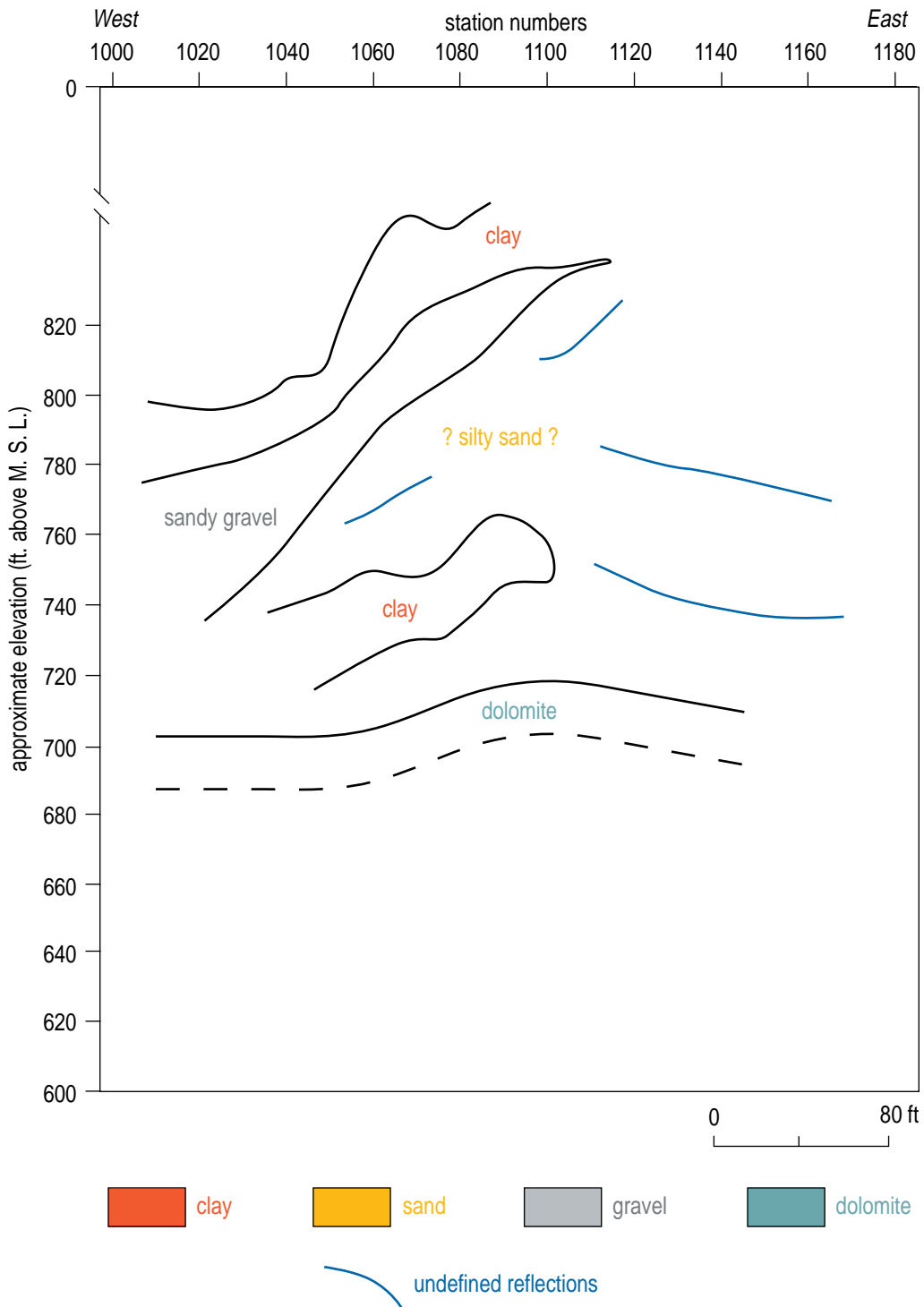
Figure 18. Interpreted CDP stacked section of line 3 using well information west of this stacked section.

Acknowledgments

References

Birkelo, B.A., D.W. Steeples, R.D. Miller, and M.A. Sophocleous, 1987, Seismic reflection study of a shallow aquifer during a pumping test: Ground Water, v. 25, p. 703-709, Nov.-Dec.

Black, R.A., D.W. Steeples, and R.D. Miller, 1994, Migration of shallow seismic reflection data: Geophysics, v. 59, p. 402-410.

Goforth, T., and C. Hayward, 1992, Seismic reflection investigations of a bedrock surface buried under alluvium: Geophysics, v. 57, p. 1217-1227.

Healey, J., J. Anderson, R.D. Miller, D. Keiswetter, D.W. Steeples, and B. Bennett, 1991, Improved shallow seismic-reflection source: building a better Buffalo [Exp. Abs.]: Soc. Explor. Geophys. v. 1, p. 588-591.

Hunter, J.A., et al., 1984, Shallow seismic reflection mapping of the overburden-bedrock interface with the engineering seismograph—some simple techniques: Geophysics, v. 49, p. 1381-1385.

Jongerius, P., and K. Helbig, 1988, Onshore high-resolution seismic profiling applied to sedimentology: Geophysics, v. 53, p. 1276-1283.

Knapp, R.W., and D.W. Steeples, 1986, High-resolution common depth point seismic reflection profiling: field acquisition parameter design: Geophysics, v. 51, p. 283-294.

Lindgren, R.J., 1990, Simulatino of ground-water flow in the Prairie du Chien-Jordan and overlying aquifers near the Mississippi River, Fridley, Minnesota: U.S. Geological Survey Water Resources Investigations Report 90-4165, 152 pp.

Miller, R.D., 1992, Normal moveout stretch mute on shallow-reflection data: Geophysics, v. 57, p. 1502-1507.

Miller, R.D., N.L. Anderson, H.R. Feldman, and E.K. Franseen, 1995, Vertical resolution of a seismic survey in stratigraphic sequences less than 100 m deep in Southeastern Kansas: Geophysics, v. 60, p. 423-430.

Miller, R.D. S.E. Pullan, D.W. Steeples, and, J.A. Hunter, 1994, Field comparison of shallow P-Wave seismic sources near Houston, Texas: Geophysics, v. 59, p. 1713-1728.

Miller, R.D., S.E. Pullan, D.W. Steeples, and J.A. Hunter, 1992, Field comparison of shallow seismic sources near Chino, California: Geophysics, v. 57, p. 693-709.

Miller, R.D., S.E. Pullan, J.S. Waldner, and F.P. Haeni, 1986, Field comparison of shallow seismic sources: Geophysics, v. 51, p. 2067-2092.

Miller, R.D., D.W. Steeples, and M. Brannan, 1989, Mapping a bedrock surface under dry alluvium with shallow seismic reflections: Geophysics, v. 54, p. 1528-1534.

Miller, R.D., and J. Xia, 1996, High resolution seismic surveys at U.S. Marine Corps Air Station, Cherry Point, North Carolina: Kansas Geological Survey Open-file Report No. 96-4.

Pullan, S.E., and J.A. Hunter, 1990, Delineation of buried bedrock valleys using the optimum offset shallow seismic reflection technique: Soc. Explor. Geophys. Investigations in Geophysics, Investigations in Geophysics no. 5, Stan H. Ward, ed., Volume 3: Geotechnical, p. 75-87.

RMI Inc., 1995, Cross-section B-B', NIROP-Fridley, Minnesota workplan for groundwater extraction system upgrade (Figure A-5): Cross section generated by RMI Inc., Madison, Wisconsin.

Schieck D.G., and S.E. Pullan, 1995, Processing a shallow seismic CDP survey: An example from the Oak Ridges Moraine, Ontario, Canada: in SAGEEP 95 Proceedings (Symposium on the Application of Geophysics to Engineering and Environmental Problems), Orlando, Florida, April 23-26.

Steeples, D.W., and R.D. Miller, 1990, Seismic-reflection methods applied to engineering, environmental, and groundwater problems: Soc. Explor. Geophys. Investigations in Geophysics, Investigations in Geophysics no. 5, Stan H. Ward, ed., Volume 1: Review and Tutorial, p. 1-30.

Yilmaz, O., 1987, Seismic data processing: Soc. Explor. Geophys. Investigations in Geophysics, Investigations in Geophysics no. 2, S.M. Doherty, ed., p. 1-30.

APPENDIX A
Walkaway Test Sites

Walkaway Site 1

The location for walkaway noise testing site #1 was selected to be as near to well D-13 as possible and along the trace of the proposed CDP production profile (Figure 1). This allowed for direct correlation with the uphole survey and to get an idea of data quality and potential along a portion of the actual proposed production line. All three sources were tested under as near ideal conditions as possible for each. The nearby four-lane East River Road and overhead power lines provided noise sources. In the case of the road, traffic noise was managed by attention to vehicle flow. The power lines, however, provided few options that would allow reduced levels of recorded electric noise (60 Hz, 120 Hz, 180 Hz, 240 Hz, etc.). The stacking source (sledge hammer) provided some advantages over single-impact sources with respect to noise by nature. The receivers were placed at 2 ft intervals with sources occupying locations on both the north and south ends of the line.

Spectral properties of each source were similar with only subtle differences in relative bandwidth and ratio of bodywaves to noise (Figure A1). The obvious difference between the three sources is the higher level of air coupled wave and the lower percentage of high frequency bodywaves on the sledge hammer in comparison to the explosive sources. The downhole 30.06 seems to have more usable energy in the frequency band between 125 Hz and 250 Hz than either of the other sources. This observation is consistent with the digitally filtered walkaway files discussed later in this report.

The downhole 30.06 provided the highest usable upper corner frequency in the reflection bandwidth and the least recorded ground roll and air coupled wave. The unfiltered shot gathers clearly show the relative amount of energy from the various types of waves (Figure A2). Wide angle reflection energy from the water table is evident as the high amplitude curved arrival that starts about 40 msec and then immediately becomes asymptotic to the direct wave. Digital filtering of the 30.06 downhole source enhances the reflection energy present and allows for very confident correlation of reflections to reflectors (Figure A3). The offsets observed in the first arrivals that appear similar to faulting are the result of changes in source location. Reflections at offsets greater than about 60 ft are from bedrock and sub-bedrock layers. The dominant reflection frequencies are around 200 Hz for most reflections, with some in excess of 225 Hz. A second shot recorded in the same hole
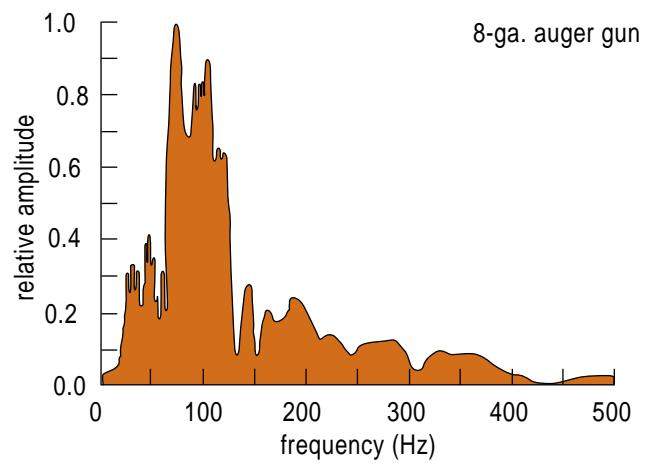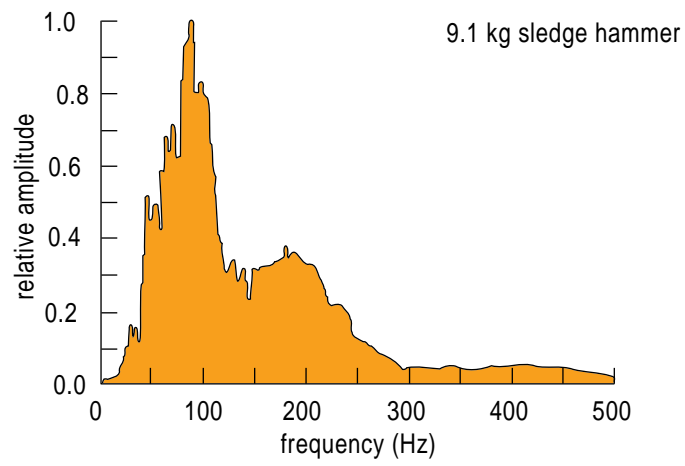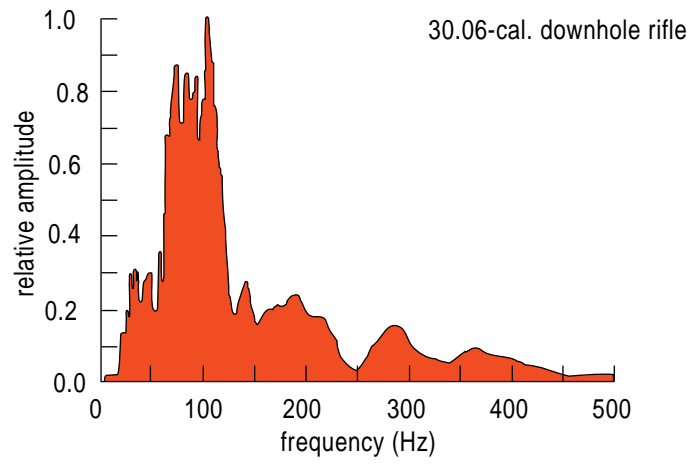
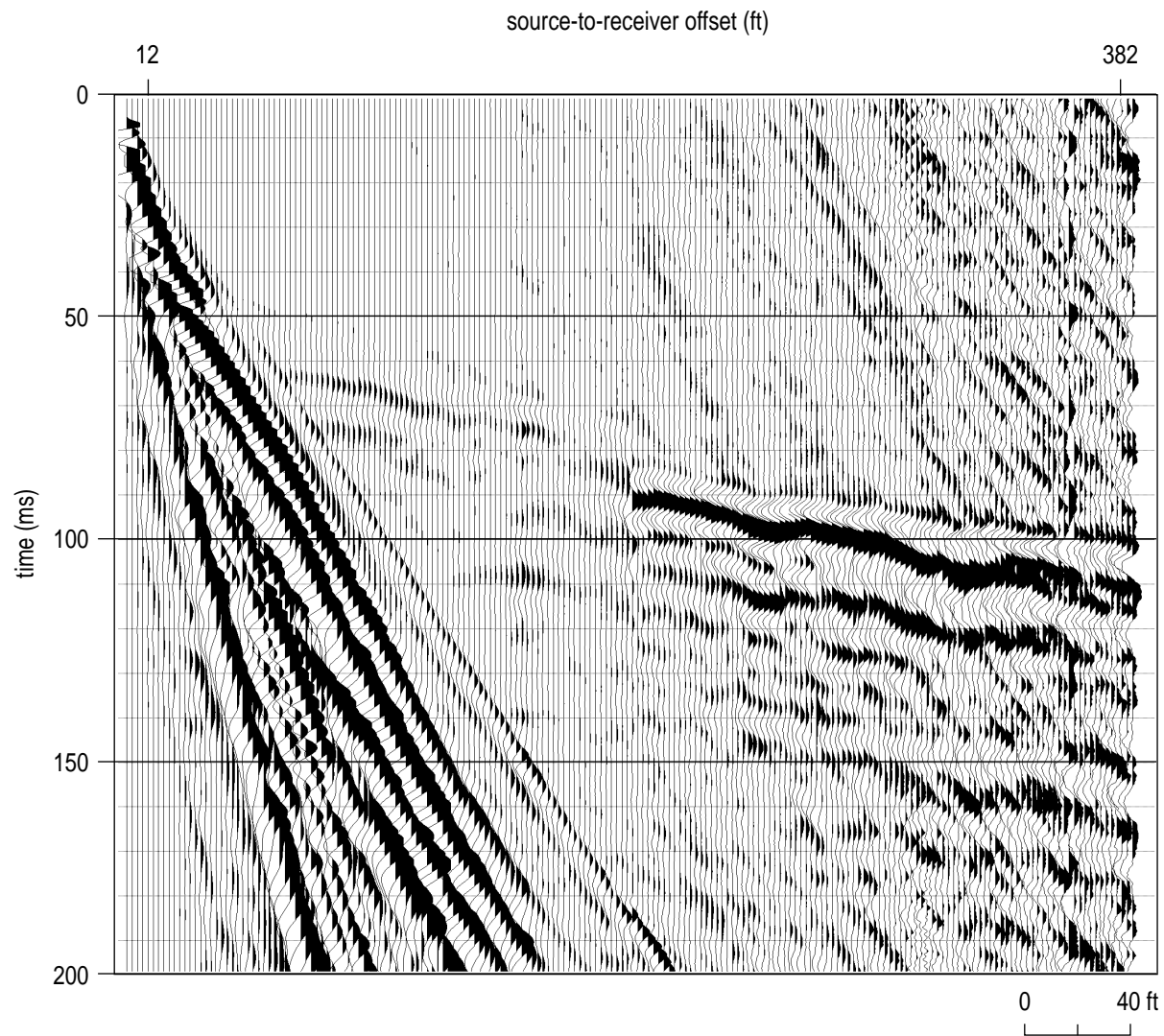Figure A1. Walkaway site #1 (WS1), whole record normalized source spectra.

Figure A2. Unprocessed 30.06 shot gather from WS1 containing 194 traces, each separated by 2 ft. The apparent offset between traces 96 and 97 are source static problems resulting from combining two field files with different source locations.
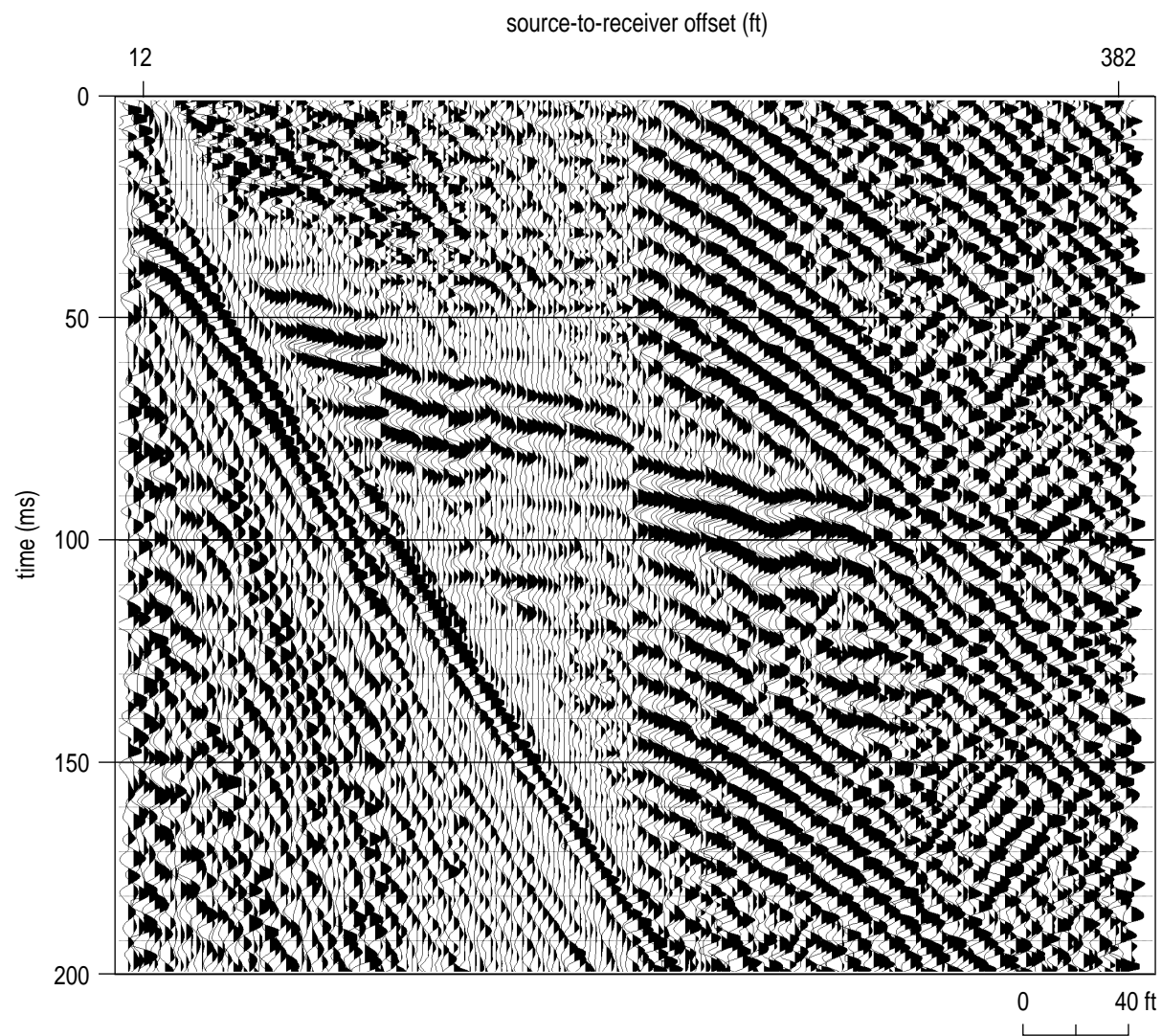
source-to-receiver offset (ft)

12   382

0   40 ft

Figure A3. Digitally filtered shot gather from WS1. The apparent time offsets in first arrivals are from either source static or timing irregularities between the two 48-channel seismographs, which was noted during acquisition and corrected at that time.

as the first was recorded to test the well documented observation that hole conditioning many times increases the amount of high frequency energy propagated from an explosion (Miller et al., 1992; 1994) (Figure A4). In this case only minor improvement was observed. To insure the arrivals are at least locally consistent, shots were recorded from opposite ends of the spread (Figures A5 and A6). These reverse shots can also provide valuable information about dip, velocity, and depth of and to the refracting layers. From the opposite end some improvement is noted with the second shot (Figure A6). All things considered, the water table and bedrock are well imaged with the 30.06 downhole.

The 12 lb sledge hammer represents the only non-invasive, vertically stacking weight drop source tested at this site. The high ratio of air wave and ground roll to reflection energy is evident on the unfiltered shot gather (Figure A7). It is also interesting to compare the dominant frequency of the 40 msec reflection on sledge hammer data with the same event on downhole 30.06 data (Figure A2). The higher dominant frequency of the gun is evident. A filtered shot gather from the north end with a single shot provides only marginally interpretable reflection arrivals (Figure A8). However, the six-shot vertical stack with the hammer provides a much higher signal-to-noise ratio and therefore permits easier interpretations of both bedrock and water table reflections (Figure A9). From the reverse direction the water table reflection is not as evident, but the bedrock reflection, on the other hand, has very nice separation (diverging) from the refraction which provides for a much higher quality and more accurate CDP stacked section (Figure A10). The six-shot stack from the reverse direction does not increase the signal-to-noise ratio quite as much as from the north. Some noise reduction is obvious while little if any reduction in dominant frequency can be detected (Figure A11). Vertically stacking many times boosts the signal-to-noise levels at the expense of resolution potential (i.e., dominant frequency).

The 12-gauge auger gun detonated a 165 grain black powder blank load in a water-saturated hole at a depth of 2 ft. The raw shot gather clearly possesses the 40 msec water table reflection and a relatively strong 60 msec reflection event from the bedrock surface (Figure A12). Visible reflections from bedrock is uncommon on unfiltered auger gun records at this site. After digital filtering the signal-to-noise ratio increases but the bandwidth decreases (Figure A13). This decrease in bandwidth is inevitable when digital filtering alone is increase the resolution potential by flattening the spectra and increasing the dominant frequency. This is true especially when the spectra is not sufficiently rich in high frequency reflection
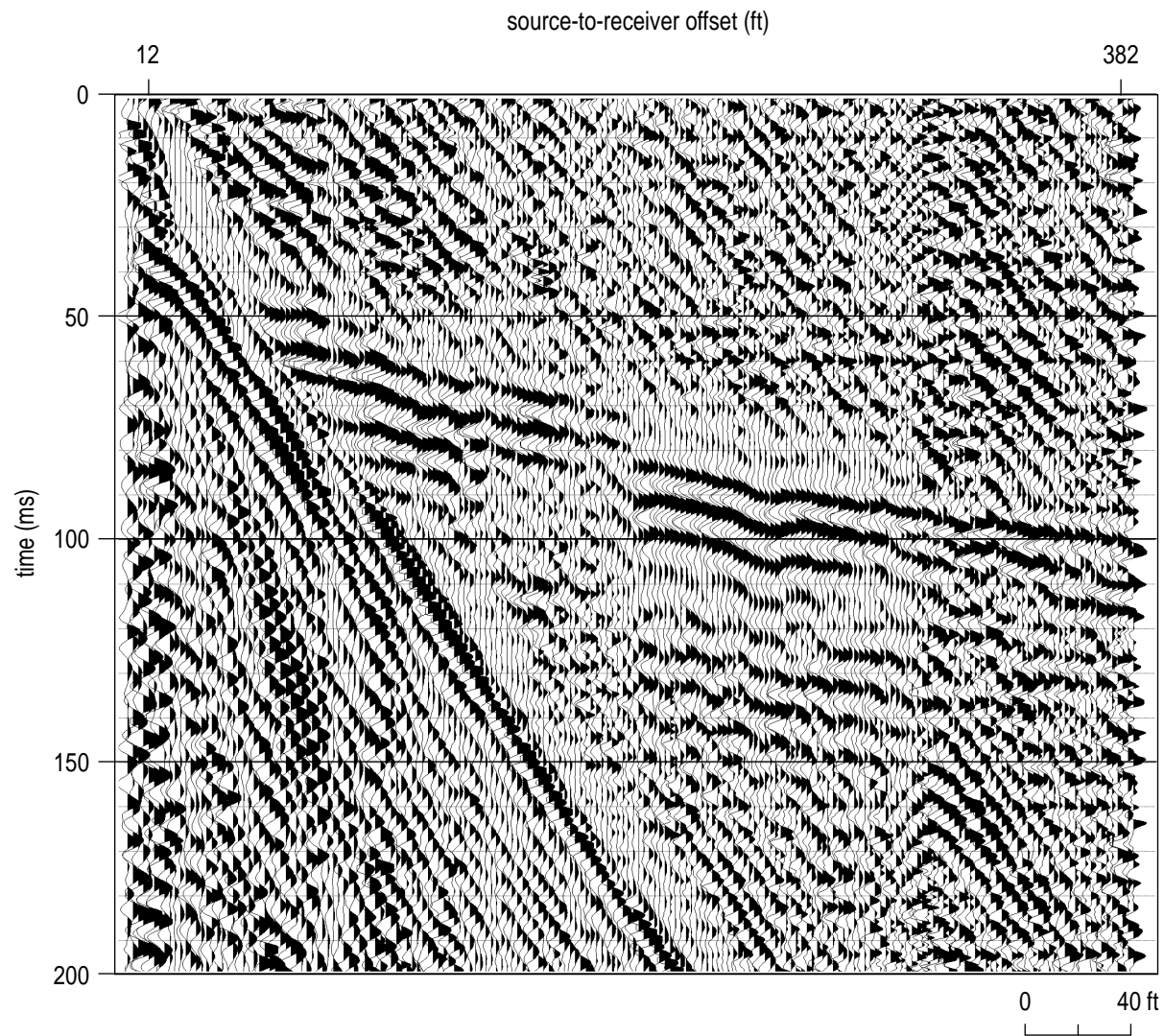
Figure A4. Second shot into the same shot hole as Figure A3. Changes in background noise are related to East River Road traffic. This digitally filtered file possesses several interpretable reflections.
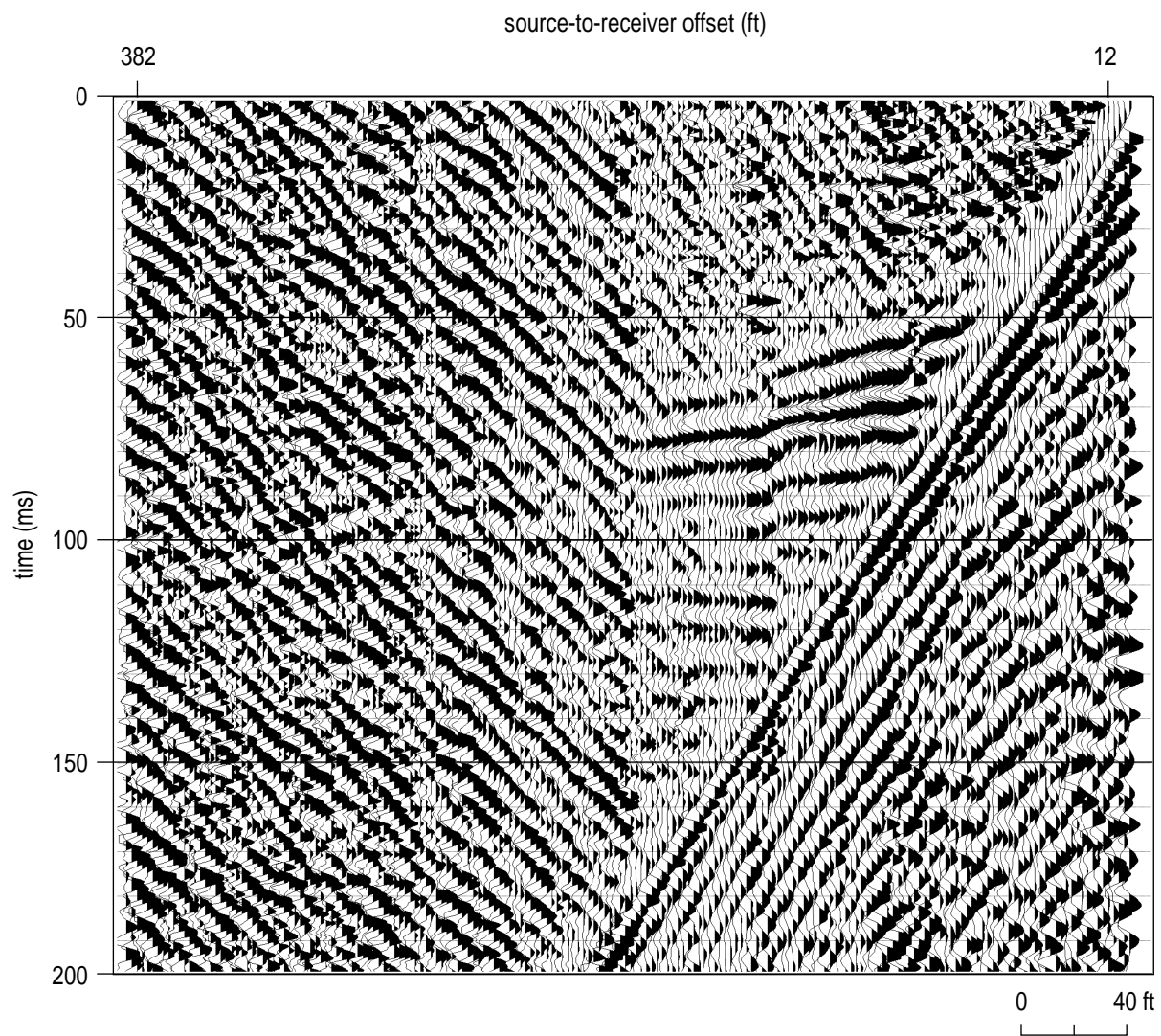
Figure A5. Reverse shot direction, digitally filtered shot gather from WS1. Reflection events and coherent traffic noise are apparent. This reverse shot possesses characteristics similar to previous forward shots (Figures A3 and A4).
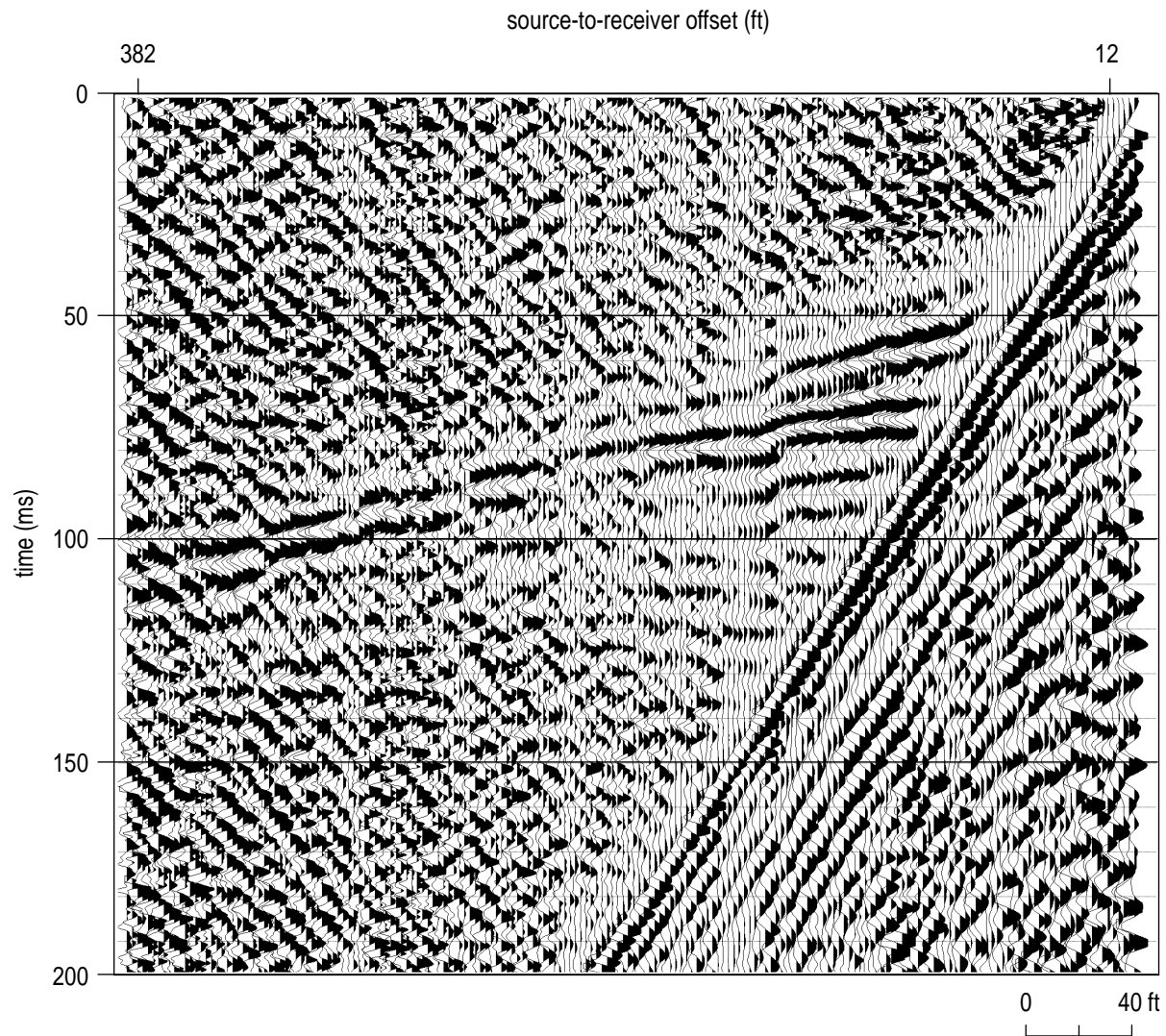
source-to-receiver offset (ft)

382   12

Figure A6. Second shot into the same shot hole as Figure A5. A strong bedrock reflection at about 65 msec is evident at close offsets.
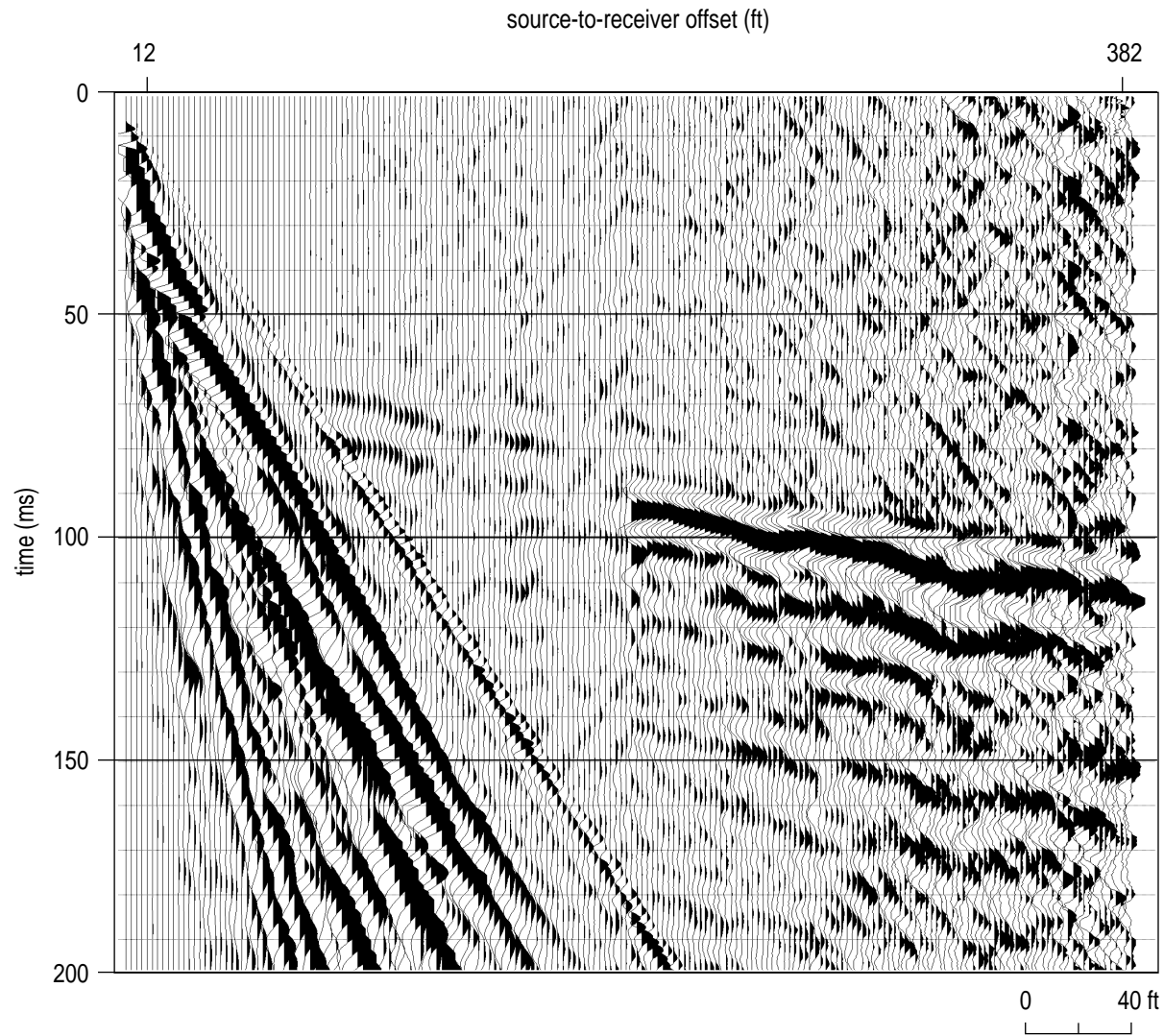
Figure A7. Unfiltered shot gather using a 16 lb sledge hammer for a source at WS1. This single shot clearly possesses more air-coupled wave and lower dominant frequency than the data from the downhole 30.06 in Figures A2 through A6.

source-to-receiver offset (ft)
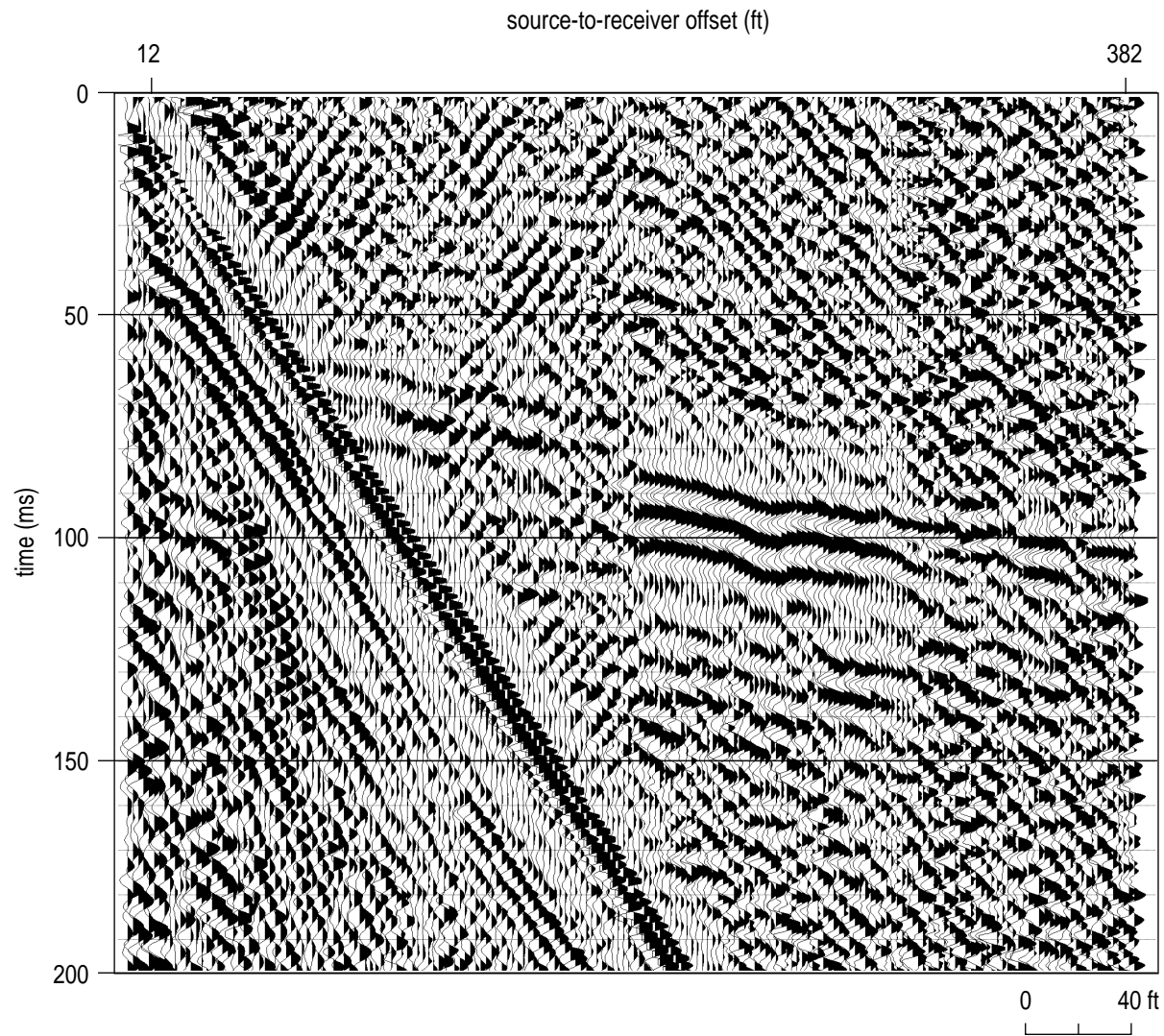
Figure A8. This digitally filtered field file of a single sledge hammer impact has interpretable reflections from about 45 msec to as deep as 100 msec. The signal-to-noise ratio is lower than on equivalent downhole 30.06 data at WS1.
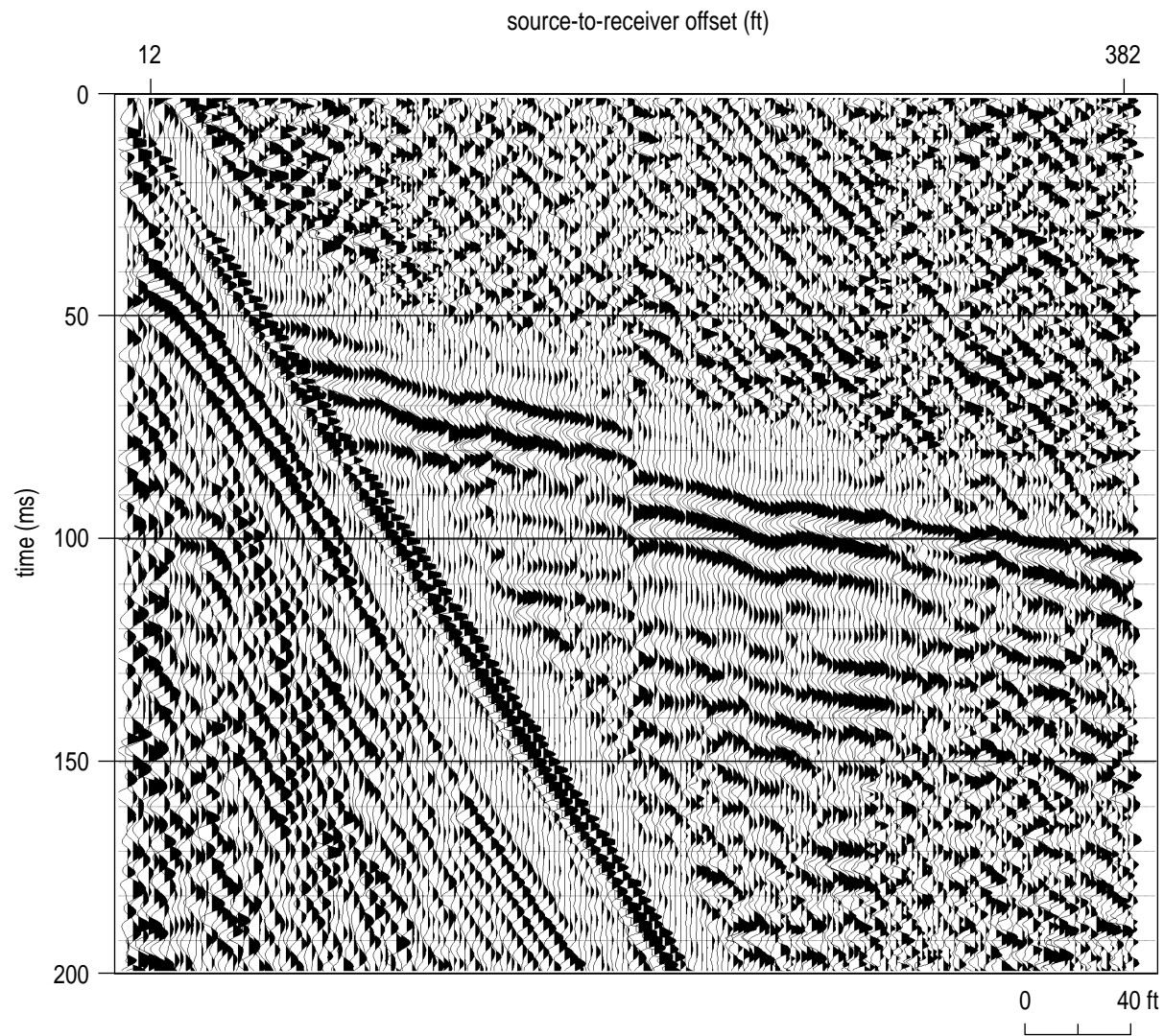
Figure A9. This four-shot vertical stack clearly demonstrates the signal-to-noise improvement with multiple impacts per shot station. The frequency content does not seem to improve with increased signal-to-noise.
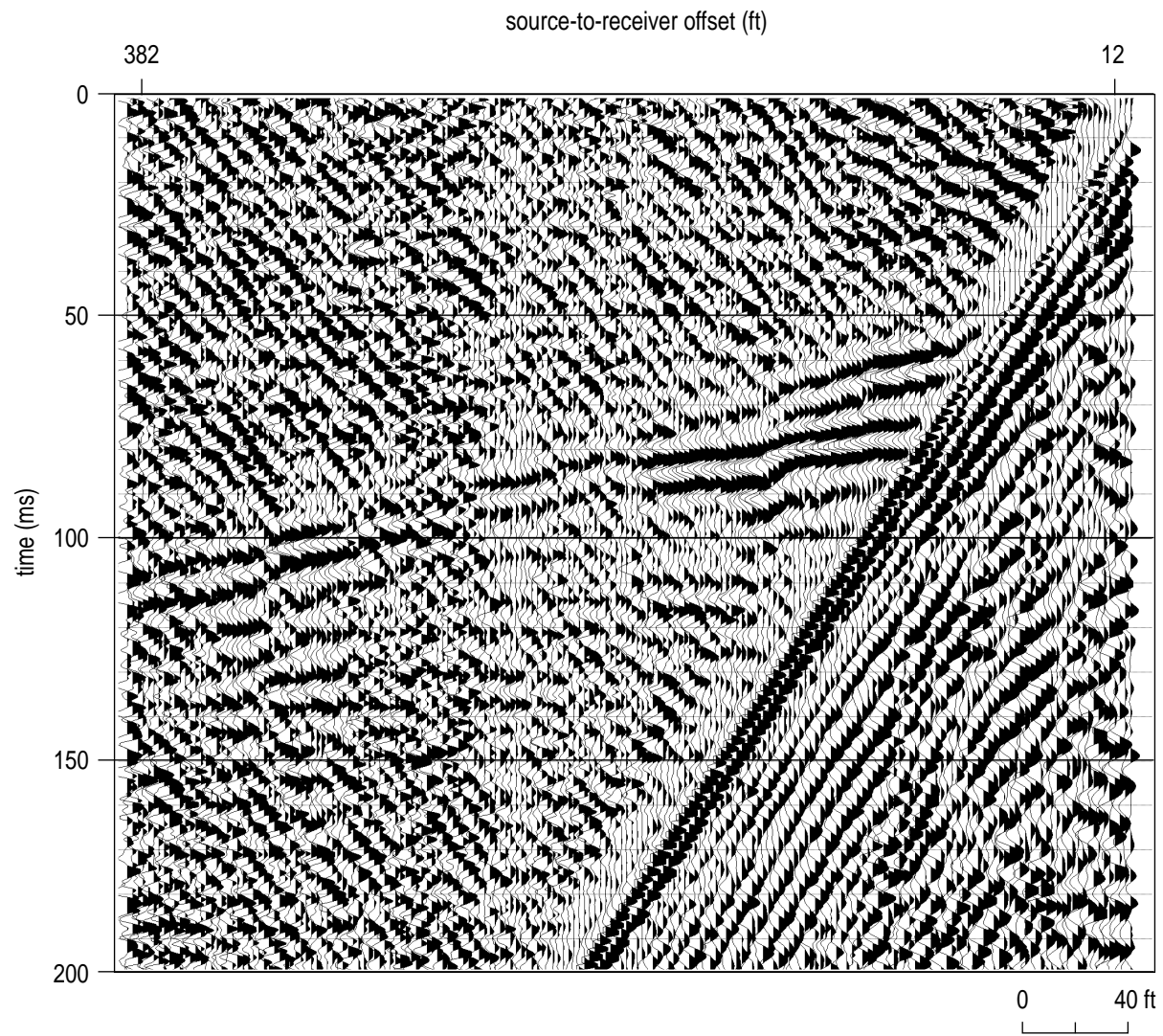
Figure A10. Single shot gather from the reverse direction with the sledge hammer at WS1.
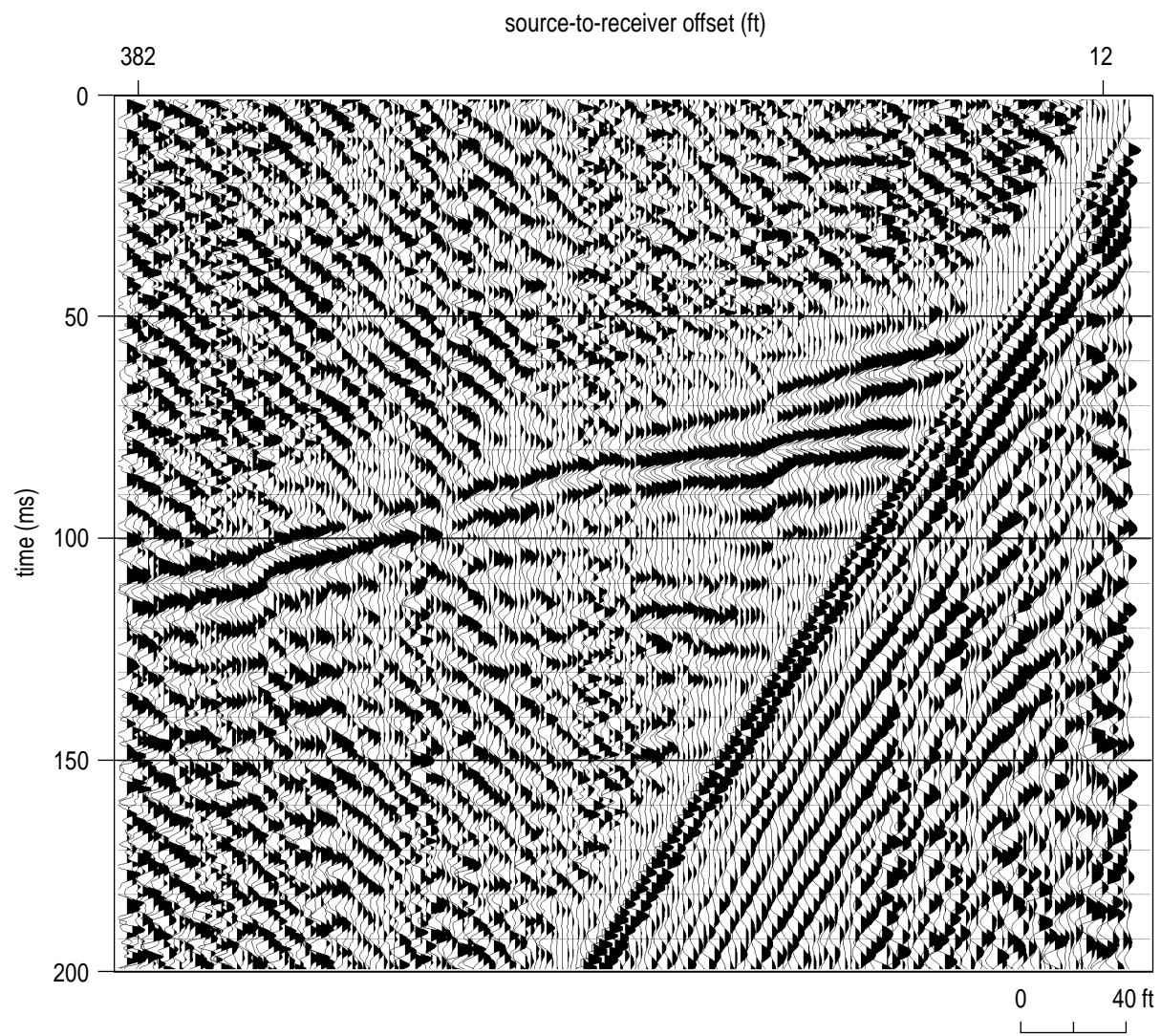
Figure A11. Again the signal-to-noise improves with the vertical stacking of sledge hammer impacts.
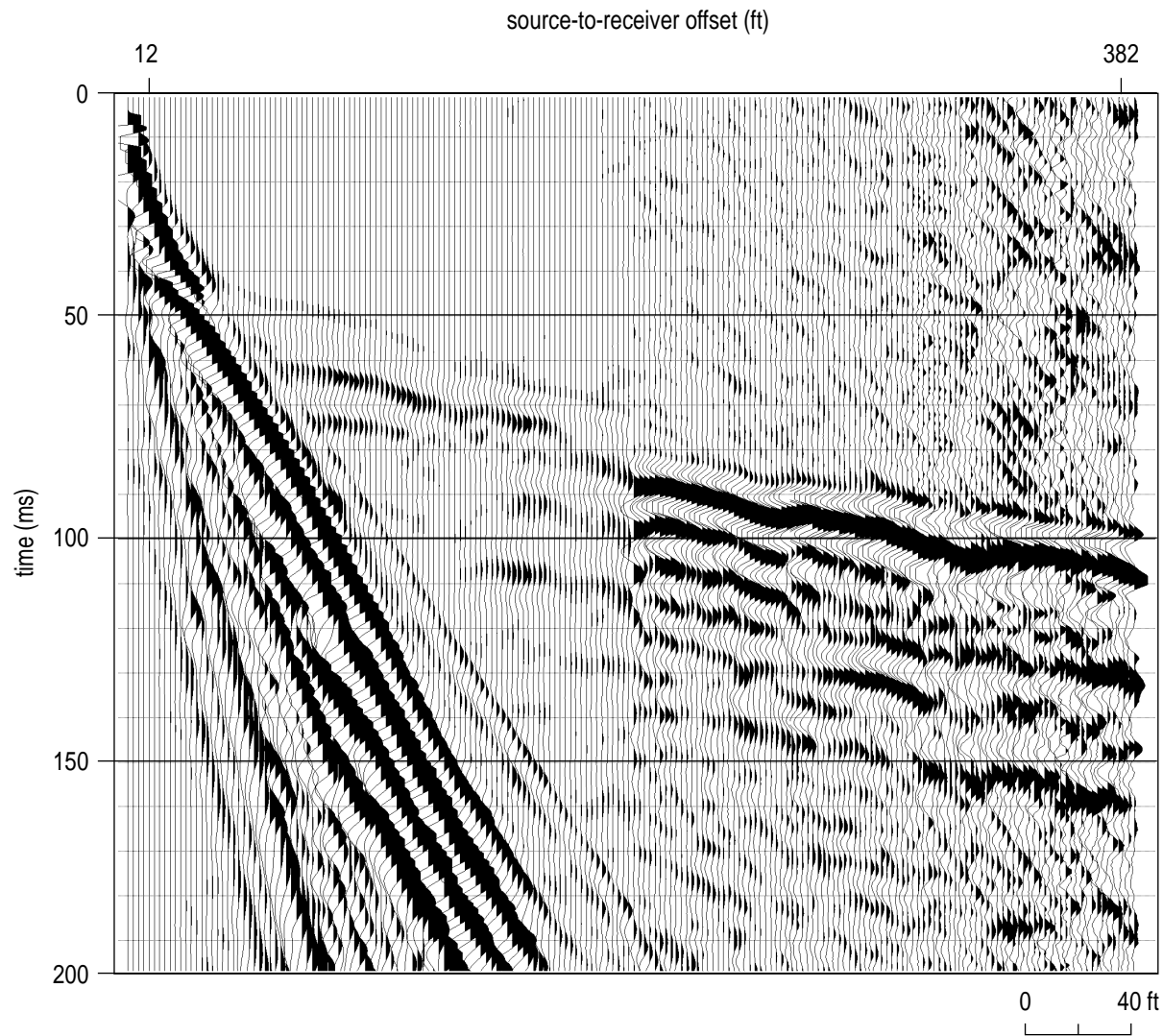
Figure A12. Raw 12-gauge auger gun shot gather from WS1. On this raw file the shallow low-velocity reflection as well as several other very pronounced reflections above bedrock and bedrock itself are interpretable.
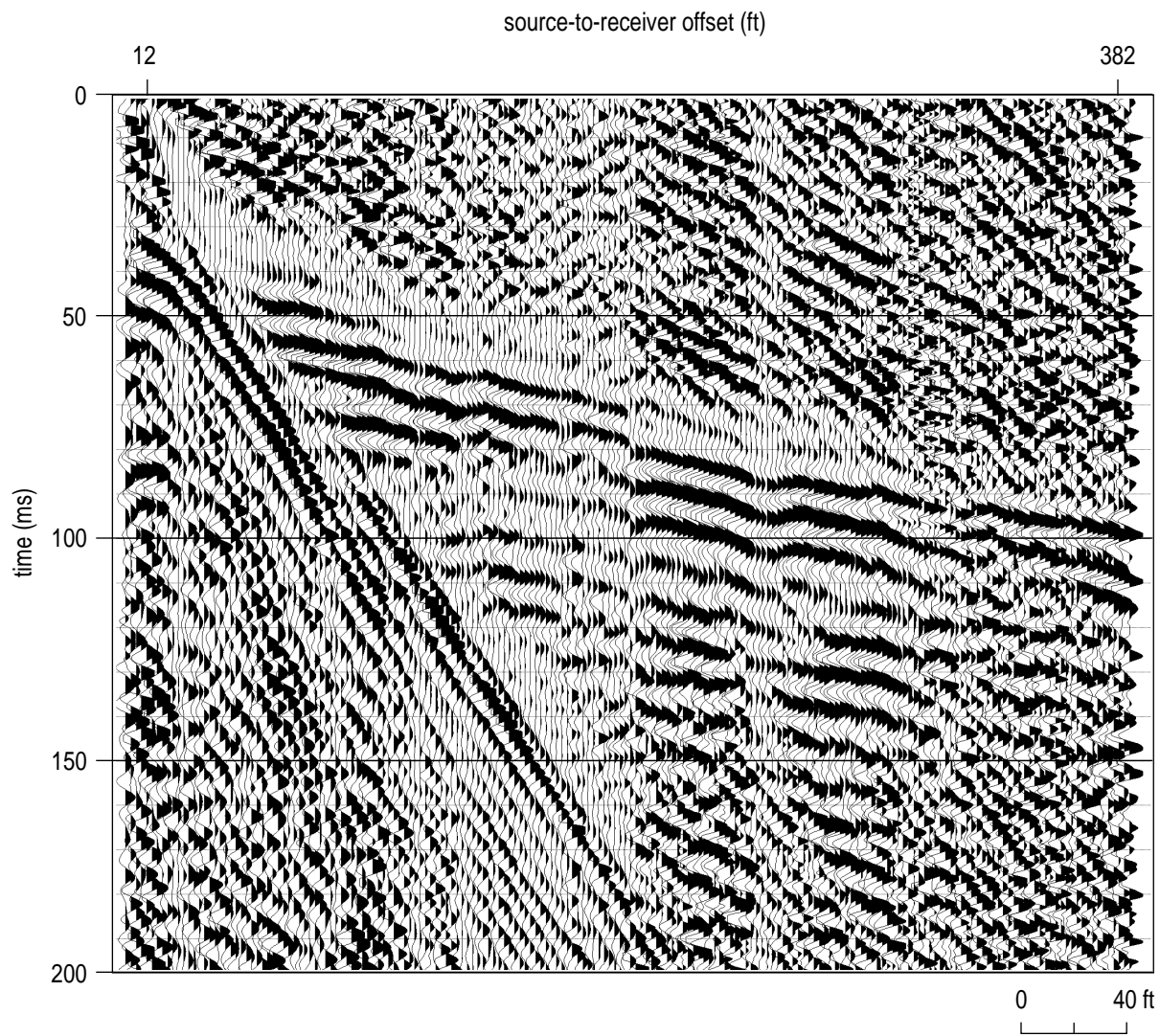
Figure A13. Digital filtering of the auger gun data deteriorated the overall quality. This is likely due to the filter design, which was focused on the 30.06 data. All auger gun records are from single shots.

signal. The second shot in the same hole (increasing depth to almost 3 ft) seems to increase the bandwidth a little, but the dominant reflection frequencies are still in the mid-100 Hz range (Figure A14), which is clearly below the 200 Hz plus obvious on the downhole 30.06 (Figure A3). As with the sledge hammer, shooting from the south end of the line results in a well separated bedrock reflection that for the most part is consistent with reflections identified on files recorded from the north (Figure A15). The deeper shot burial does not seems to significantly change the reflection wavelet properties or characteristics.

Results of the walkaway noise test in conjunction with the uphole survey were the basis for selection of equipment and acquisition parameters optimized for reflections to stack on CDP profiles along the west perimeter fence. Reflections arriving from between the water table and bedrock surface will arrive within a narrow time window from 30 msec to 60 msec and require at least a 200 Hz dominant frequency to have the potential to image clay layers at around 40 ft (40 msec). Based on the results of the site #1 walkaway and the uphole survey, data were recorded using the downhole 30.06, single 100 Hz geophones, 2 ft receiver spacing, 4 ft source spacing, split-spread source/receiver geometry, source off-line offset of 4 ft, 96 channel recording, one shot per station, and no analog filters.

Walkaway Site #2

Walkaway site #2 was selected to determine the feasibility of collecting reflection data on the asphalt or cement around and/or within the building (Figure 1). The site was proposed as an intermediate step between recording in a grassy area along the western boundary (i.e., site #1) and recording on 100% asphalt/cement. The geophones were planted in a grassy median strip immediately north of the north business entrance to the building. Geophone placement in the grass and source stations on asphalt or gravel allowed comparisons of the influence source coupling/environment has on the seismic wave field. Site #2 is also an area that has been heavily worked and reworked during building construction and later renovations. The goal and attractiveness of this particular site was the ability here to study the effects of changing one parameter at a time. Due to the limited amount of room available to plant receivers, only 90 phones were deployed as opposed to the 96 laid for test sites #1 and #3. The geophone spacing was also reduced to 1 ft to allow improved event coherency and easier identification of the anticipated very weak and offset limited reflection arrivals.
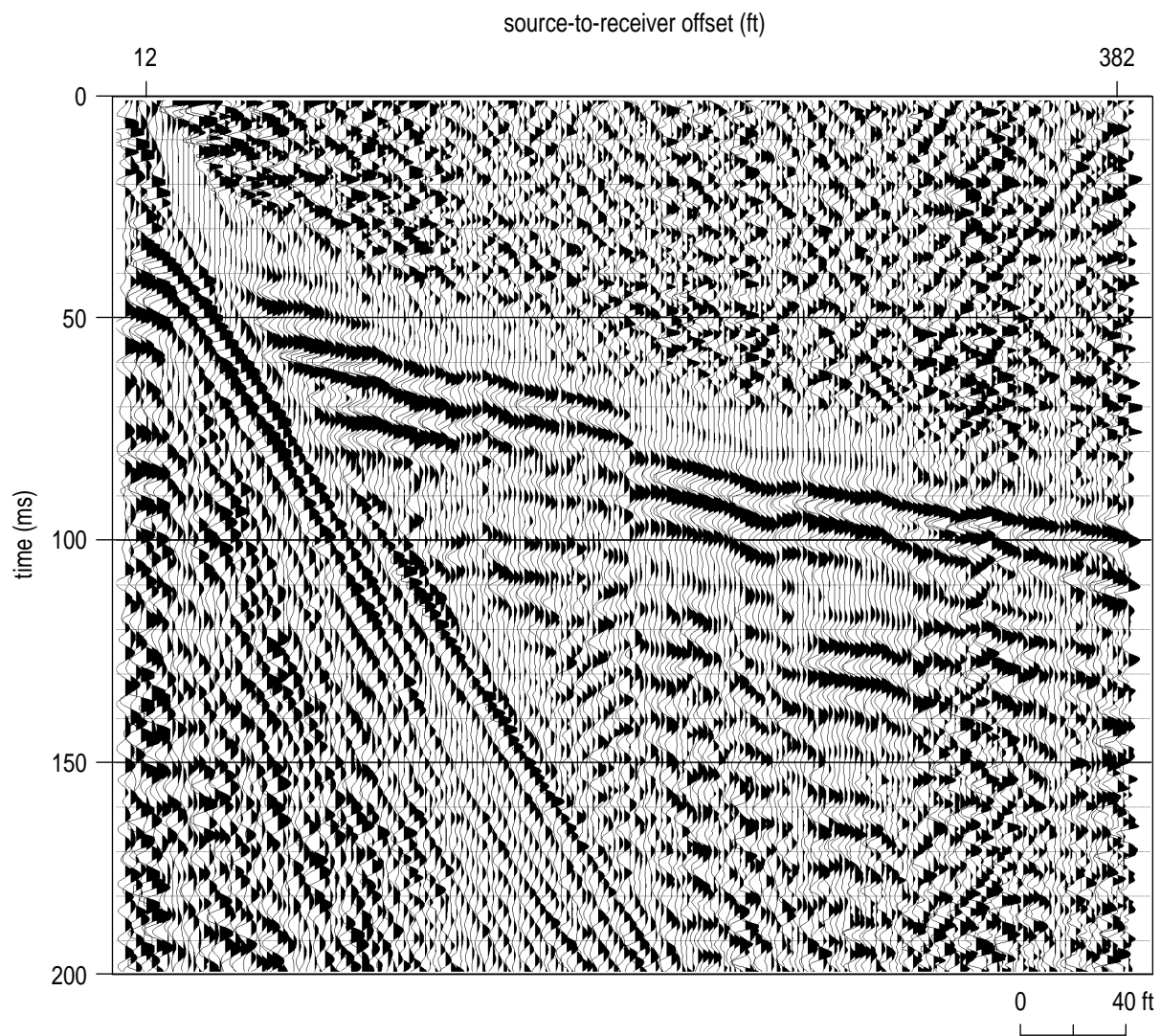
Figure A14. The second shot in the auger gun hole resulted in a noticeable improvement in reflections within 100 ft of the source.
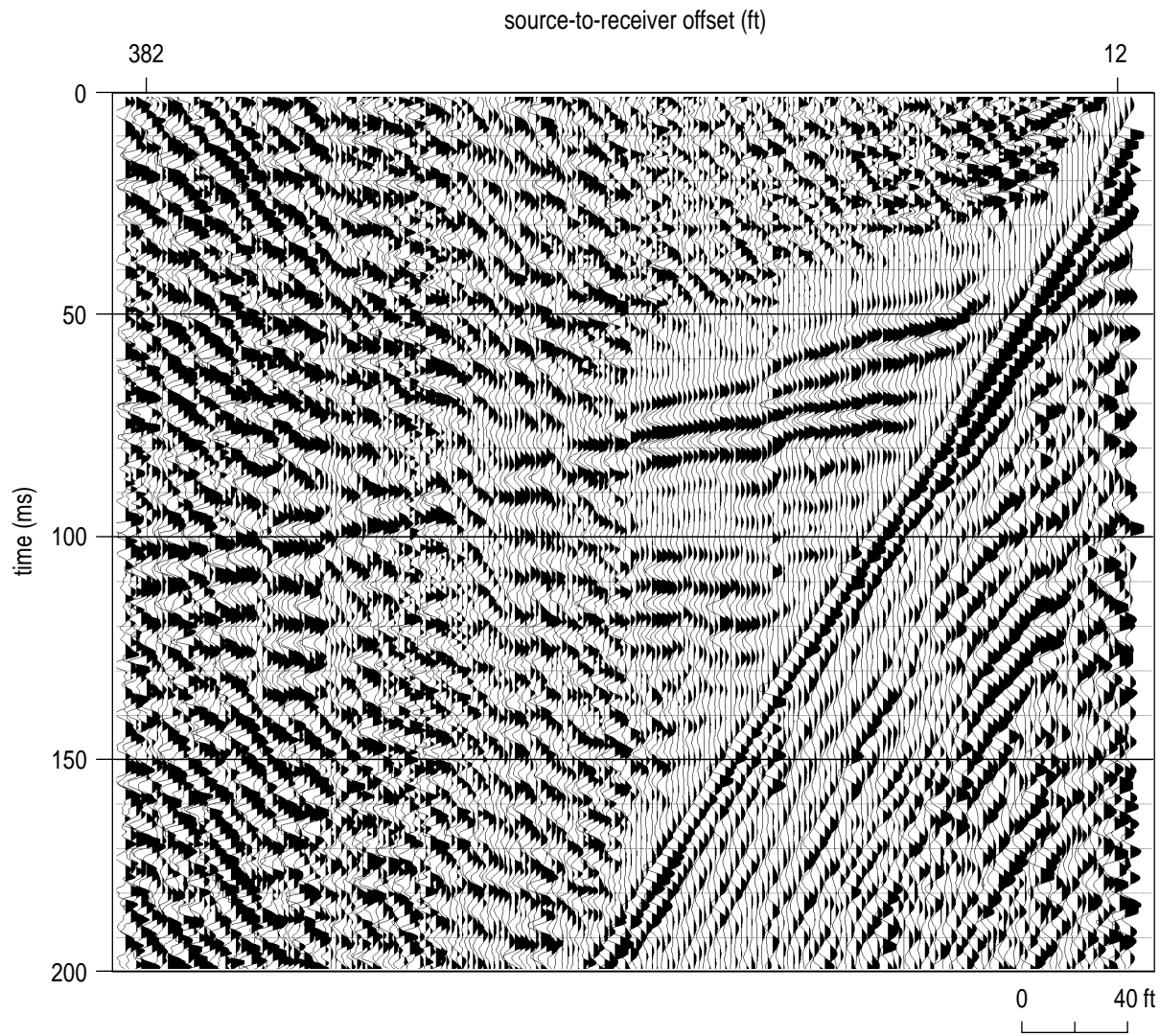
source-to-receiver offset (ft)

382

12

time (ms)

0

50

100

150

200

0   40 ft

Figure A15. This reversed direction auger gun record possesses signal quality similar to the 30.06, but at slightly lower dominant frequencies.

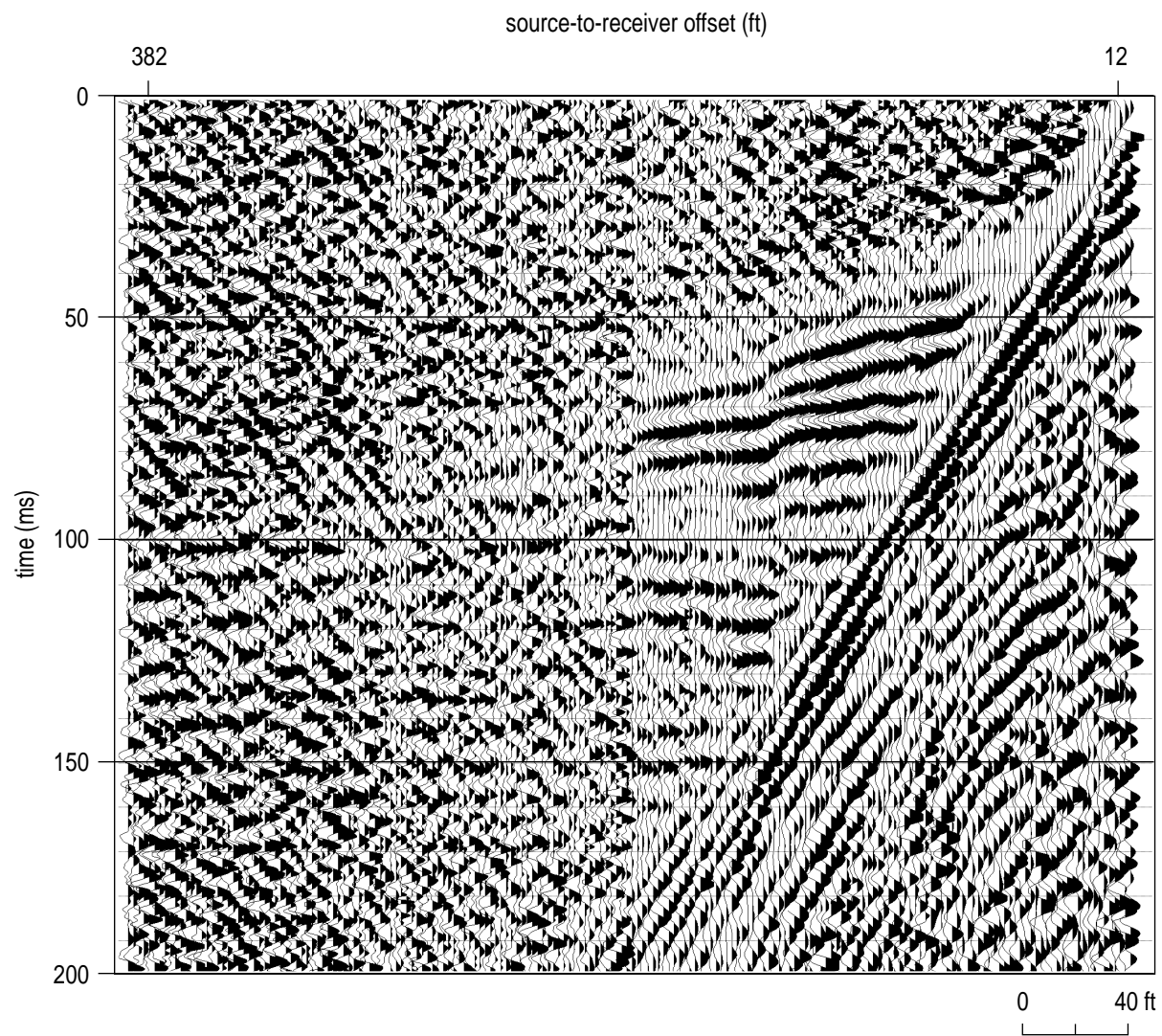source-to-receiver offset (ft)

Figure A16. The second shot into the auger gun shot hole again improved the signal-to-noise but did little to the resolution potential. This record is from a single shot.

The spectral properties of the sources were adversely effected by the change in near-surface material (Figure A17). This is no surprise for the downhole sources since moist, fine grained, and native materials are optimum for generation and propagation of high frequency energy for these sources, however, the obvious reduction in the high frequencies in hammer data suggests it too is negatively affected by this environment. It is also evident that the dominant frequency range for all three sources is 80 to 100 Hz with the two downhole sources possessing broader acoustic bandwidths. Frequency and wave field observations on the time section reveal this increased bandwidth to be predominantly noise from sources in or near the building. The effective bandwidth of the reflection signal is slightly narrower than even the sledge hammer spectrum suggests since a portion of that energy is noise remaining even after the 5 to 10 vertically stacked shots per station.

Since it was not easily possible to get a hole deep enough to safely fire the 30.06 downhole in the gravel area adjacent to the asphalt, in the asphalt, or in the cement, a single offset was acquired in the grassy median near the geophones. The median area had clearly been altered during construction of the building and parking lot, hence the gun did not couple effectively enough to transmit the broad bandwidth compressional wavetrain observed at site #1 (Figure A18). The water table reflection is evident with origin time of 40 to 45 msec. A possible bedrock reflection could be interpreted on longer offset traces at times around 70 msec. The water table reflection can be interpreted with a degree of confidence; the bedrock, however, is very speculative. The two most noteworthy events on this section are 1) the strong set of reflections that are air wave echo from the building arriving at times of 90 msec and 120 msec, and 2) the high velocity direct wave through the cement curb arriving at times between 10 and 20 msec (Figure A19). Little in the way of improvement or even change is noted in the second shot in the hole (Figure A20). The reverse shot (from the east) clearly shows the detrimental effects of not recognizing an air wave echo (Figure A21). The building echo is absent, or at least subdued or different, from the reverse direction shot gather. On CDP stacked data, if not carefully removed during processing, such an artifact could appear as a discontinuous undulating reflecting interface, much like a clay stringer. Or worse yet, a line that paralleled a wall for longer distances might be interpreted on stacked reflection data as a continuous confining layer that really is not present.

Sledge hammer data from this site possess both a very strong air coupled wave component and only minimal background noise (Figure A23). The low noise levels are of course due to the vertical stacking possible with weight drop style
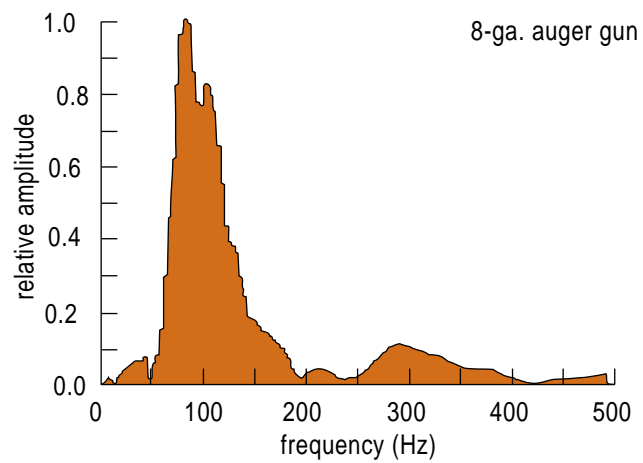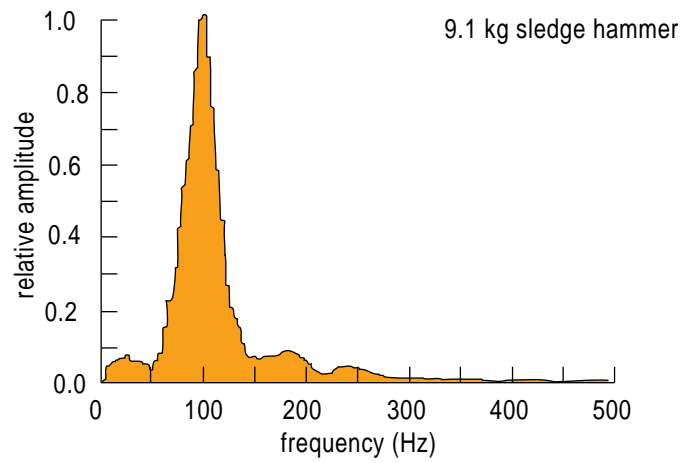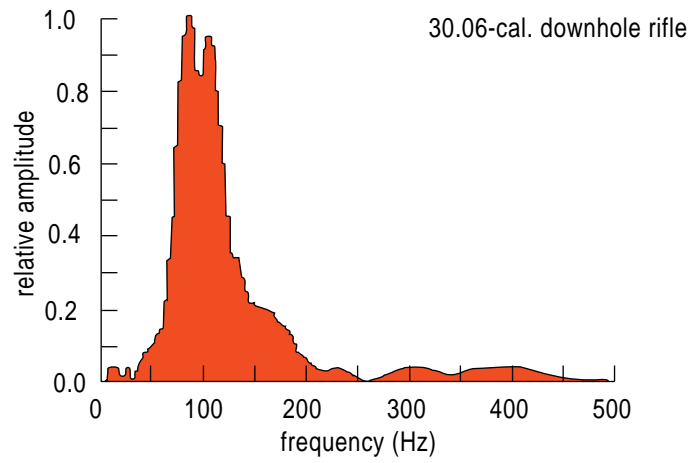
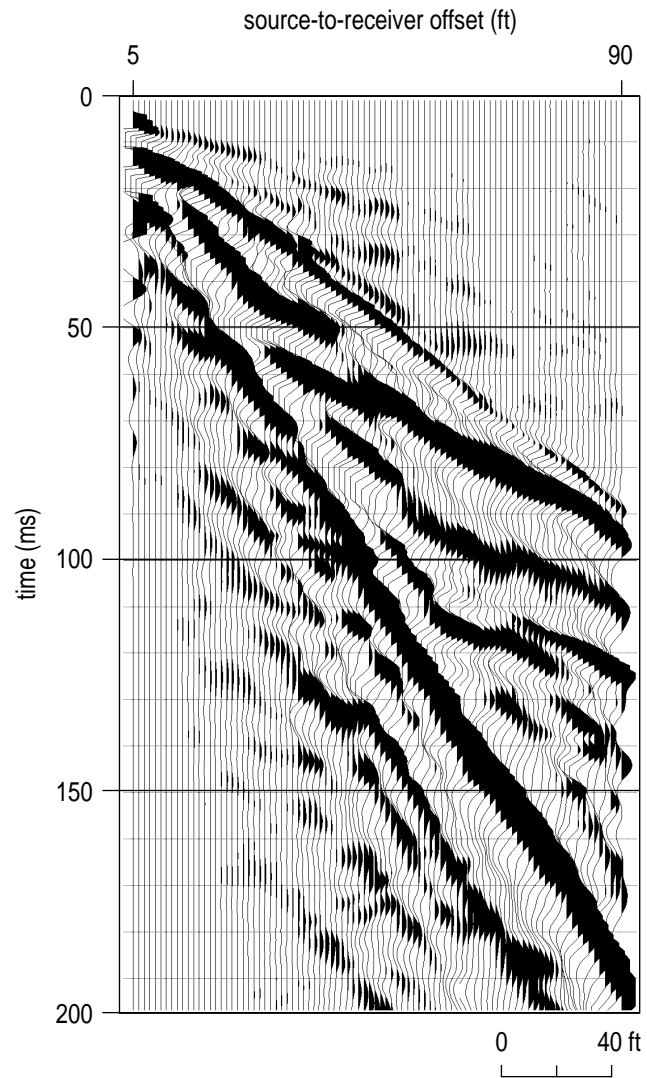Figure A17. Walkaway site #2 (WS2), whole record normalized source spectra.

Figure A18. This 85-channel shot gather from the 30.06 was collected in a manicured grassy strip between the parking lot and the main building identified in this report as WS2.
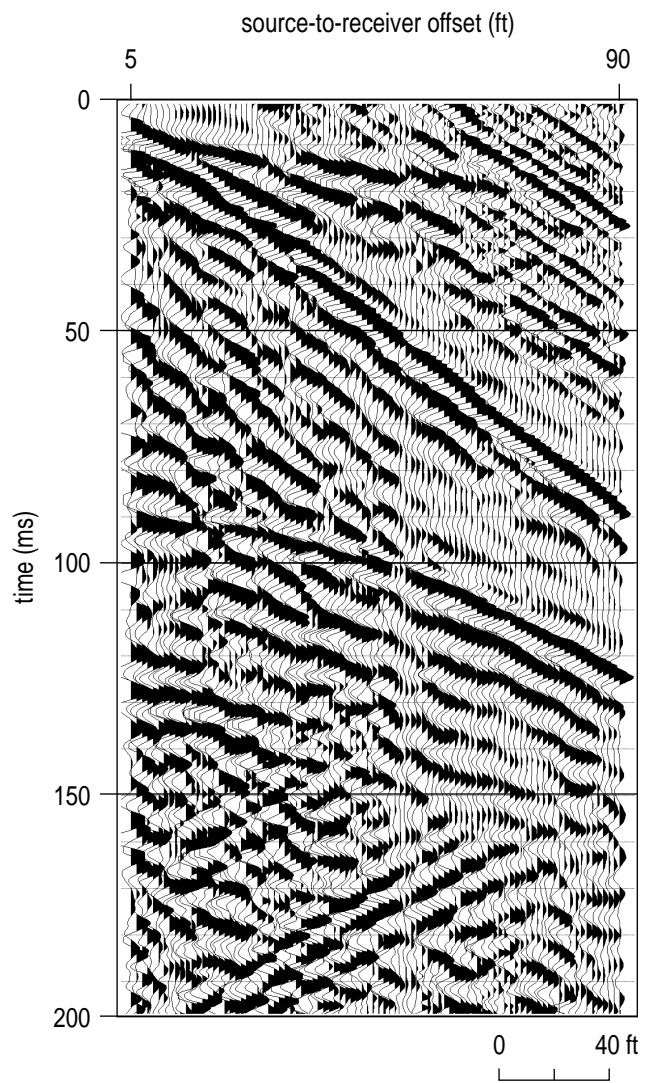
source-to-receiver offset (ft)

Figure A19. Digital filtering of this 30.06 record provides a very clear view of the various coherent
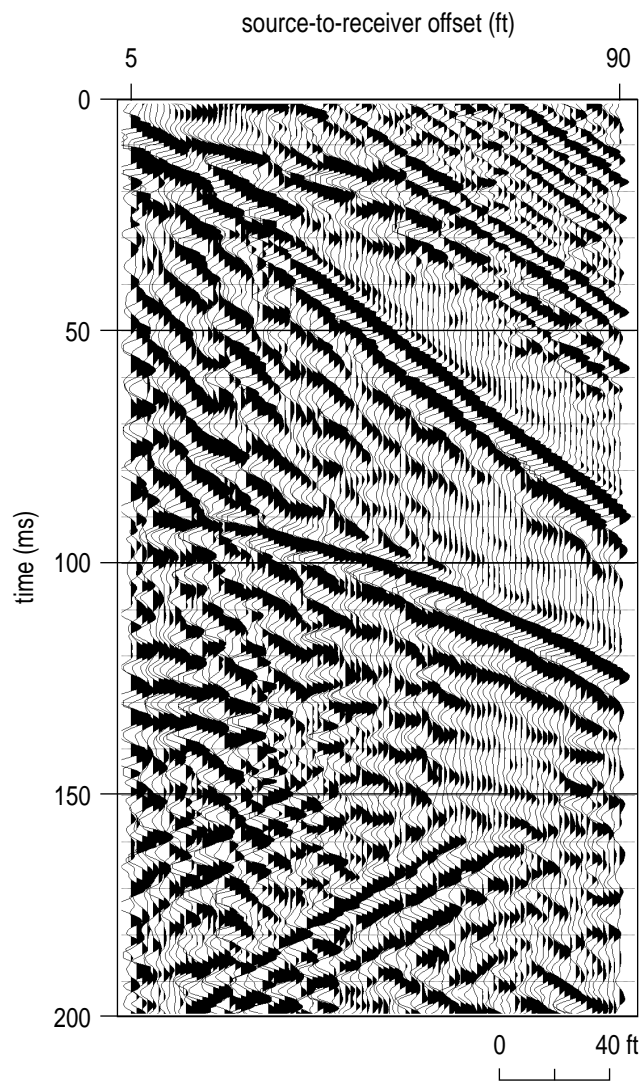noise sources and unique arrival patterns from each.

Figure A20. The second shot into the existing 30.06 shot hole does little to enhance reflections from subsurface geologic interfaces.

source-to-receiver offset (ft)
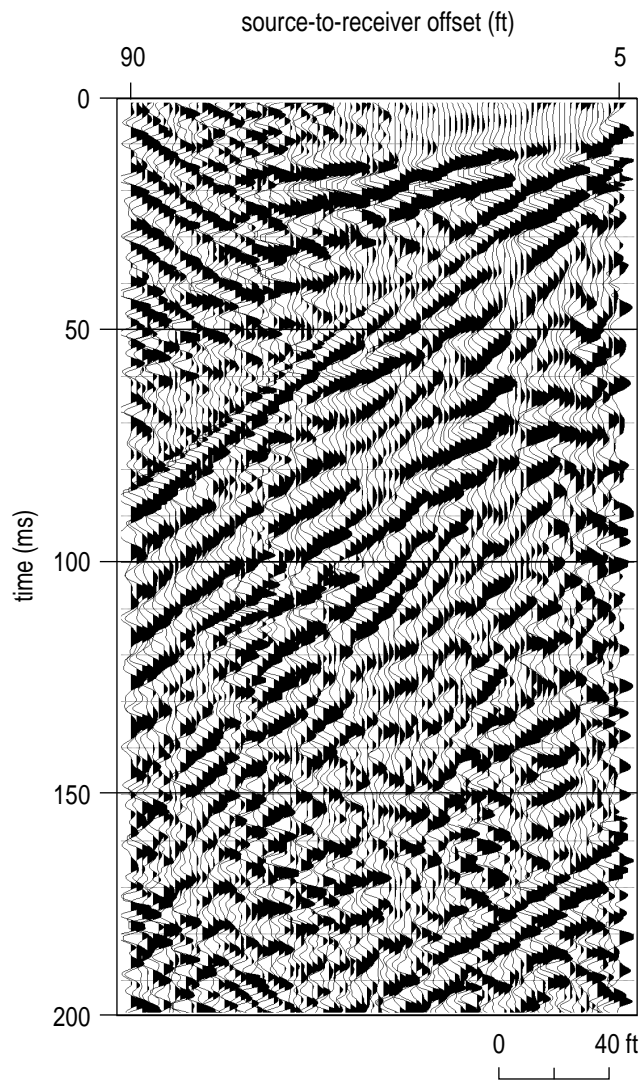
Figure A21. Acquiring this 30.06 record from the opposite direction relative to the receiver line demonstrates the potentially adverse effects of incomplete event identification on shot gathers.
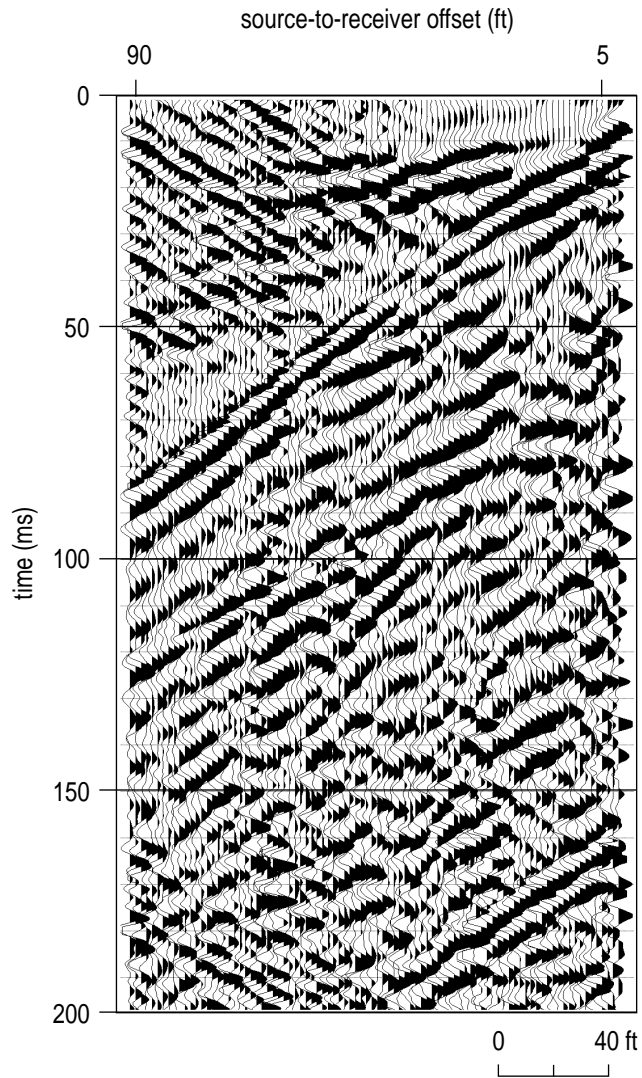
Figure A22. This second shot from the reverse direction does not seem to have as pronounced an effect on the data quality at this site (WS2) (which has been significantly altered during construction) in comparison to WS1.
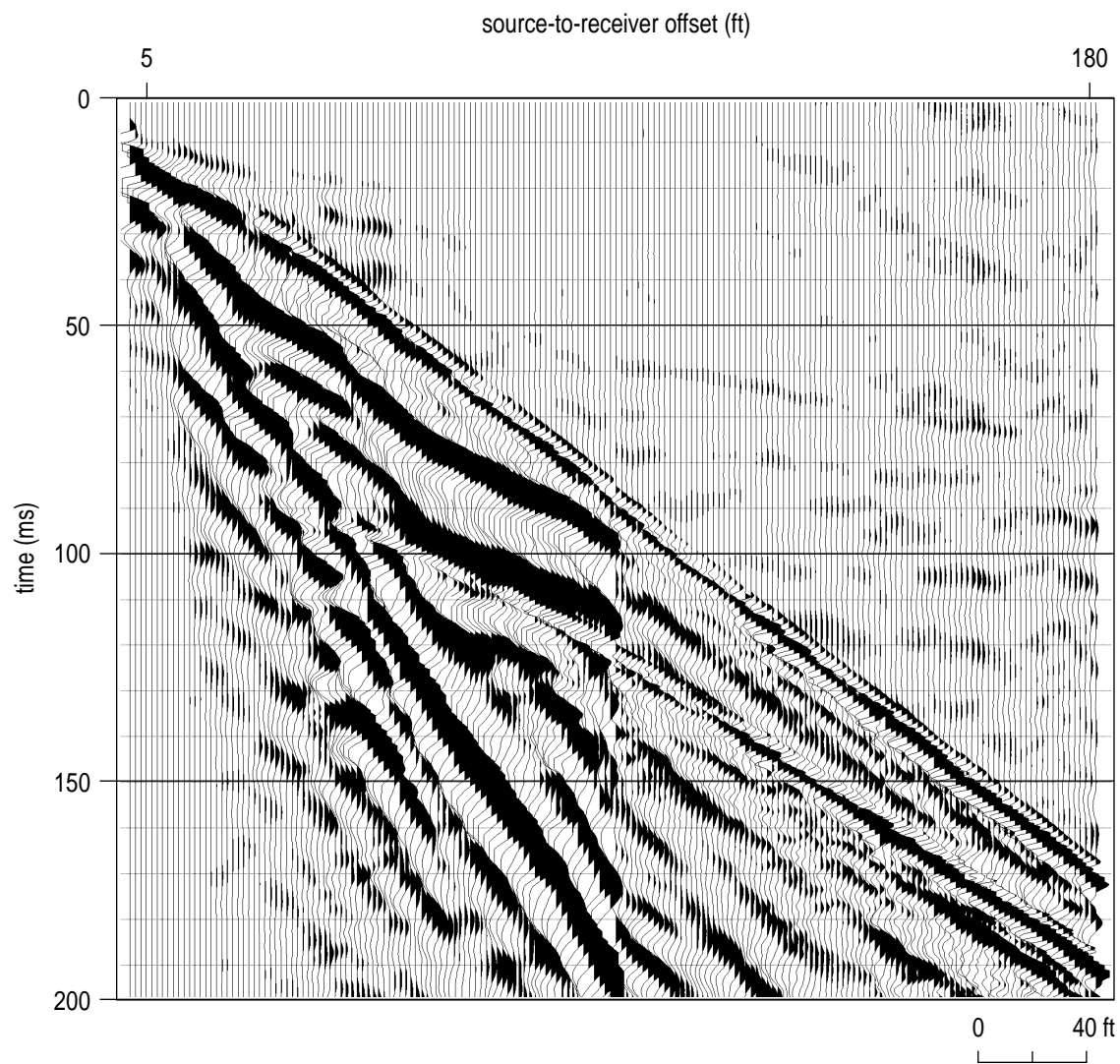
Figure A23. Shot gather of a single impact from the 16 lb sledge hammer. The air-coupled wave direct arrival and air-coupled wave building reflection are both pronounced high frequency events on this record.

sources. The high frequency air coupled wave is clearly interpretable as well as the building reflection. Interesting to note is the similarity between the frequency components of the air coupled wave reflection and the reflection interpreted on shot gathers from site #1. Misinterpretation is a definite possibility. The offset in the first arrival about halfway across the shot gather is the result of combining two different source locations to expand the total spread length (Figure A24). The hammer source is definitely not the best source in or around surface reflecting objects (Figure A25). The reverse direction shot again shows how the arrival patterns and intensities of the air wave reflections change with orientation to buildings or walls (Figure A25). There are not any obvious subsurface reflection arrival present on the sledge hammer data.

The auger gun data show the detrimental effects caused by changes in near surface conditions (Figure A26). Two source locations were occupied and as evidenced by the raw shot gather, the bandwidth was severely altered by changing from gravel to replacement sod (Figure A26). From comparisons of raw data (Figure A26) with digitally filtered shot gather (Figure A27) it appears the gravel shot record retains a relatively rich high frequency portion of the spectrum with reductions evident in the more detrimental low frequencies. As with the other sources, the building reflection, curb direct wave, and noise from a building exhaust fan are prevalent (Figure A28). Energy arriving at very close offsets and about 40 msec into the record appears to have a geometry consistent with modeled reflection curves from the water table. The reverse direction shot record possesses the same building reflection but with slightly different geometries (Figure A29). The deeper shot had no obvious effect on data quality (Figure A30).

Based on the significant drop in data quality experienced by moving from a moist sod/ditch environment present at site #1 to this disturbed/infilled geophone environment with a hard surface source setting like site #2, moving inside the building or even within 50 ft of any building at this site would severely compromise the interpretability of the resulting data set.

Walkaway Site #3

Walkaway site #3 was selected to get as near the building as possible and allow geophone and source coupling into a dirt/soil environment. Much of the site selection criteria was based on the better data quality obtained at site #1 than at site #2 (Figure 1). This site was also intended to estimate the amount of variability in data quality and reflection times that could be expected if a seismic line were
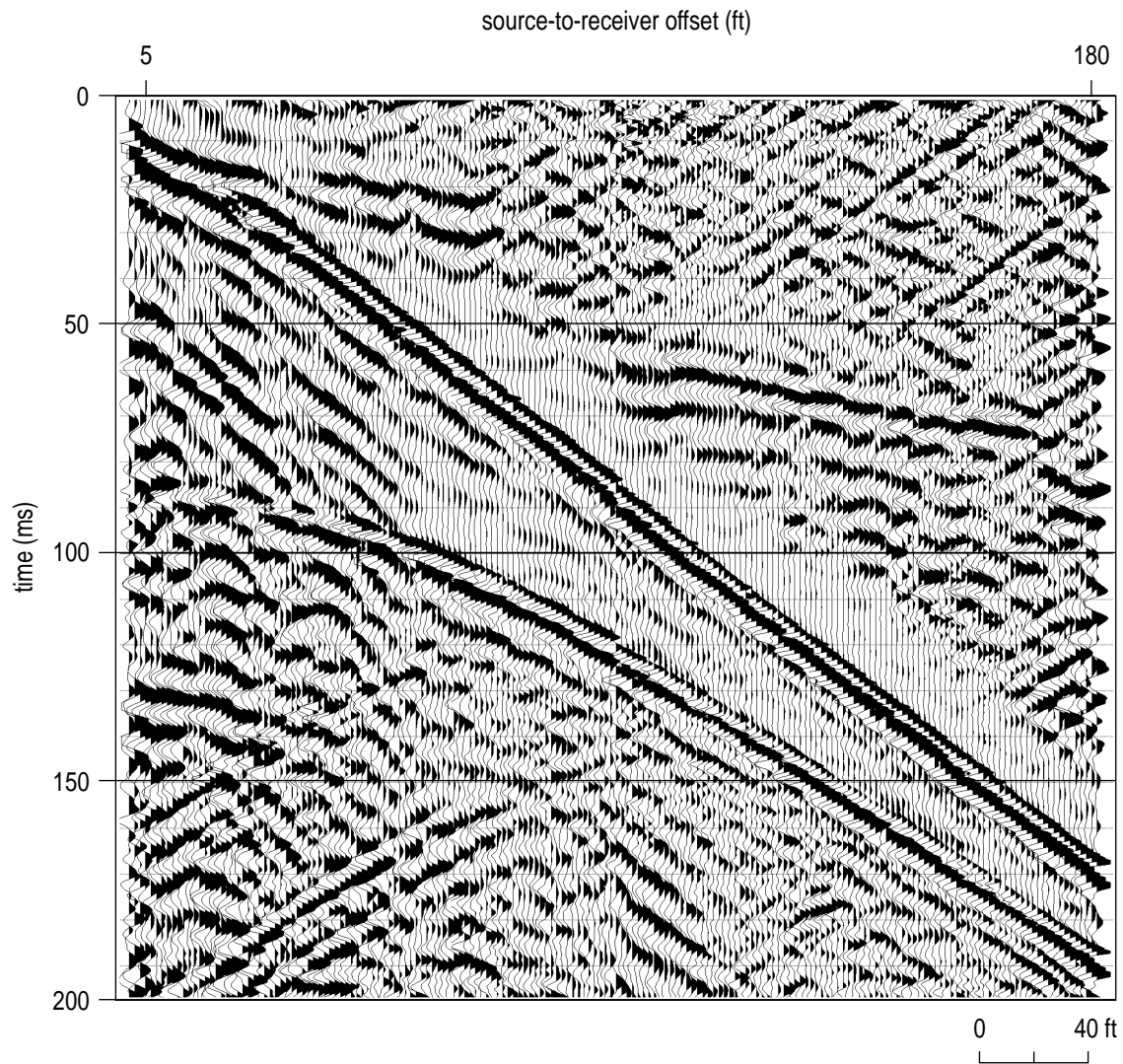
Figure A24. Digital filtering of Figure A23 enhances the air-coupled wave and allows easy interpretation of the direct/refracted wave associated with the concrete/asphalt surfaces.
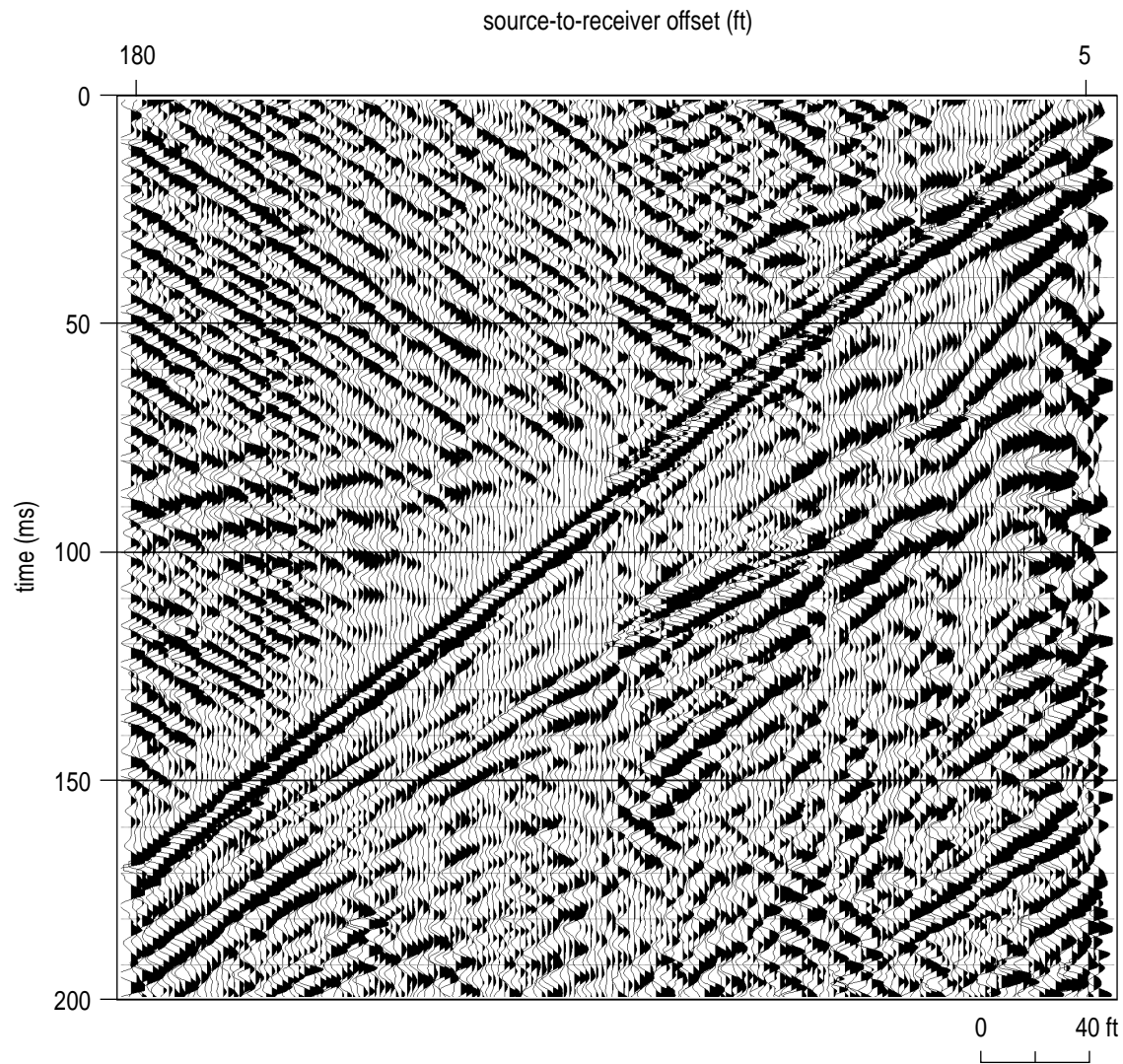
Figure A25. Digitally filtered shot gather of sledge hammer recorded from east to west as opposed to Figure A24, which is recorded west to east at WS2. The chaotic nature of building echoes makes interpreting arrivals after the direct air wave almost impossible. Pre-arrival noise from the building ventilation system is evident as well.
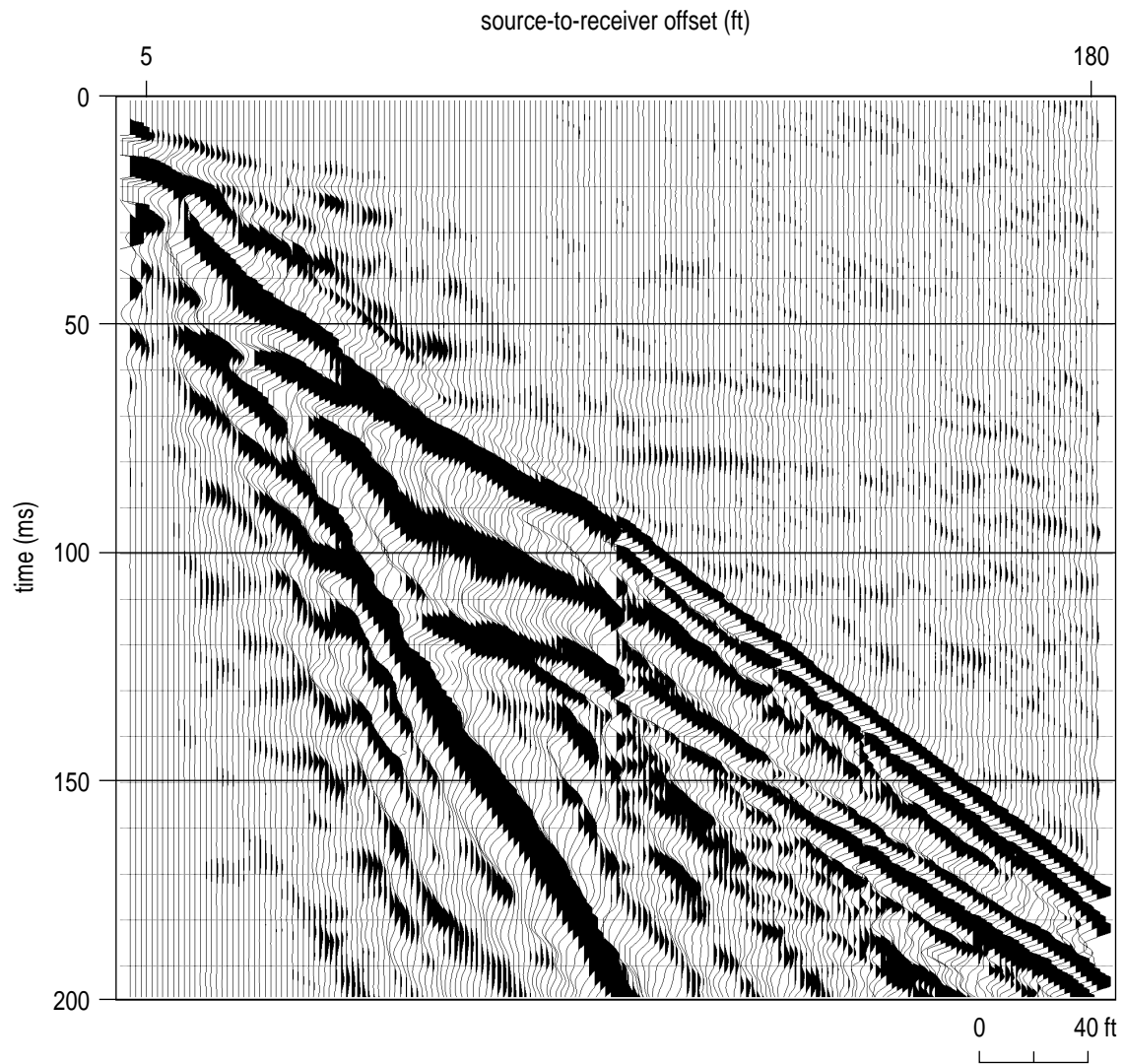
Figure A26. Raw shot gather from the auger gun at WS2. The abrupt change in data characteristics at source offset of about 90 ft is due to a change in source location.
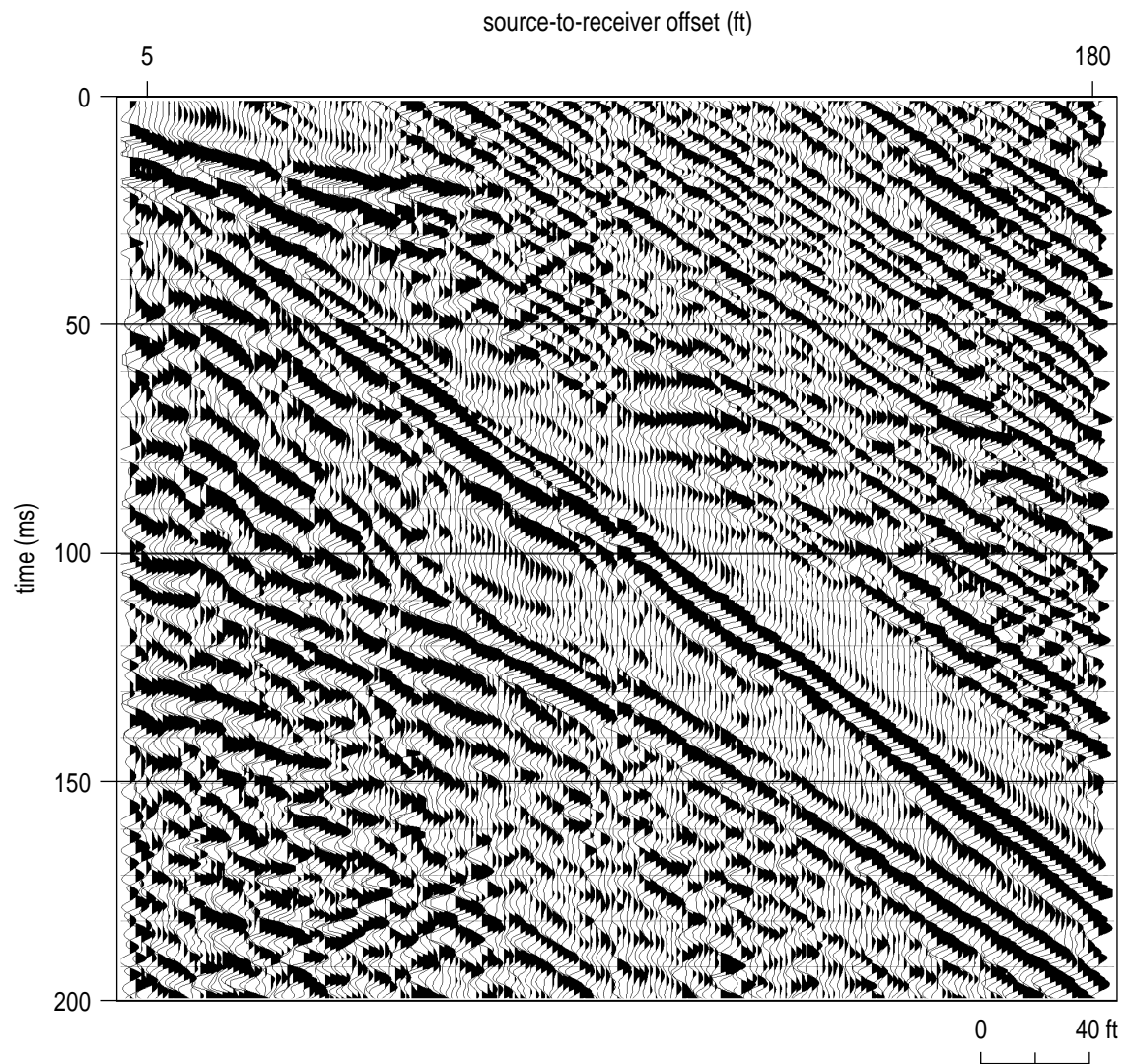
Figure A27. Digitally filtered shot gather from the auger gun allows easy interpretation of asphalt/concrete direct/refracted arrivals, air wave echo from the building, noise from the building ventilation system, and hints of coherent reflection energy.
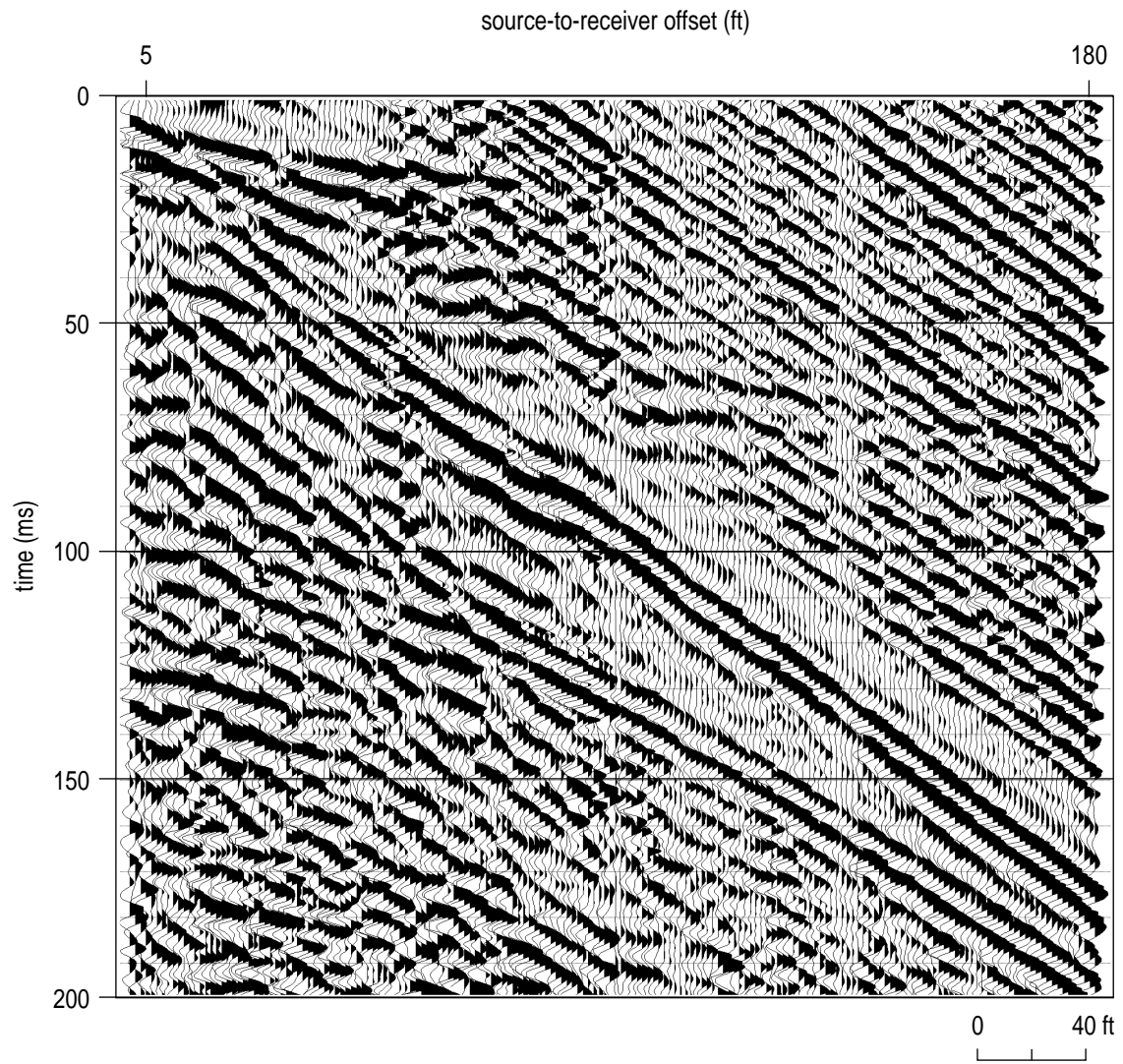
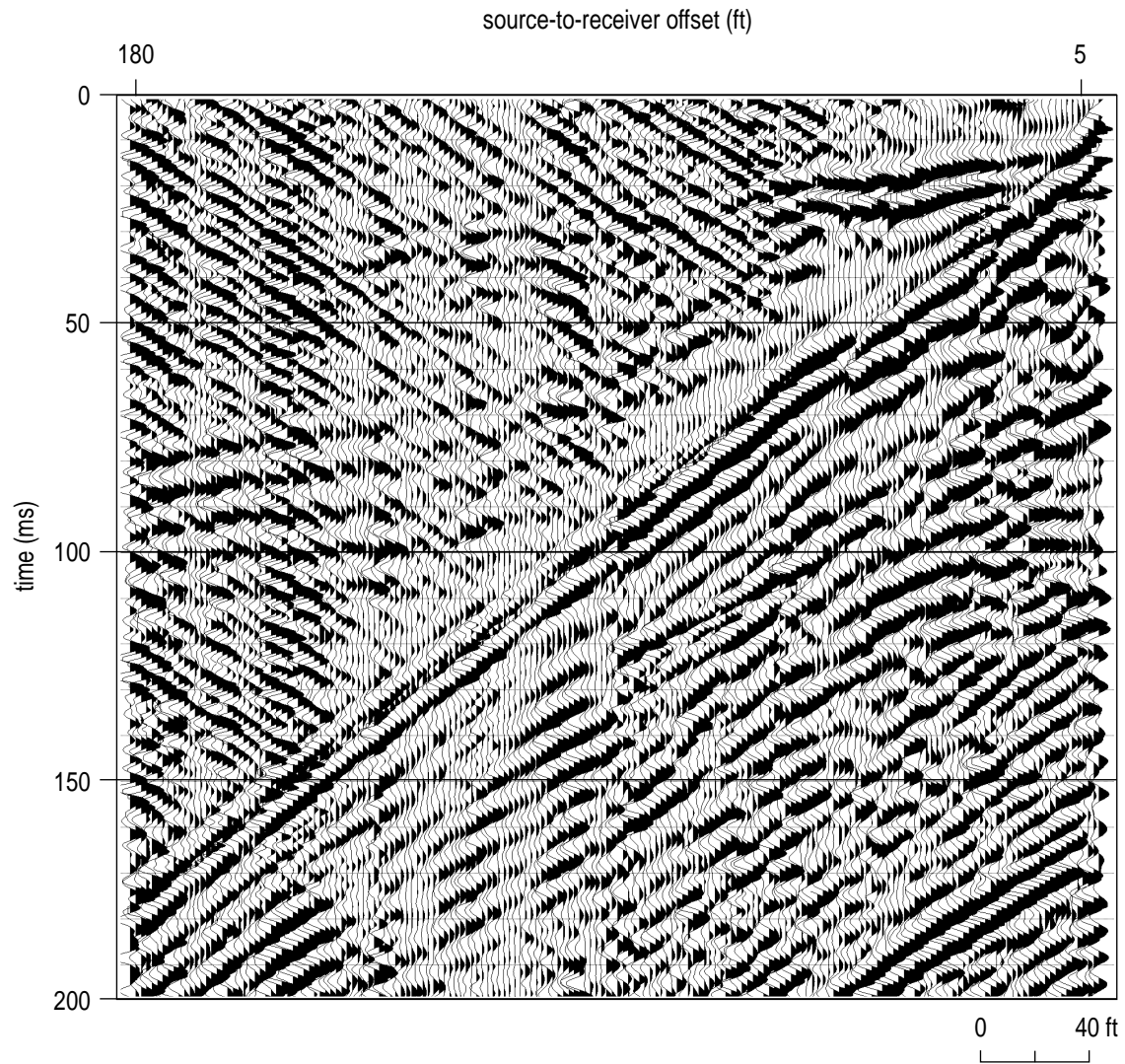Figure A28. The second shot in the same auger gun hole provides little obvious improvement.

source-to-receiver offset (ft)

Figure A29. This digitally filtered auger gun shot gather from the east (reverse direction of Figure A28) is consistent with records recorded with the sledge hammer from the east.
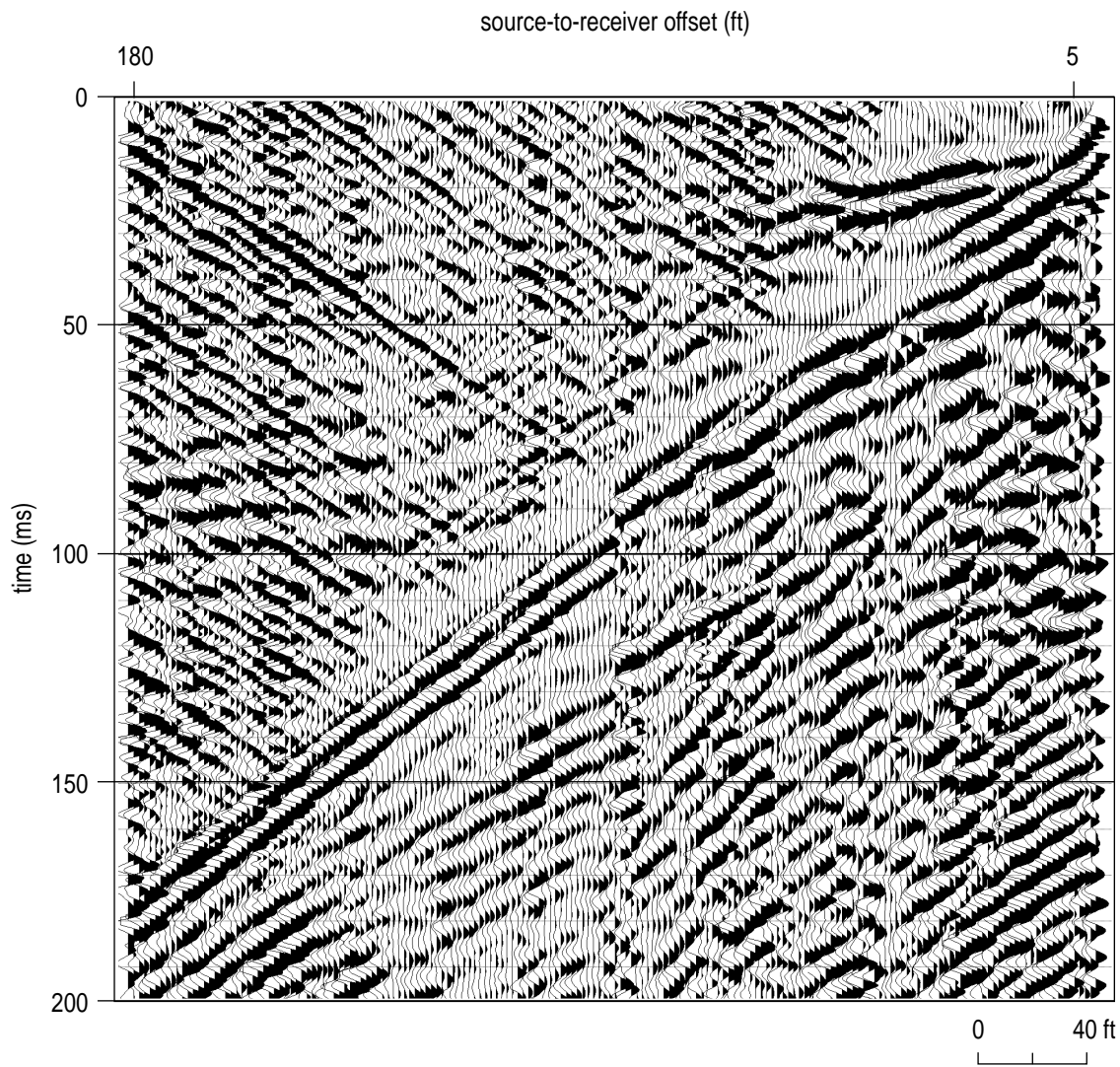
Figure A30. A second shot with the auger gun from the east resulted in poorer quality data. The decrease in data quality is likely due to an extremely disturbed (blown out) shot hole resulting from the initial shot.

acquired along the east perimeter fence. The spread layout was very similar to site #2 except there was sufficient room to get the entire 96-channel, 96 ft spread deployed. The source and receivers were coupled into a dry but relatively undisturbed near surface. The site had some years ago been the location of a small installation but nothing remained at the time of this noise test. Testing at this site included the same as previous sites plus an extensive set of hammer experiments attempting to determine what if any difference delivery of impact energy to the ground had on wavelet characteristics and signal-to-noise ratio.

The spectra from this site were very consistent with those observed at site #1 with the exception of the auger gun (Figure A31). The deviation in spectral properties of the auger gun is probably related to underground remnants of previous structures at this site which, is likely due to the deeper placement of the 12-gauge shell as compared to the surface fired 30.06 projectile. The air wave component is visible on the sledge hammer and 30.06 spectra in the form of a slight increase in amplitude between 250 Hz and 350 Hz. An interesting set of sawtooth looking peaks between 150 Hz and 250 Hz on the sledge hammer are likely part of the ground roll wedge.

The raw shot gather of the 30.06 downhole possesses several interpretable reflections with no spectral shaping (Figure A32). It is also obvious that the refracted arrival arrives later in time here than along the west perimeter fence. This is indicative of a deeper water table and/or lower velocity material between the water table and the ground surface. The water table reflection is present at about 50 msec, which is 10 msec deeper than at site #1 and consistent with the observation of a later refraction arrival. The digitally filtered gathers possess several high quality reflection arrivals with dominant frequencies above 180 Hz (Figure A33). The water table reflection is coherent and high amplitude with arrivals interpretable to near vertical incidence. The effects of two source locations are evidenced at this site as well as the previous sites by the apparent offset in the refraction at about station 2397. Little improvement is noted on the second shot recorded in the same shothole (Figure A34). On this shot gather it is interesting to note the time displacement of otherwise continuous reflection events. Reverse direction shots provide a much more interpretable bedrock reflection (Figure A35). The obvious separation between the water table refraction and bedrock reflection makes meticulous removal of refraction energy from the data set much easier (removal of refractions is an absolutely mandatory step when processing CDP reflection data of this type). The second shot at this site seems to be a little worse than the first (Figure A36). This is likely the
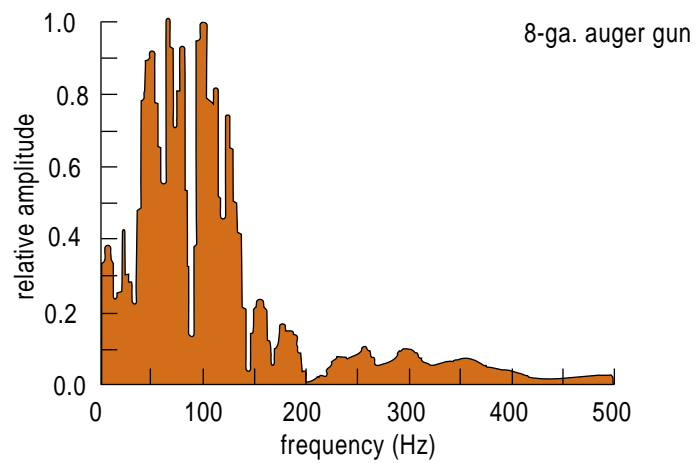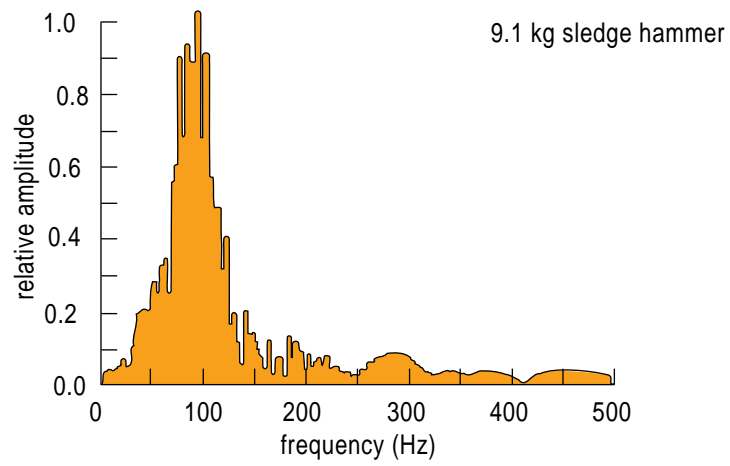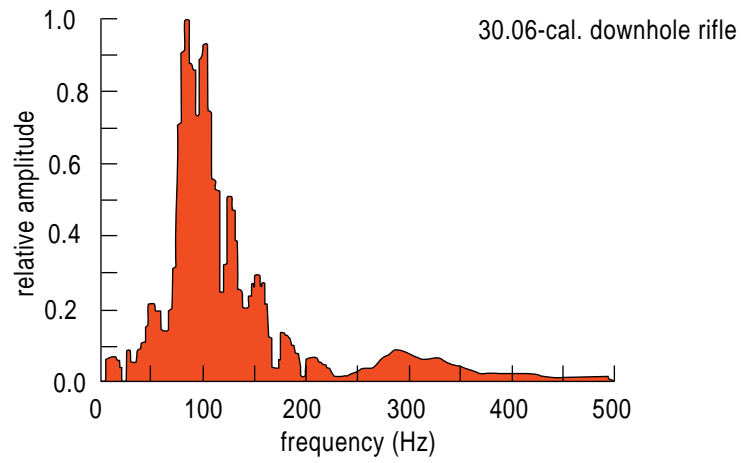
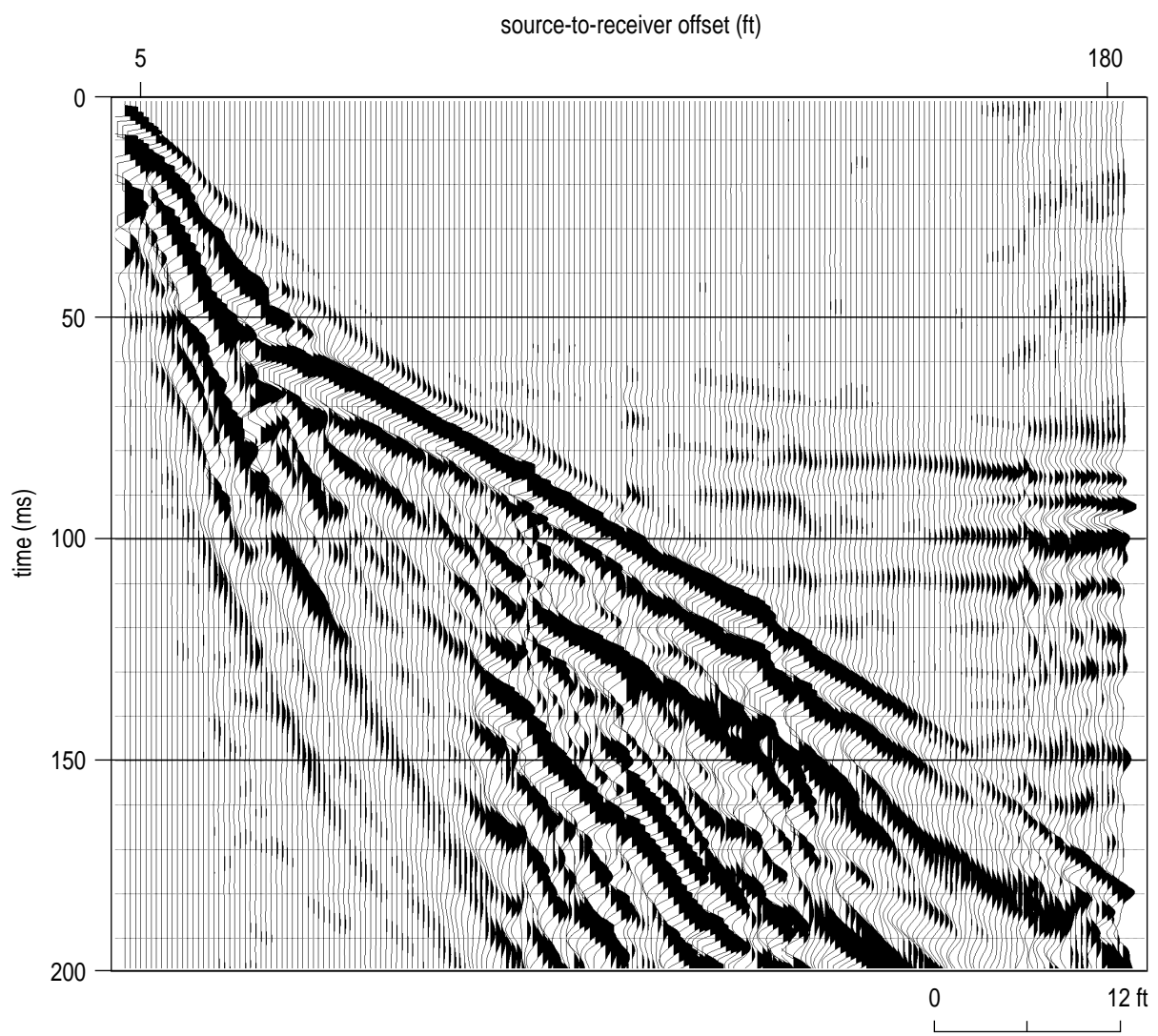Figure A31. Walkaway site #3 (WS3), whole record normalized source spectra.

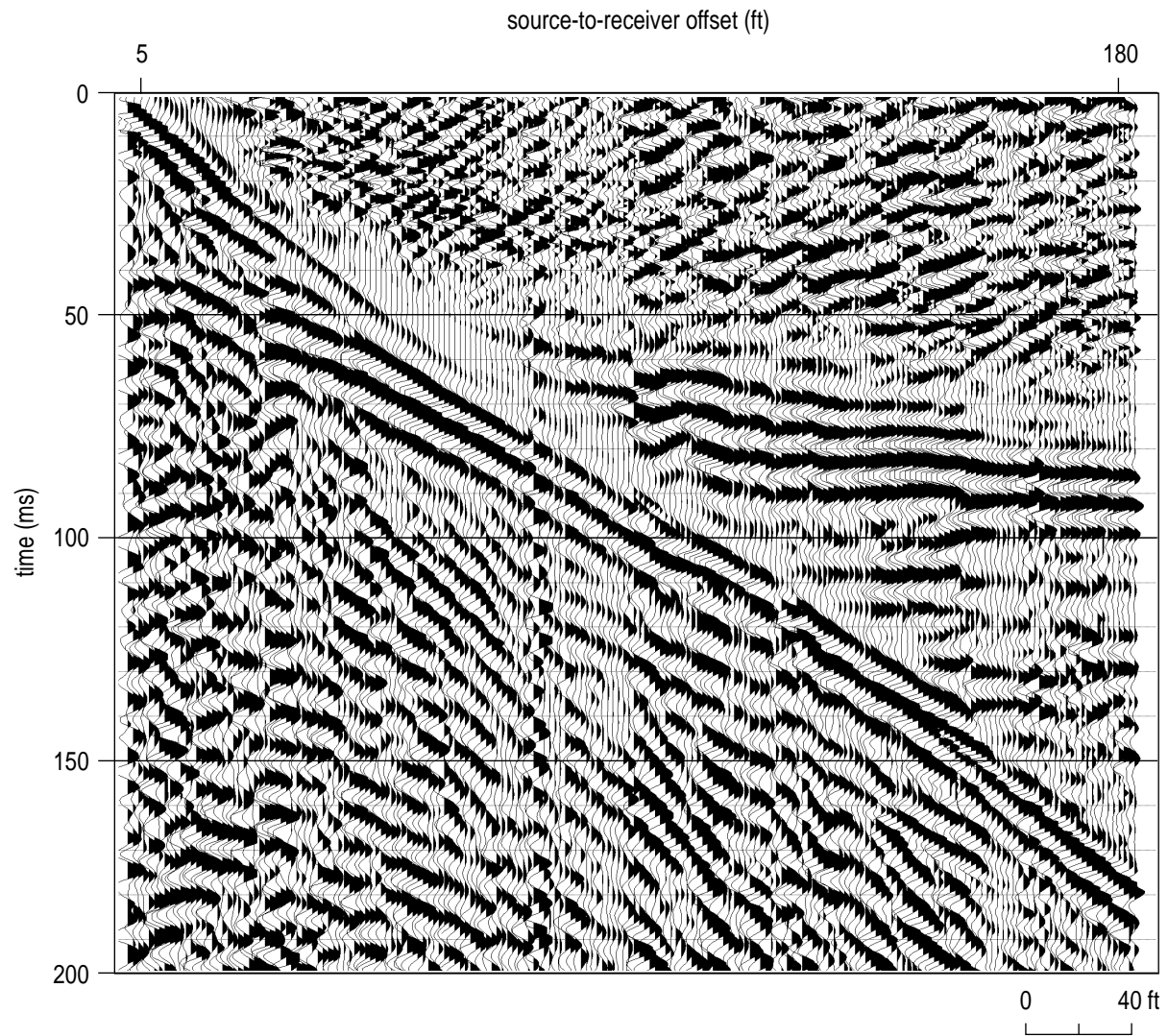Figure A32. Raw 30.06 downhole shot gather from WS3.

Figure A33. Digitally filtered shot gather from WS3. Coherent reflection events can be interpreted from 40 msec to depths in excess of 130 msec.
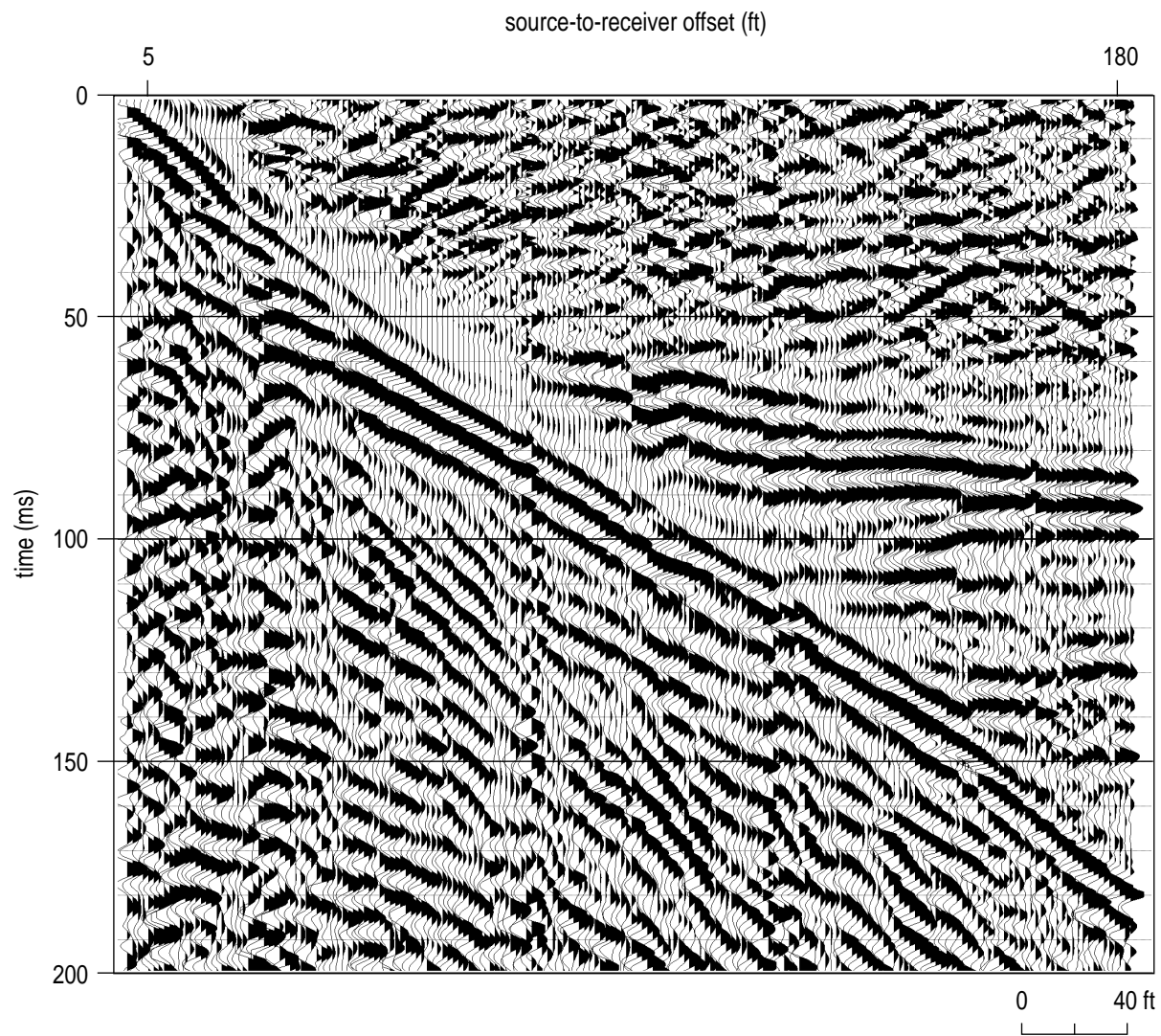
Figure A34. This second shot in the same shot hole using the 30.06 shows little in the way of improvement in signal-to-noise or resolution potential.
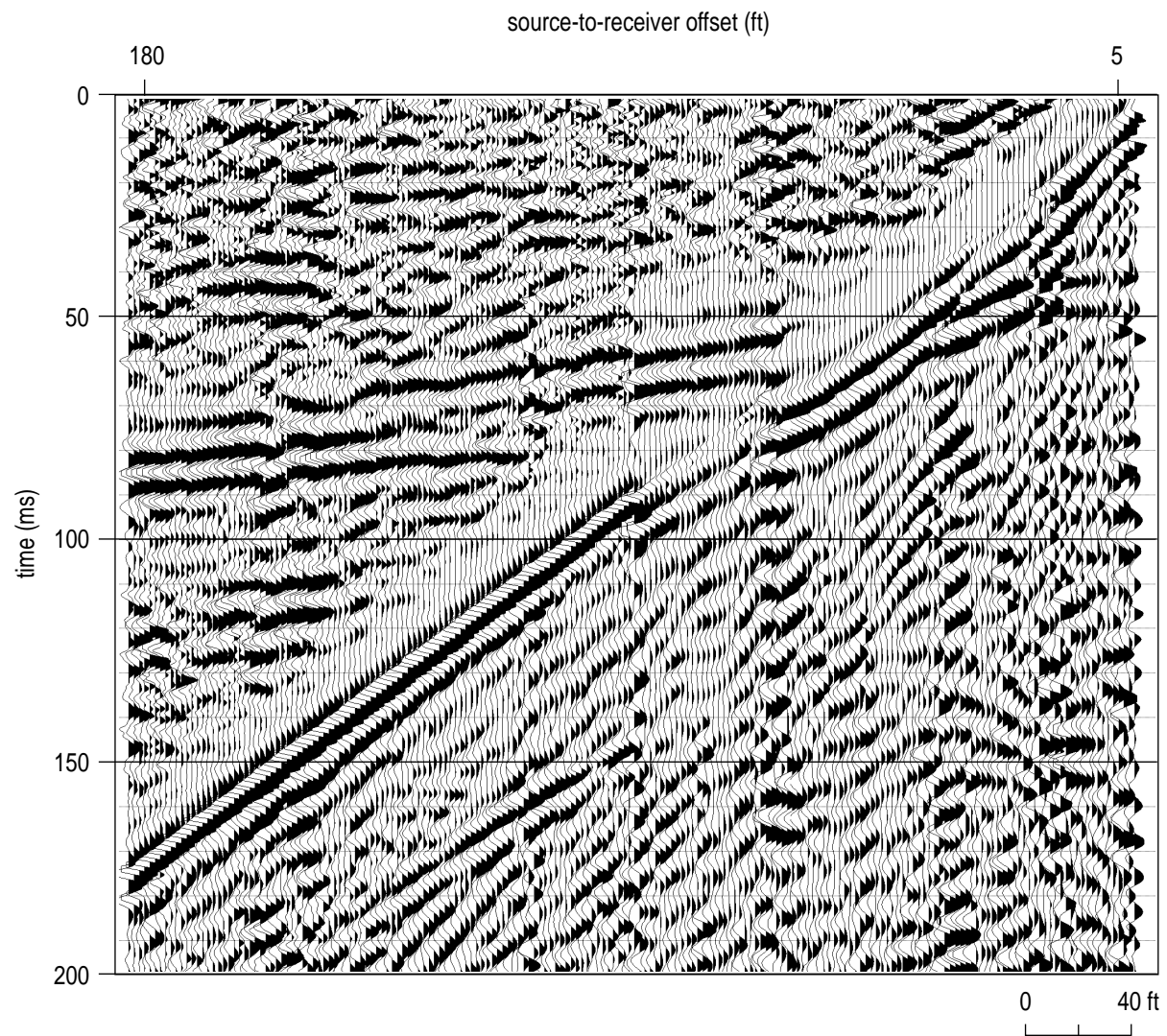
Figure A35. Reverse direction shot gather from WS3. Several reflection events are interpretable across the entire spread.
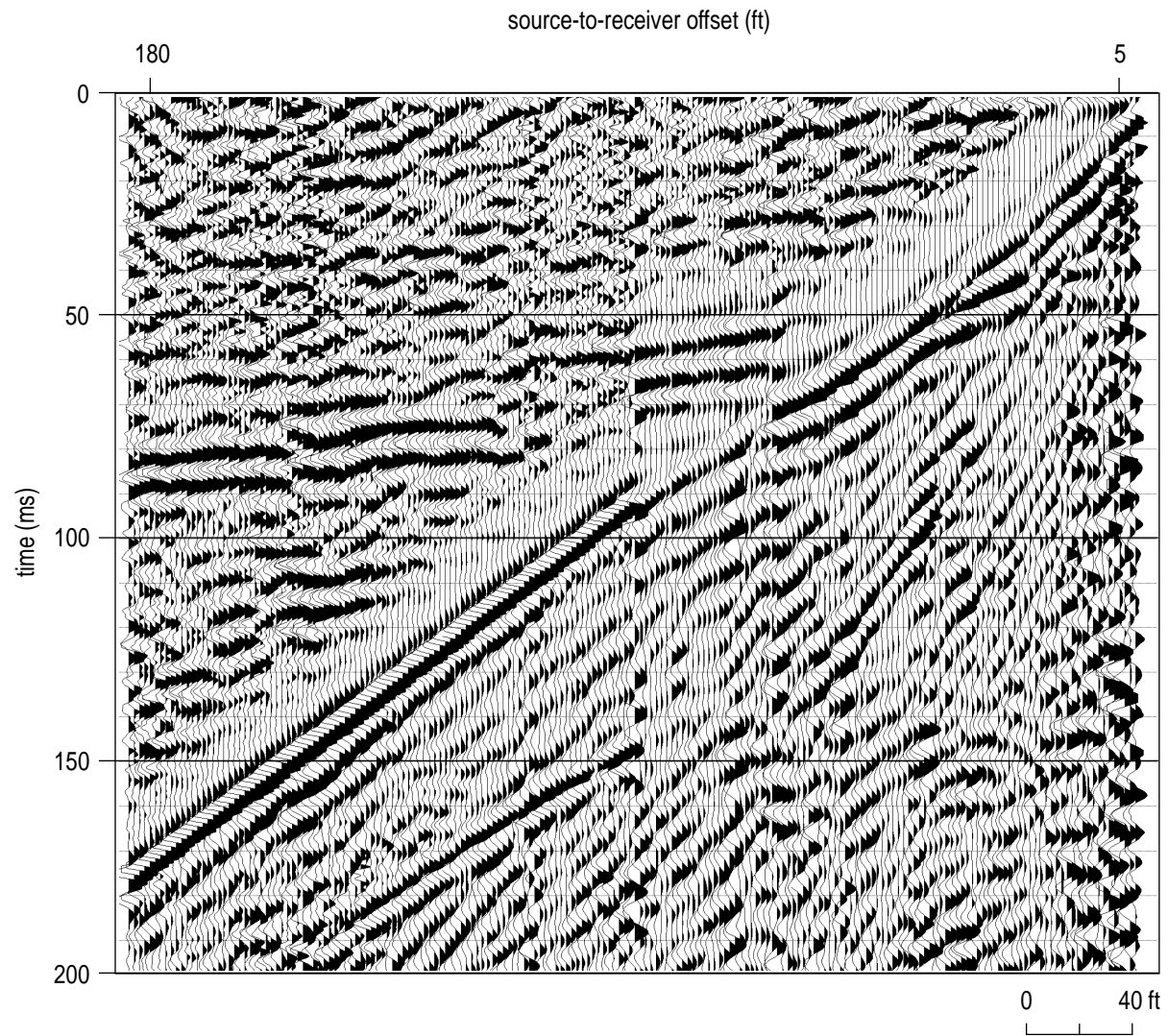
Figure A36. Second shot in original reverse direction shot holes provides no obvious improvement and may even result in a deterioration in overall data quality.

result of reduced coupling caused by the distortion of the ground in and around the shothole by the first shot.

The sledge hammer raw shot gather possesses many of the same properties observed in the 30.06 data set from this site (Figure A37). It is apparent on digitally filtered sledge hammer data that even at distances as great as several hundred feet from the building a substantial amount of noise is recorded with spectral properties similar to reflections from this site (Figure A38). The air coupled wave is a very strong arrival and arrives coincident with a critical portion of the reflection energy frequency and time arrivals. The reflection from the water table is not as well defined on the sledge as on the 30.06. This is most evident at offset less than about 40 ft. Vertical stacking improves the signal-to-noise ratio of the sledge hammer (Figure A39). The noise originating from within the building is still present, but not as coherent as with the single shot data. The destructive adding of any non-source related noise through vertical stacking should reduce both its overall relative amplitude and coherency on time sections. Data recorded from the reverse direction does not possess as high a signal-to-noise ratio as from the front (east) of the line (Figure A40). The water table reflection is more evident at this site with the sledge than previous, but at the expense of deeper reflections which are not as obvious. Vertical stacking improved the signal-to-noise and allowed identification of both the water table reflection and bedrock (Figure A41). The source location of the reversed shotpoint (west location) was near the edge of a cement drive while the east source location or the forward shot was in a grassy area near the fence.

The 12-gauge auger gun provides a shot record very similar to the downhole 30.06 with the exception of total amplitude or power, which is more than 9 dB greater with the auger gun (Figure A42). There appears to be very distinguishable reflections from the water table and bedrock with some indication of reflection energy between the water table and bedrock (Figure A43). The main distinction between the two explosive sources (auger gun and 30.06 downhole) is the bandwidth and corner frequency of body wave energy. The second or deeper shot with the auger gun did nothing to improve the potential of the data (Figure A44). Reversed shots (west end of the spread) provided high frequency bedrock and water table reflections (Figure A45). The improvements of uniqueness of the opposite end files are consistent with findings on 30.06 data. Building noise stopped at about this point during testing so there is little indication that coherent out-of-the-plane noise noted on previous shot gathers from this location is present. The second or deeper shot seems to have generated a record with decreased signal-to-noise but retained a
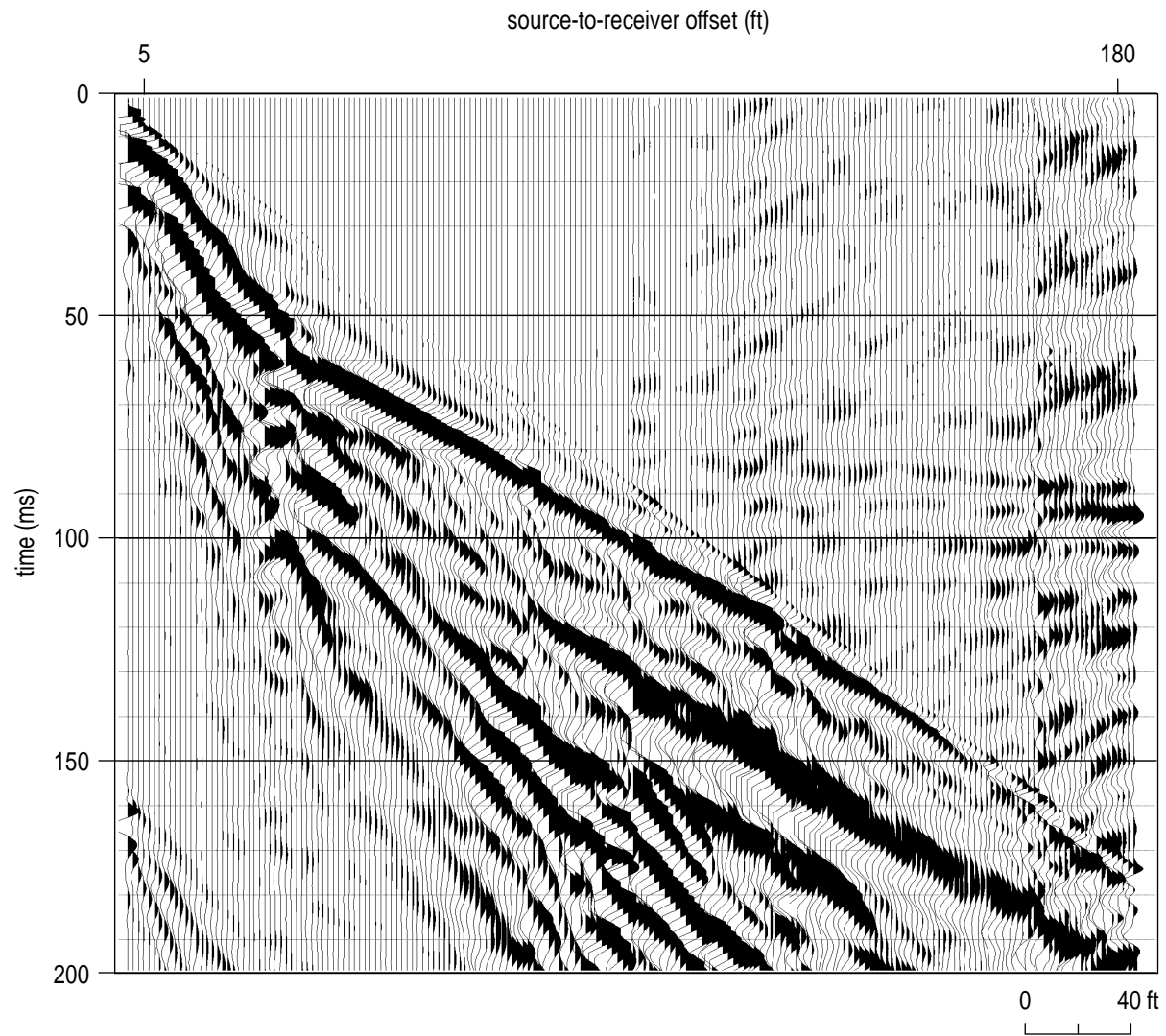
Figure A37. Single impact with 16 lb sledge hammer at WS3. The long offset wavelets of the shallow low-velocity reflection are very evident on this shot gather.
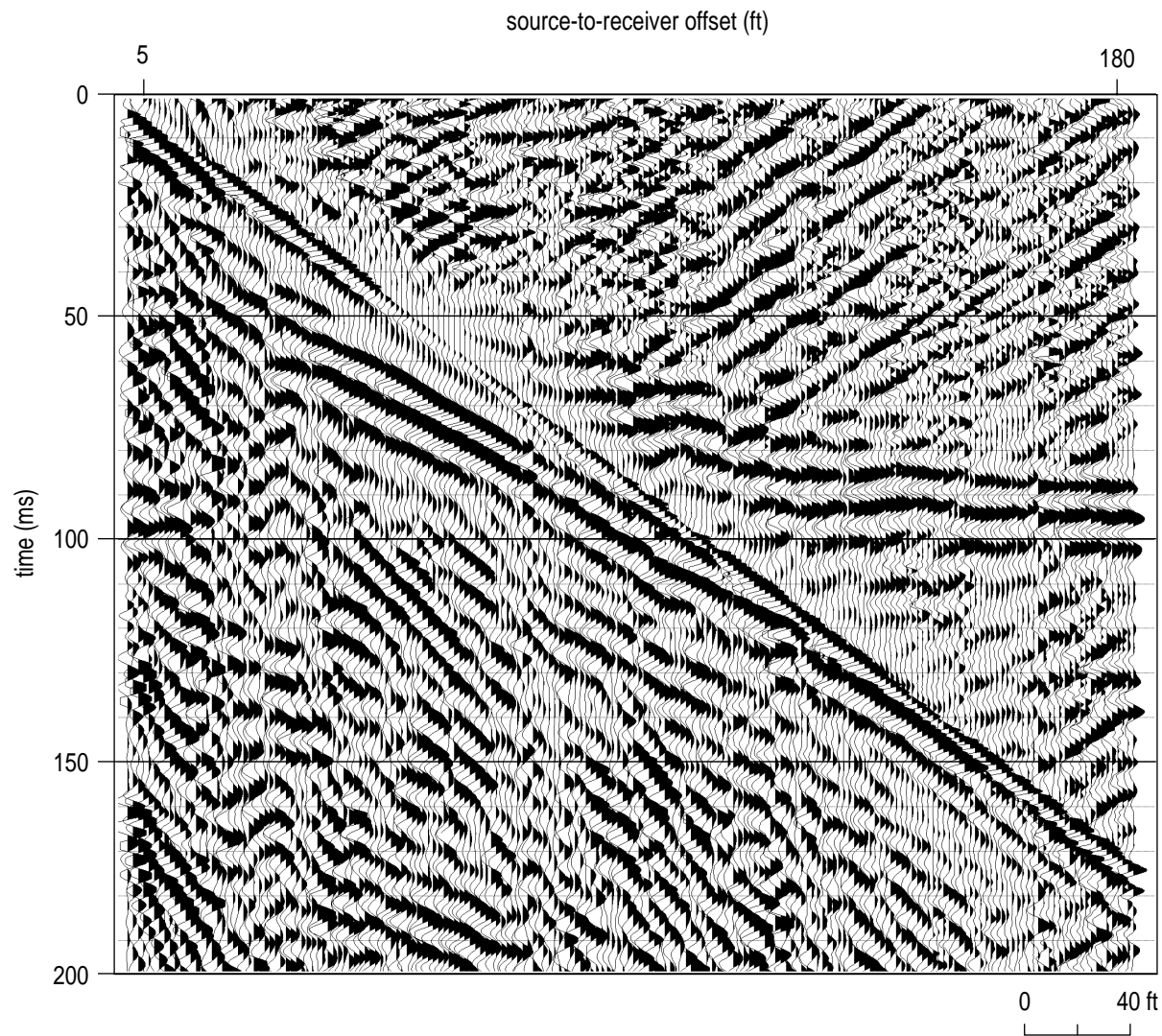
Figure A38. Due to the narrow band nature of the sledge hammer data, digitally filtering the shot gather (Figure A37) results in a "ringy wavelet." Little is evident in improvement to the signal-to-noise or bandwidth after filtering.
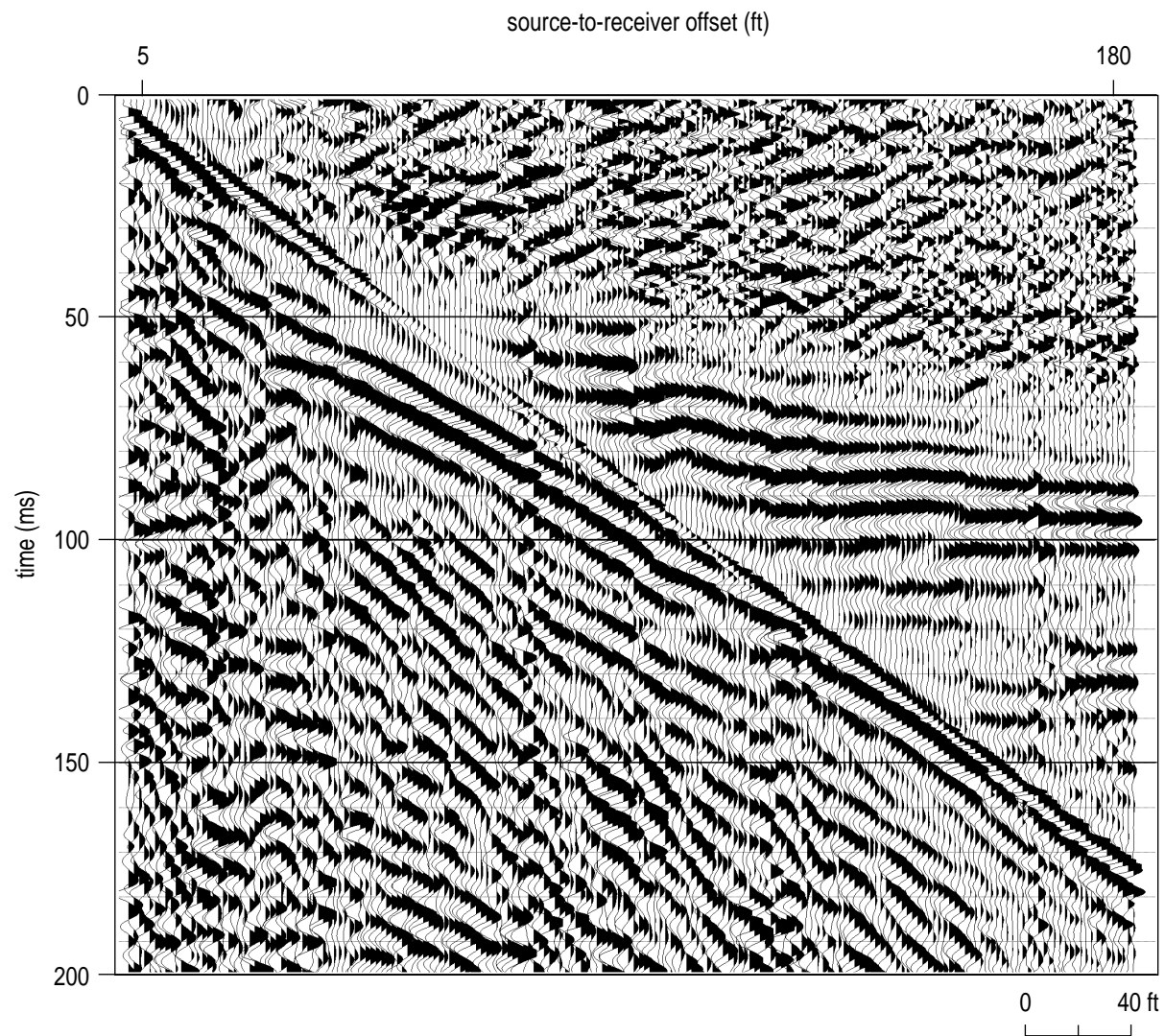
Figure A39. A vertical stack of four sledge hammer shots improves signal levels, especially from deeper reflectors, but the narrow band nature of the data (relative to the filter) results in the "ringy" wavelet appearance.

source-to-receiver offset (ft)

180   5

time (ms)

Figure A40. A single shot from the reverse direction with a digital filter applied possesses a very limited amount of interpretable
reflection energy.
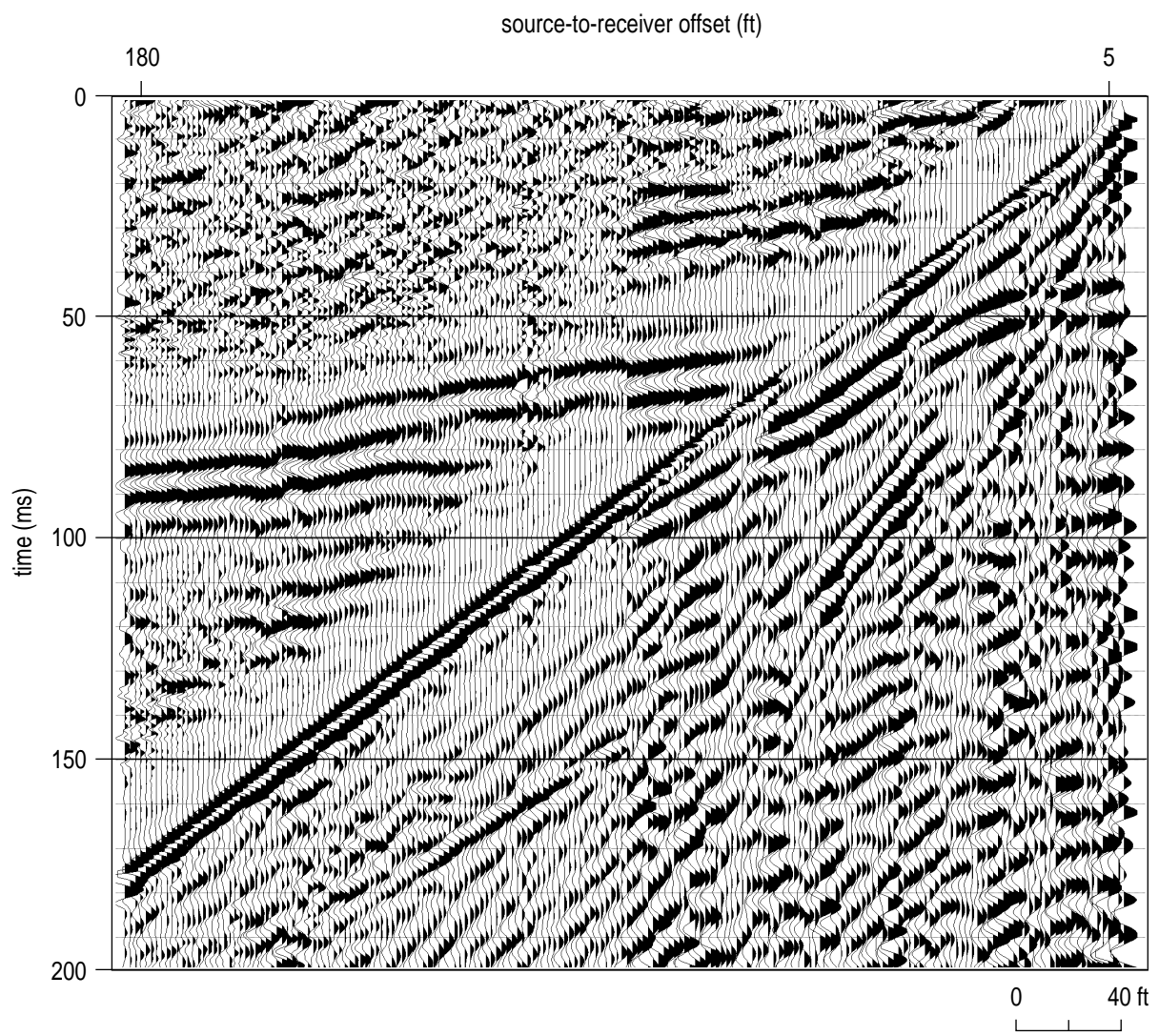
Figure A41. The four-shot vertical stack of sledge hammer impacts from the reverse direction along WS3.

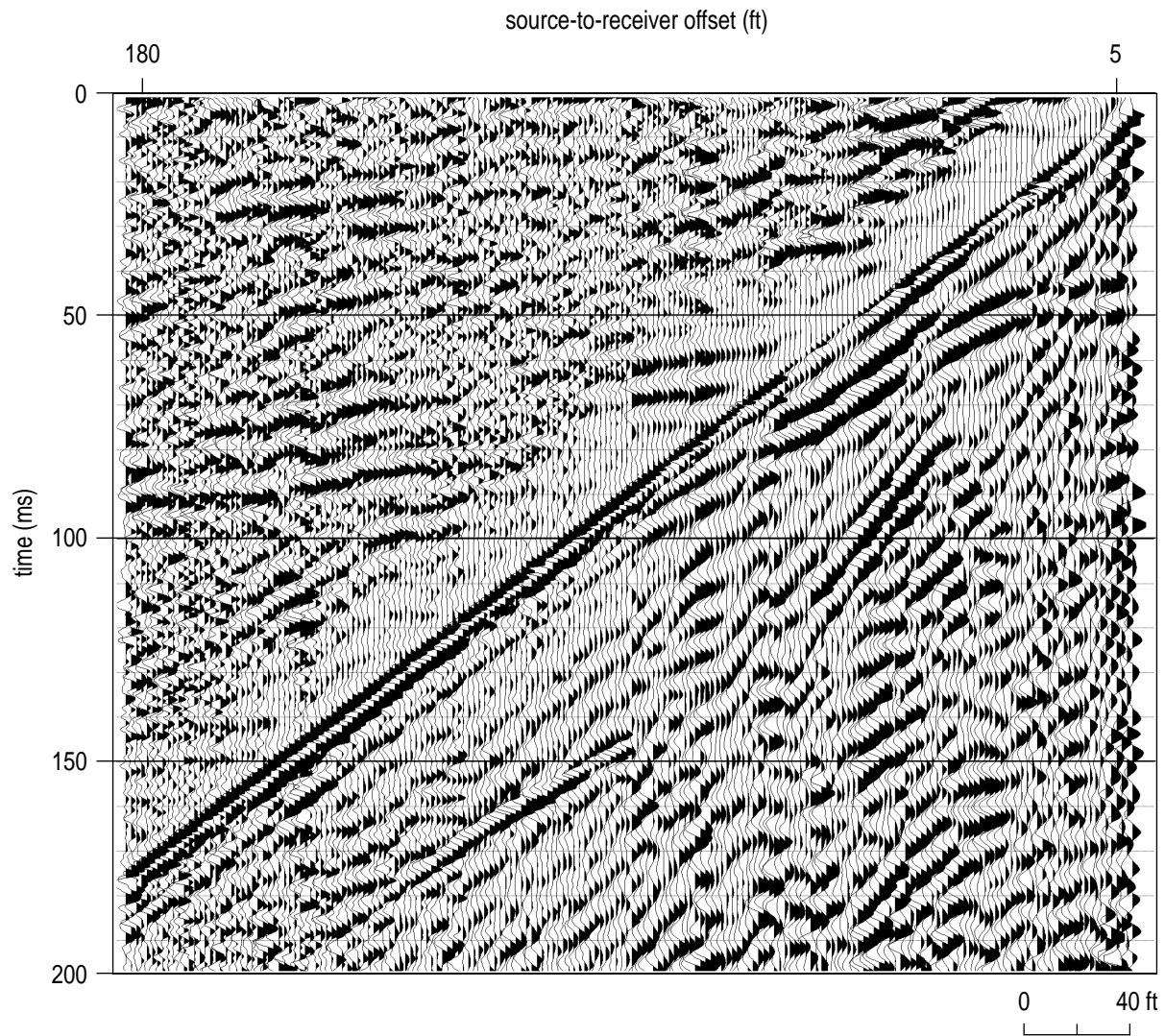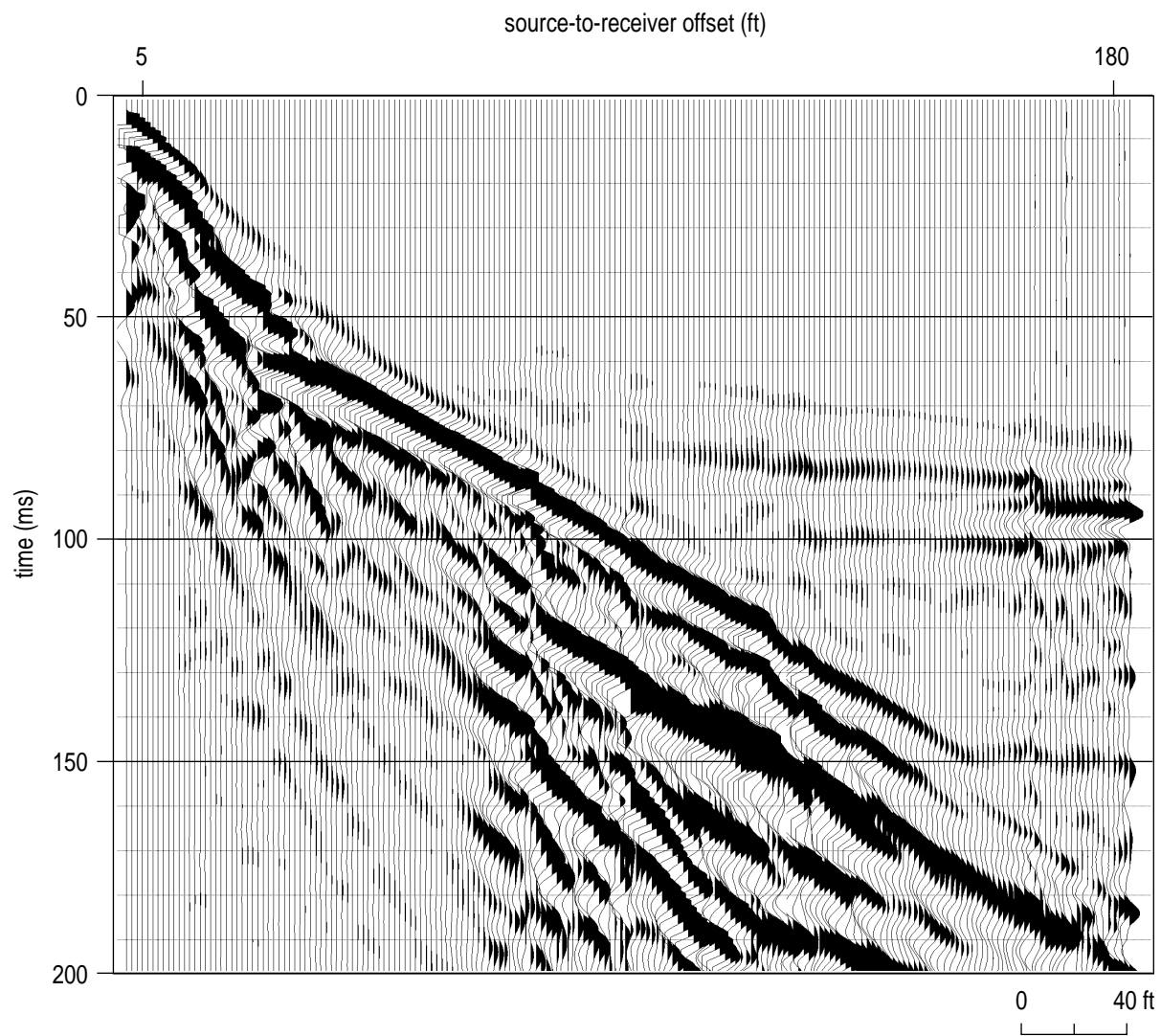Figure A42. Single shot from 12-gauge auger gun at WS3. The significant reduction in ground roll and air-coupled wave in comparison to the sledge hammer is evident.
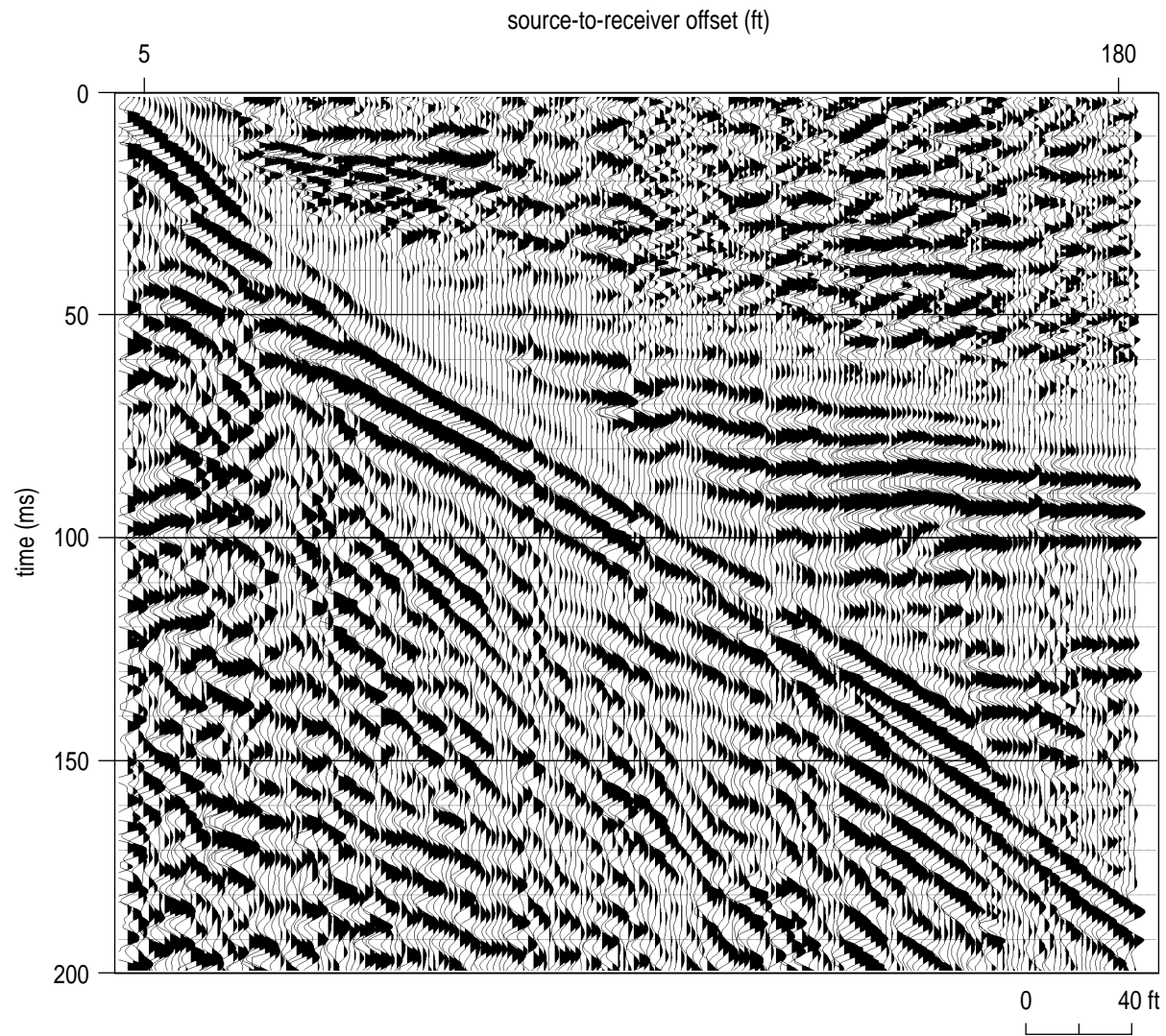
Figure A43. This digitally filtered auger gun shot possesses very "ringy" wavelet characteristics. This ringiness is due to the lower bandwidth nature of the auger gun in comparison to the 30.06 data, which was used to design the filter.
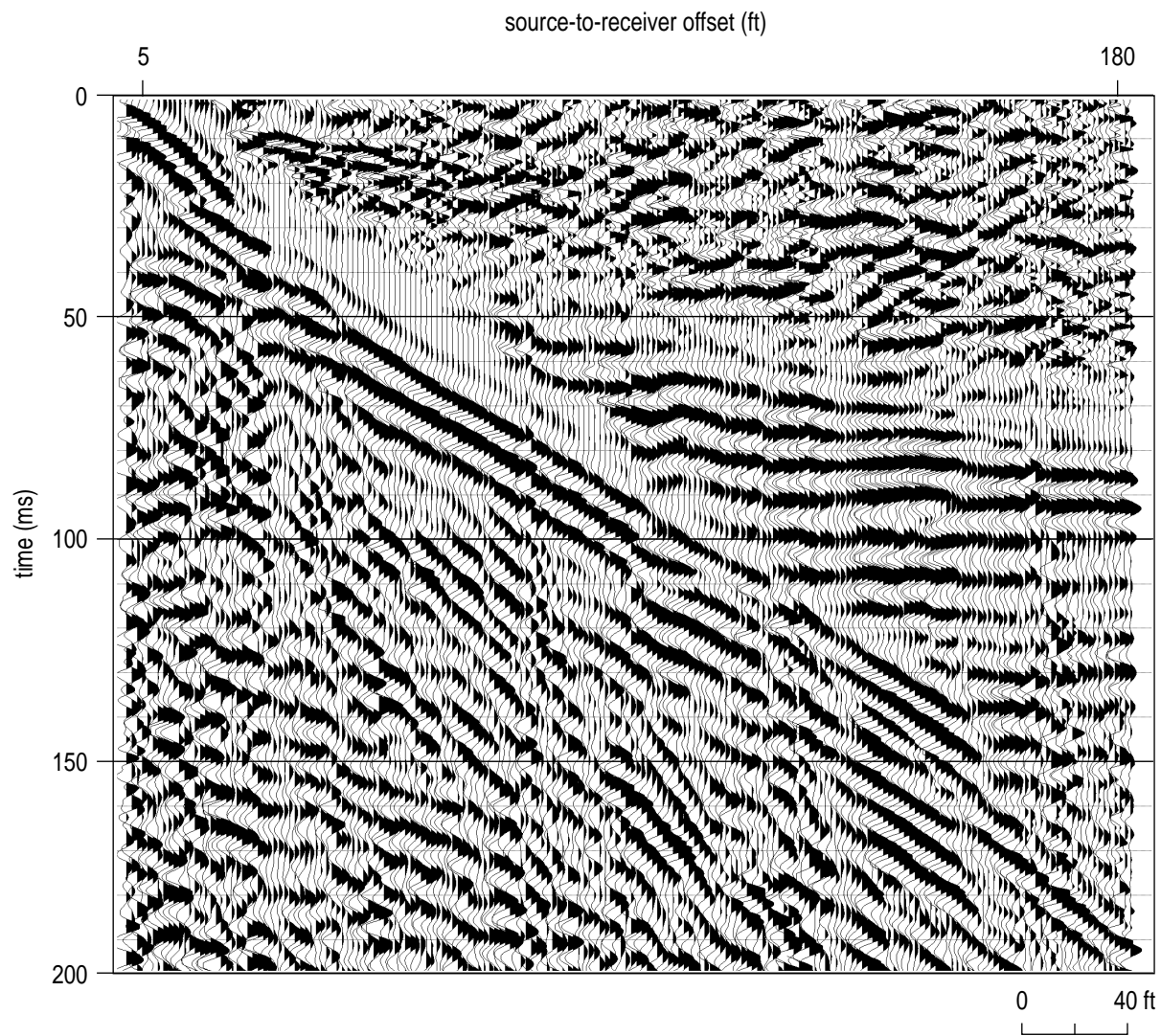
Figure A44. The second shot in the auger gun hole resulted in recorded data with a higher-signal-to-noise but no obvious improvement in bandwidth.
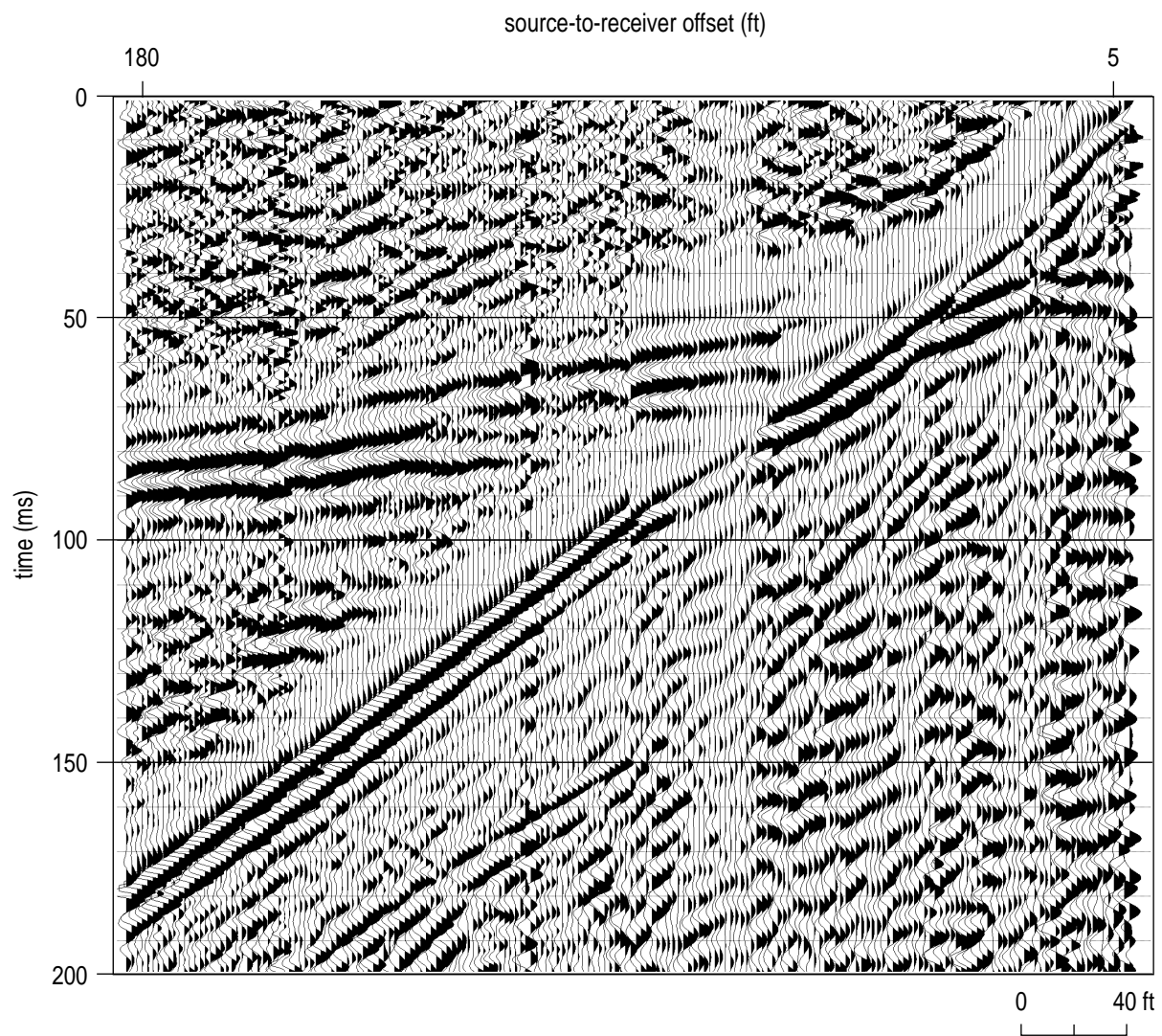
Figure A45. A reversed direction shot with the auger gun at WS3 permits interpretation of several reflecting events.

very interpretable reflection arrival (Figure A46). Very subdued back ground noise appears coherent prior to the initial arrival of source generated energy.

Site #3 provides more insight into the limitations of the technique in this very noisy environment. The sledge was least effective when data were recorded in areas with a paved surface or with a significantly altered near-surface. The down-hole explosives seemed to be very effective on first shot records. Sufficient body-wave energy was being generated to interpret good reflection arrivals even in the presence of coherent noise generated at or in the building a couple hundred feet away.

Figure A46. The second shot from the reverse direction with the auger gun seems to have resulted in lower quality data at the longer offsets. This is likely related to deterioration in hole conditions after the first shot.

APPENDIX B
Shallow Seismic Reflection Techniques

Introduction

Seismic-reflection techniques depend on the existence of discrete seismic velocity and/or mass density changes in the subsurface, known as acoustic impedance contrasts. Mathematically, acoustic impedance is simply the product of mass density and acoustic wave veloci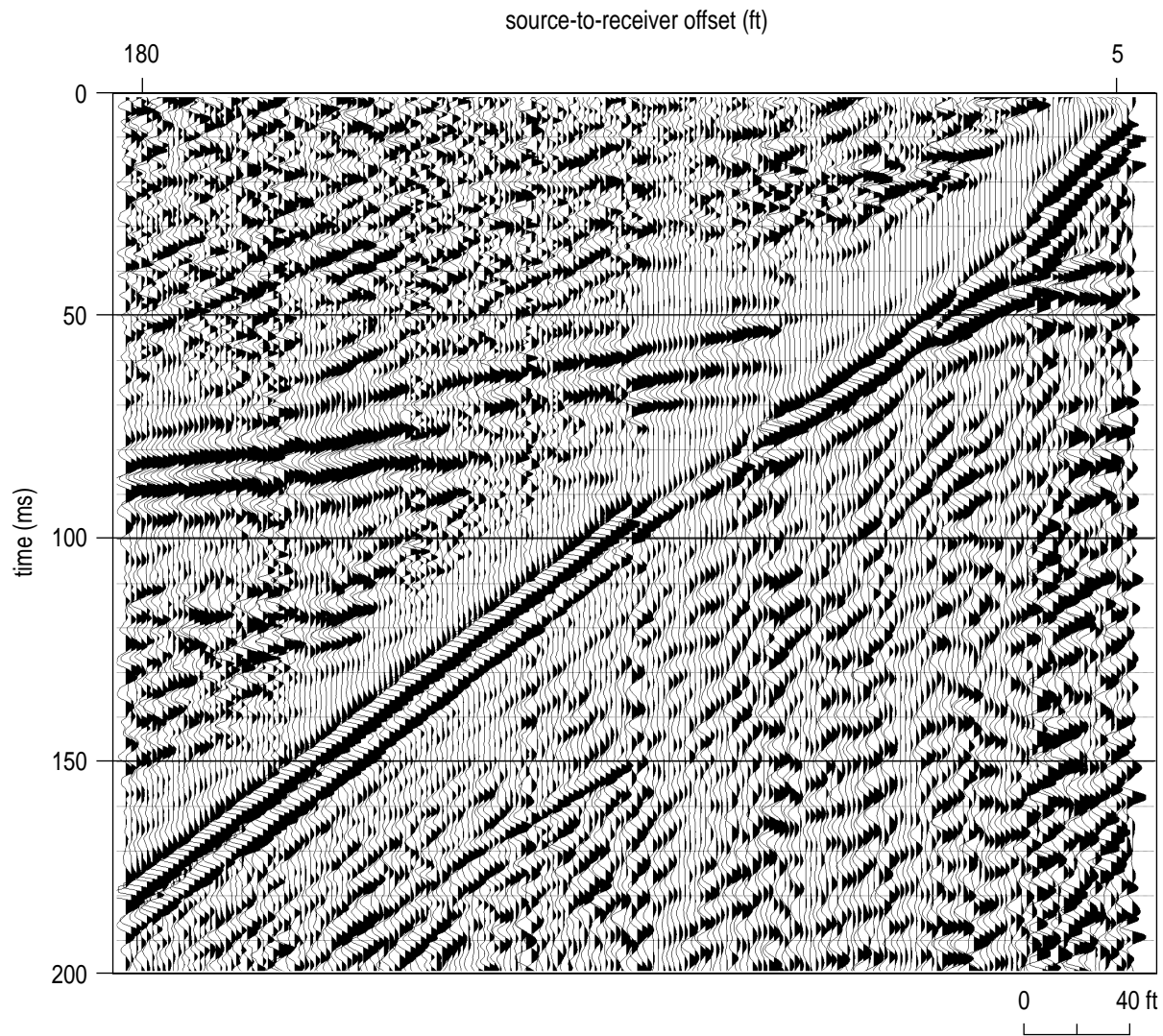ty. Acoustic impedance contrasts occur at natural boundaries between geologic layers, although man-made boundaries such as tunnels and mines also represent contrasts. The classic use of seismic reflection is to identify the boundaries of layered geologic units; however, the technique can also be used to search for localized anomalies such as sand/clay lenses and cavities.

Compressional waves (P-waves) propagating through the earth behave similarly to sound waves propagating in air. When sound waves (voices, explosions, horns, etc.) come in contact with a wall, cliff, or building (all acoustic contrasts), it is common to hear an echo. When a P-wave comes in contact with an acoustical contrast underground, echoes (reflections) are also generated. P-wave reflections can be thought of as sound wave echoes from underground acoustic impedance contrasts. In the underground environment the situation is more complex because some P-wave energy impinging on a solid acoustical interface can also be transmitted across the interface, refracted at the interface, and/or converted to other types of seismic waves at the interface.

Seismic methods are sensitive to the physical properties of earth materials and relatively insensitive to the chemical makeup of contained fluids in earth materials. Electrical methods are sensitive to contained fluids and to the presence of magnetic or electrically conductive materials. The measurable physical parameters upon which the seismic methods depend are quite different than the important physical parameters for electrical and magnetic methods. In the world of shallow geophysics, there are similarities among seismic reflection, seismic refraction, and ground-penetrating radar. There are also similarities with cross-hole seismic tomography and vertical seismic profiling. The similarities with electrical and potential fields methods are substantially less.

Shallow Seismic Reflection Fundamentals

The simplest case of seismic reflection is a single layer over an infinitely thick medium (Figure B1). Seismic energy induced into the ground from a point is radiated spherically away from that point in much the same fashion in three dimensions as waves from a pebble tossed into a still pond radiate outward in two dimensions. An arbitrarily large number of ray paths can be traced outward from the seismic energy source. One particular ray path will direct energy to a subsurface layer, reflect from that subsurface layer, and return as an echo to the ground surface first, following Fermat's principle of least travel time. In the case of a single flat-lying layer and a flat topographic surface (Figure B1), the path of least time will be from the energy source to a reflecting point mid-way between the source and the receiver, and then back to the receiver. The incident angle of the down-going ray will be equal to the angle of reflection of the up-going ray from the subsurface layer.
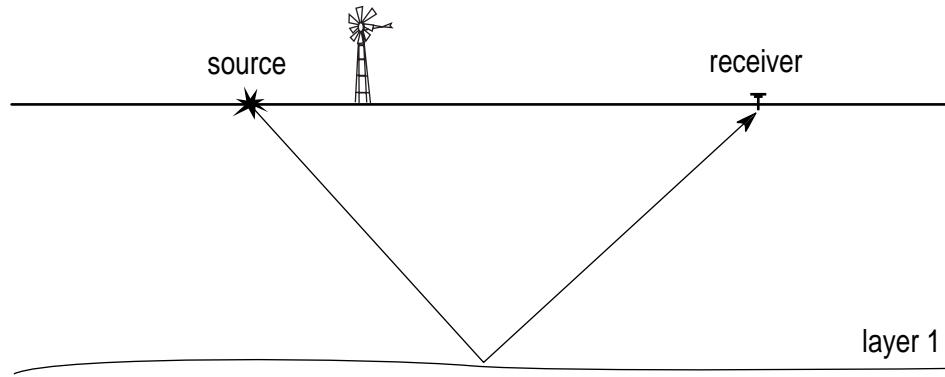
Figure B1. Reflection from one subsurface layer. The angle of incidence of the downgoing ray is equal to the angle of reflectance of the upgoing ray.

Commonly several layers beneath the earth's surface are targeted by a single seismic reflection survey (Figure B2). Seismic data are more complex when several layers are involved. Seismic energy can be converted from one wave type to another at layer interfaces. The simple one-layer case (Figure B1) becomes slightly more complicated when considering all the possible raypaths and wave conversions. The apparent complexity of a seismogram directly relates to the variety of types of seismic waves and their associated characteristic velocities and travel paths. Complexity is often increased as well by the presence of seismic energy that has bounced more than one time off layers in the subsurface (multiple reflections). Reflected energy from successively deeper and deeper boundaries appears on a seismic trace at greater and greater time.

Expanding the multilayer case of Figure B2 to multiple receivers allows travel path versus arrival time determinations and comparisons (Figure B3). Rays reflected from different points in the subsurface are recorded by receivers appropriately spaced on the ground surface. The distance between these subsurface reflecting points is exactly half the distance between receivers, providing a closer subsurface sampling interval than the surface receiver spacing. The recording of multiple receiver/channel locations for each individual shot allows determinations of apparent velocity (travel path/arrival time) and apparent reflector dip.

Source and receiver locations can be placed so that path S1–R2 reflects from the same location in the subsurface as path S2–R1 (Figure B4). The subsurface point that is in common for both source and receiver pairs is called a common-reflection point (CRP) (Mayne, 1962), a common-depth point (CDP), or a common-midpoint (CMP), depending upon the preference of the author (Figure B4).

The power of the CDP method is in the redundancy in sampling of a particular subsurface location. By gathering traces in a computer according to CMP and time-adjusting them for different travel-path lengths, traces with the same CMP can be added to enhance the reflection signal. The degree of redundancy or multiplicity of data at a particular point is known as "CDP fold." A 24-channel seismograph, for example, is typically used to gather 12-fold CDP data. From a theoretical standpoint, signal-to-noise ratio of reflections improves proportionally to the square root of the CDP fold. For shallow reflection data in particular, it is important to remember that 1-fold of good data is better than many-fold of bad or marginal data.

The seismic-reflection method is generally used to determine the spatial configuration of underground geological interfaces. Displaying all the CDP stacked traces consistent with their spatial locations results in a reflection-time cross-section of a portion of the earth (Figure B5). The peaks of the seismic reflections (wiggles) are generally blackened to assist in interpretation. This schematic example (Figure B5) is a very simple version of typical near-surface geology that depicts a buried sand lens in a river valley. Resolving a fixed size target becomes more difficult with increasing depth below the ground surface, but the physical principles remain the same. Resolving power is a linear function of increasing the frequency and bandwidth of the seismic reflection data.

Obtaining high quality shallow seismic reflection data is still somewhat of an art where an individual's ability improves with experience. Improving the quality
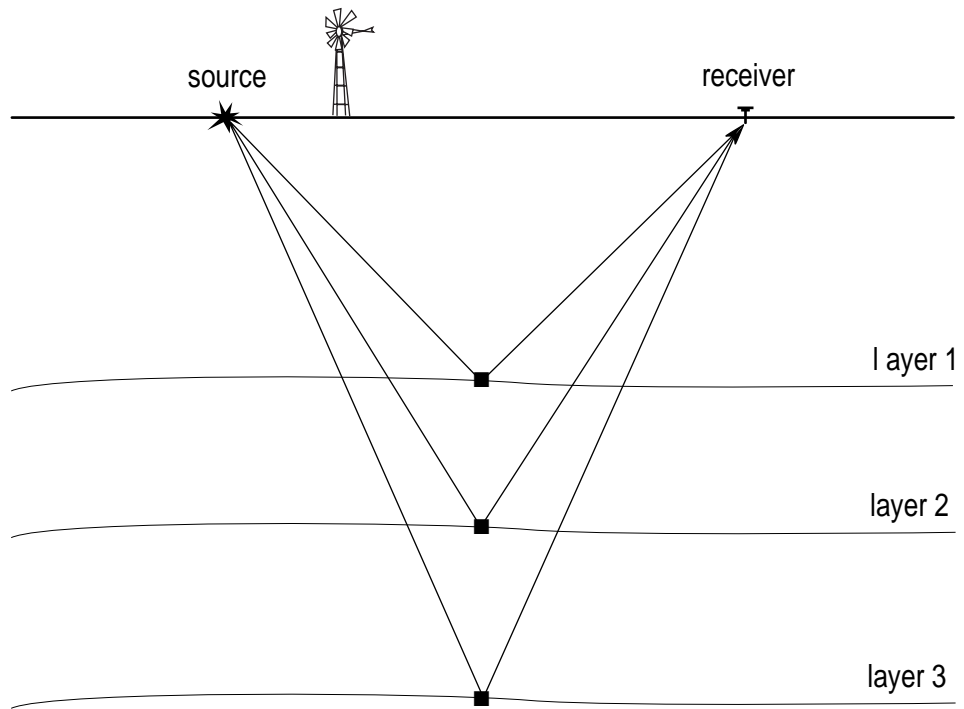
Figure B2. Reflection from three subsurface layers. The angle of incidence is different for each layer/ray but the reflecting points are vertically equivalent.

source

geophone spacing

receivers

receivers

Common Depth Point spacing

subsurface coverage
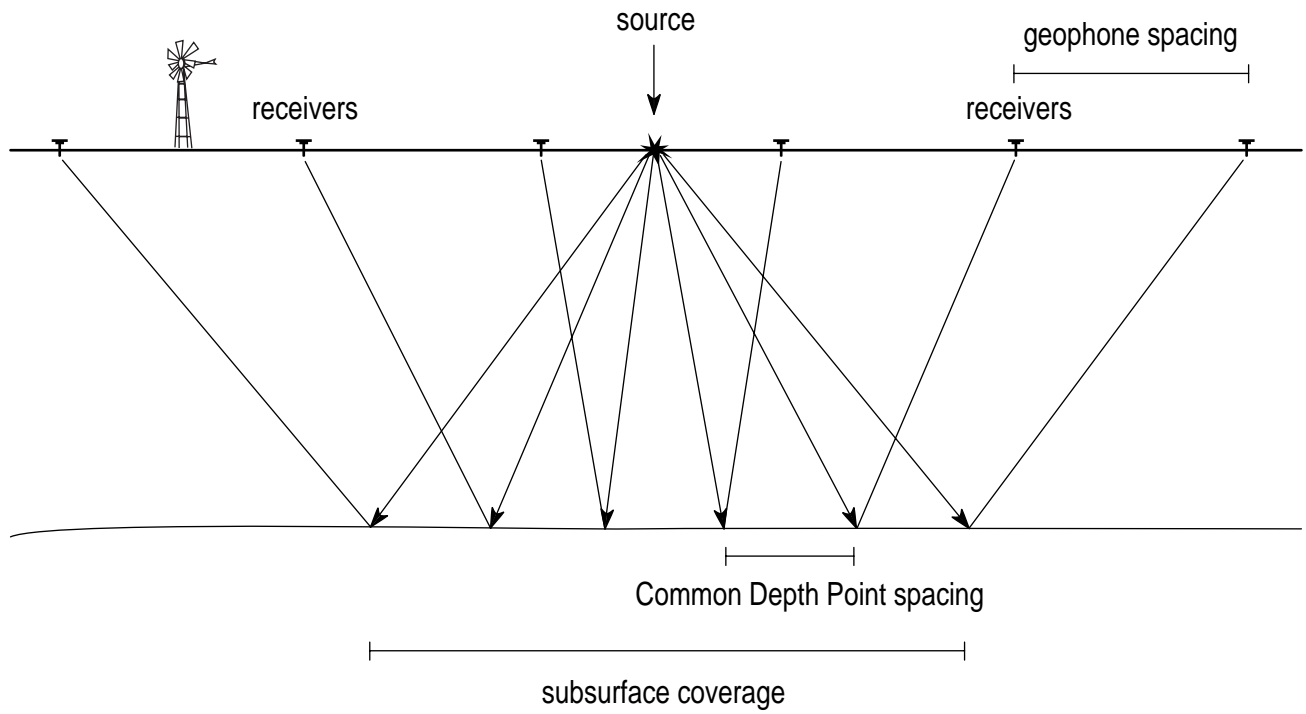
Figure B3. Schematic drawing of seismic ray paths for a single shot with a six-channel reflection seismograph.

Figure B4. The concept of Common Depth Point (CDP). Note that ray paths from two different shots (S1 and S2) reflect from a common point in the subsurface.

Figure B5. Schematic showing a seismic section relating to real-world geology.

of shallow reflection data is dependent on careful, meticulous procedures based on sound scientific observation and theory, step-by-step data analysis, stringent quality control during all aspects, and avoiding invalid assumptions during the acquisition, processing, and/or interpretation of shallow reflection data.
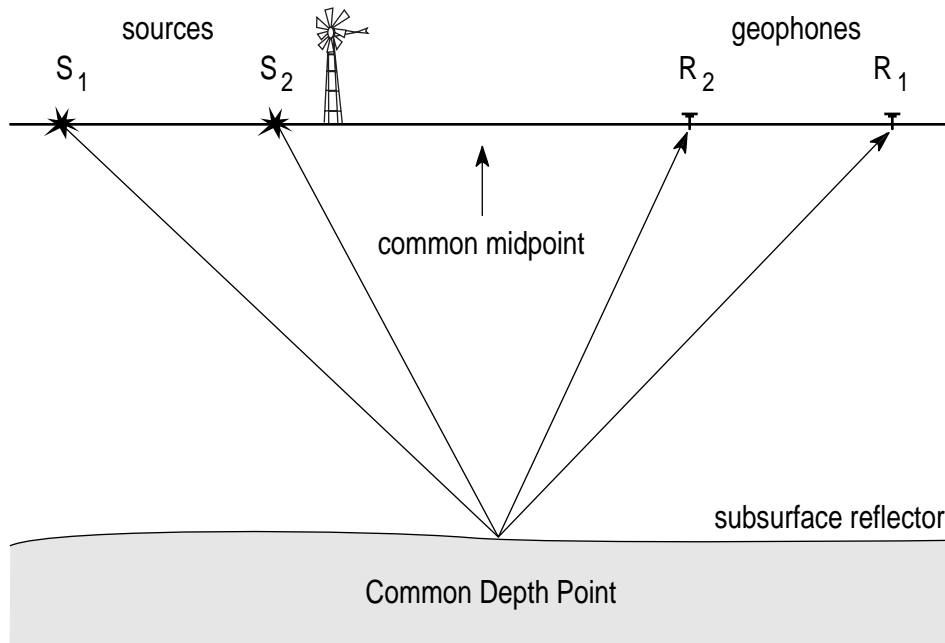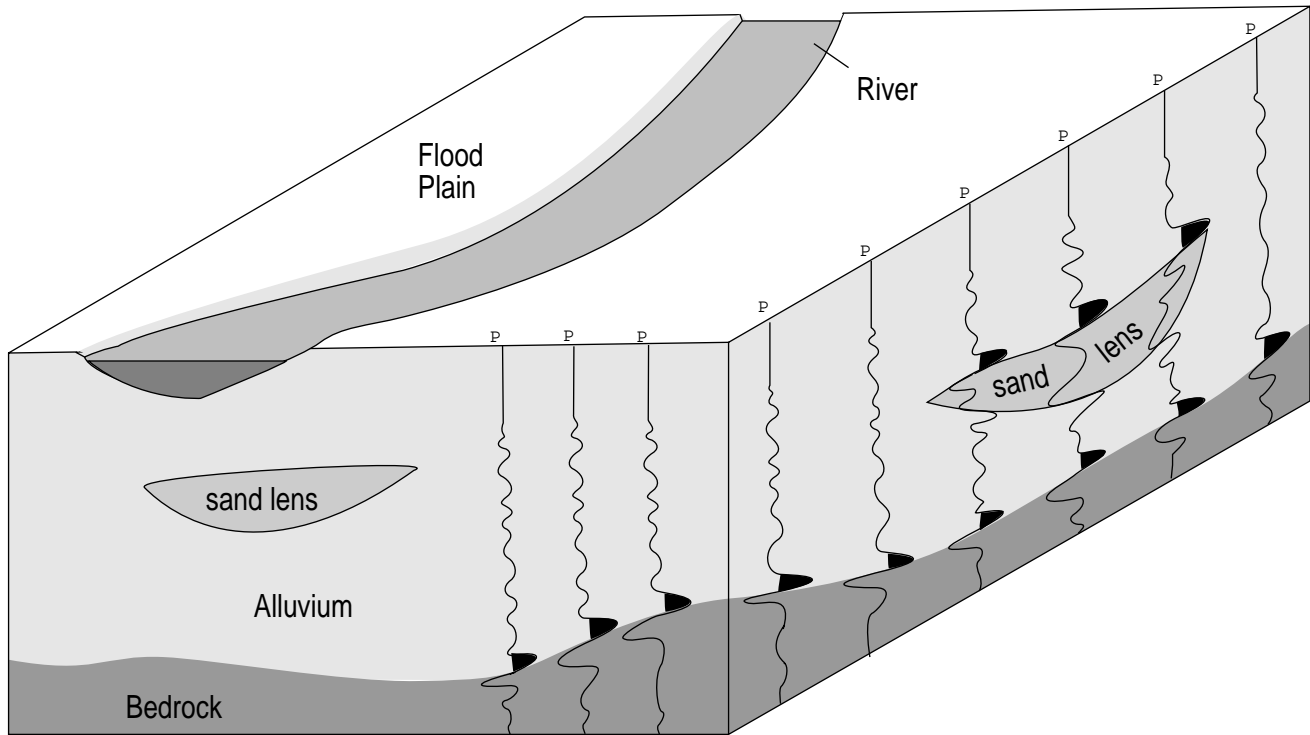
Practical Shallow Reflection Surveying

Seismic reflection surveys routinely involve three basic parts: acquisition, processing, and interpretation. A variety of selectable parameters and methods are possible at each of these three distinct stages. Pronounced differences exist between shallow and conventional seismic reflection techniques during the acquisition and processing stages. The basic principles of interpretation for both shallow and conventional seismic reflection are consistent, except for scale differences. The underlying theoretical basis for the seismic reflection method is consistent for both conventional and shallow applications.

Acquisition

The basic instrument for seismic studies is a seismograph, which is analogous to a stereo music system. The better the music system, the more detail the listener can ascertain from subtle background instruments. Likewise, the better a seismograph's dynamic range, the more the potential for distinguishing subtle geologic features. A stereo music system has variable controls to enhance high frequencies (like a flute) or low frequencies (like a tuba). A seismograph has similar selective capabilities for emphasizing recorded sound frequencies. A seismograph that can record and enhance high-frequency sound waves is necessary to detect small geologic features. The use of high-frequency seismic waves (> 80 Hz) in reflection seismology is known as "high-resolution" seismic exploration (Sheriff, 1991). A stereo system also has an amplifier volume control where a seismograph has amplifier gain control, either fixed (selectable) or floating point (automatic). Selection of the frequencies to be enhanced and the amplifier gain necessary to maximize the recorded relevant geologic information depends on the depth and size of the underground geologic features of interest and the acoustic properties of the near-surface material.

Receivers for detecting reflected acoustic signals in the ground are called geophones, which are very specialized microphones similar in principle to those used in voice recording. The operation of a geophone is based on the voltage induced in a coil of wire when it moves through a magnetic field. For most geophones a magnet is rigidly attached within the geophone case. A coil of wire mounted on a spring surrounds the magnet. When the case experiences movement, the coil moves relative to the magnetic field (set up by the magnet), which in turn induces a voltage proportional to the velocity of the ground motion. Selection of the appropriate geophone for a particular survey should be based on dominant frequency and amplitude of the signal.

The most site dependent part of the acquisition system is the acoustic energy source. A wide variety of sources have been developed and are in routine use on shallow seismic reflection projects. As a human voice is a source of acoustic energy, so is an explosion, a book dropped onto the floor, a car horn, or an electric razor.

The method of generating and transmitting acoustic energy into the ground is what determines the quality of a source at any particular site. There are basically two types of sources: impulsive and vibratory. Impulsive sources are the predominant type of shallow seismic source while vibratory sources are the predominant conventional seismic source. The frequency-limited nature of vibratory sources is what has held them to very limited used on shallow reflection surveys. Most shallow reflection surveys employ weight drop (accelerated) or explosives as the source of acoustic energy.

Processing Shallow Reflection Data

The purpose of acquiring and processing seismic reflection data in a CDP format is to enhance reflections at the expense of everything else. There are a wide variety of filtering, display, and static correction techniques that can be employed to improve the quality of the reflections. Discussion here will have to be limited to only those techniques that are necessary to understand the fundamentals of CDP processing. There are many places in the scientific literature to obtain more details (Waters, 1987; Yilmaz, 1987; Robinson and Treitel, 1980).

Raw seismic data are in a field file or shot gather format with each seismograph channel or seismic trace for a particular shot ordered according to channel number. The number of seismic traces within each shot gather is equal to the total number of seismograph channels. Prior to the gathering or sorting of the data into a CDP format, dead or unacceptably noisy traces are removed and the location of each station is defined in three dimensions. CDP gathers from a simplistic point of view, is a collection of seismic traces that have a common midpoint in the subsurface.

Before stacking (adding) seismic traces with equivalent subsurface sample points it is necessary to compensate for different travel-path lengths (arrival time of the reflection) and localized variability in the near-surface material. The arrival pattern of reflection wavelets across receivers with linearly increasing distance from the source is a hyperbolic function. This hyperbolic arrival pattern or normal moveout curve is a result of the non-linear increase in travel path for a ray traveling down to a reflector and back to the surface with a linear increasing in distance from source to receiver.

To properly correct for different ray path lengths the average velocity above the reflector must be known. The simplest procedure to determine the seismic velocity for good seismic-reflection data is to fit a hyperbola (X^2,T^2) to the data. The degree of curvature of the hyperbola or normal moveout curve of the reflection arrival (assuming horizontal surfaces) is dictated by the average seismic velocity above the reflector, depth to the reflector, and distance between geophones.

Once corrected, the data emulate what would be observed with zero distance between shot and geophone, known as zero-offset (vertical incidence). Proper time adjustment to correct for offset allows traces with common midpoints to be directly added without sacrificing any wavelet properties. The correct velocity gives the highest frequency and the best coherency on the stacked data.

Variations in the velocity and thickness of the near-surface material cause errors known as statics, which uncorrected can produce apparent geologic structures that have no geologic significance. Static variations are most commonly

determined using cross-correlation techniques such as surface consistent statics, residual statics, common offset statics, and refraction statics. Correcting static variations is accomplished through whole-trace time shifts representative of variability in the near-surface, generally in a relatively localized area.

A variety of filtering, scaling, display, and analysis techniques much less significant to the understanding of shallow data CDP processing are routinely used to improve overall data quality. The basics of CDP processing discussed here should provide a general understanding what is most significant to the generation of high-quality stacked sections.

Interpretation

Seismic reflection data can be displayed in a variety of forms including CDP stacked section, shot gather (field file), CDP gather, and common offset section, to name a few. Data displayed in any of these formats have features that require special considerations when trying to interpret the significance of the wiggles. First and foremost, with shallow reflection data not every wiggle necessarily has special geologic significance. Noise is present on any seismic data set and overly optimistic interpretations that draw meaning from every wiggle will eventually lead to misinterpretations. CDP stacked sections are corrected to represent vertically incident time arrivals and, therefore, of all the data display formats, CDP stacked data most closely equate to a geologic cross-section. Common offset data are similar to CDP in the similarity to a geologic cross-section. However, common offset data generally are not corrected from non-vertical travel paths and conversions from time to depth must compensate for the increased time of arrivals. Data in either shot gather or CDP gather format are generally ordered according to distance from shot to receiver. In this arrangement a single reflecting interface will be recorded at ever-increasing times at longer offsets. Interpretations based on shot or CDP gathered data are generally limited to approximate reflector depths and occasionally the inference (in a qualitative sense) of faulting or dipping beds. Seismic reflection data are almost always displayed relative to two-way travel time, which can be converted in a general sense to depth if velocity is known.

Seismic reflection data in a CDP stacked or common offset format can be thought of as the time equivalent to a highway road cut where geologic units are exposed for viewing. The accuracy of the conversion of a time seismic reflection section to a depth geologic cross-section is dependent on how well the average velocity from the surface to each reflector is known. The wiggles on a reflection seismogram represent amplitude (loudness from a sound wave perspective) of an echo that arrived at the geophone at a particular time. That time, when multiplied by the average seismic velocity within the earth, equates to twice depth. If the travel time of an acoustic pulse from the surface to a variety of depths in the subsurface can be determined from borehole geophones, conversion of time to depth can be very accurate. If, on the other hand, no borehole seismic velocity information is available, the NMO velocity must be used to approximate depth. NMO or stacking velocity is always 0-20% greater than the real average velocity. Reflector depths estimated from NMO or stacking velocities cannot be more than 20% deeper than the actual reflecting interface.
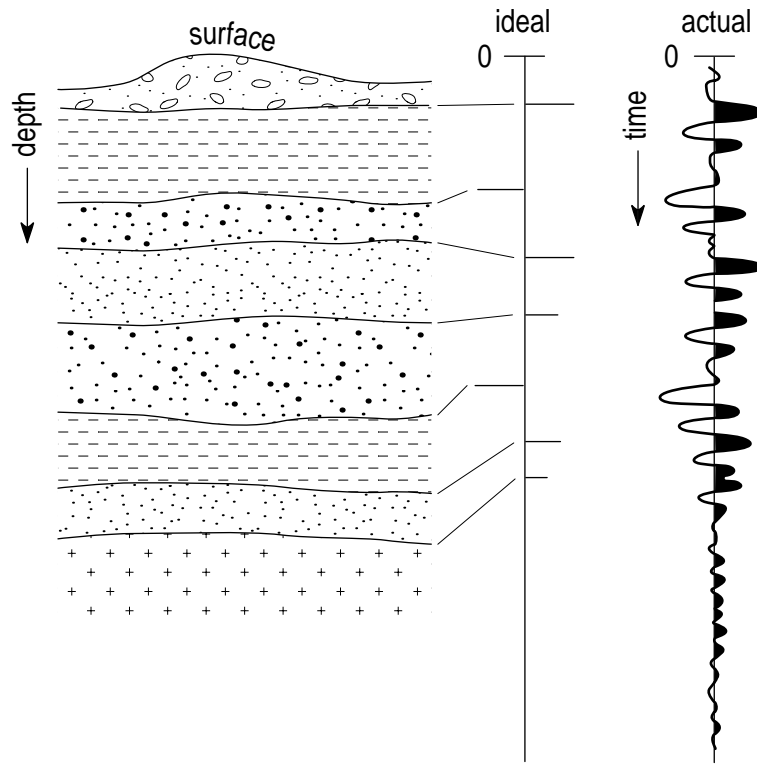
Figure B6. Actual seismic trace (with simulated noise) that would result from a reflection survey over the geologic model. The spike or ideal trace represents the acoustic impedance contrasts at each interface.

The nature of seismic energy is responsible for the representation of recorded signal in the form of a wave (wiggle) (Figure B6). Extracting discrete geologic boundaries or anomalies from the series of wiggles present on seismic data requires the actual or inferred removal of the source wavelet or characteristic sound of a source. Seismic data recorded using the perfect source (flat frequency spectrum from zero to infinity) have spikes that represent each acoustic impedance contrast with the height of a spike directly related to the acoustic impedance contrast at the interface. Unfortunately, since no perfect source exists, the spikes of the perfect source are spread out in time and become waves whose appearance or characteristics are related to the unique spectral properties of the actual source. The narrower the bandwidth of the source the farther from a spike and the 'ringier' the reflection wavelets become. In some cases a reflection may be represented by a wavelet with as many as three zero crossings (3 positive and 3 negative deflections). The interpretation of seismic data requires a good understanding and working knowledge of the source wavelet for a particular source and experience with distinguishing interference between wavelets from two closely spaced reflectors.

Conclusion

Seismic reflection is a powerful geophysical tool for exploration of the subsurface. Applications of the technique to engineering, environmental, and groundwater problems has only recently become cost effective. As with any geophysical technique as long as the basic principles and limitations are understood and no assumptions are made shallow seismic reflection can provide subsurface continuity not possible by any other means at some locations.

References

Mayne, W.H., 1962, Horizontal data stacking techniques: Supplement to Geophysics, v. 27, p. 927-938.

Robinson, E.A., and Treitel, S., 1980, Geophysical signal analysis: Prentice-Hall, Inc., Englewood Cliffs, N.J., 466 p.

Sheriff, R.E., 1991, Encyclopedic dictionary of exploration geophysics, 3rd ed., Society of Exploration Geophys., Tulsa, Okla., 376 pp.

Steeples, D.W., and R.D. Miller, 1993, Basic principles and concepts of practical shallow seismic reflection profiling (a tutorial): Mining Engineering, October, p. 1297-1302.

Waters, K.H., 1987, Reflection seismology–A tool for energy resource exploration, 3rd ed.: John Wiley and Sons, New York, 538 p.

Yilmaz, O., 1987, Seismic data processing; S. M. Doherty, Ed.; Investigations in Geophysics series, No. 2, Edwin B. Neitzel, Series Ed.: Soc. of Explor. Geophys., Tulsa, Oklahoma.